UNIVERSITÀ
DELLA CALABRIA

Dipartimento di Biologia, Ecologia e Scienze della Terra

Scuola di Dottorato: Scienze della Vita

Curriculum: Biologia Vegetale

Ciclo – XXIX

Settore Scientifico Disciplinare **BIO/01**

Impact of DNA methylation on plant growth and development: a study on a methylation-defective mutant of *Arabidopsis thaliana*

Direttore della Scuola:
Prof. Marcello Canonaco

Supervisore:
Dott. Leonardo Bruno

Co-Supervisore:
Prof.ssa Mieke Van Lijsebettens

Dottorando:
Dott. Forgione Ivano

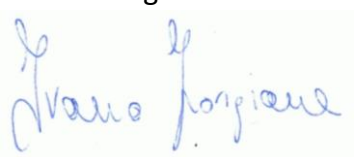

Table of Contents

CHAPTER 3: RESULTS

Abstract

Epigenetic modifications of DNA contribute to chromatin remodeling process and gene expression regulation playing a relevant role on the development of eukaryotic organisms. DNA methylation is an important epigenetic mark consisting in the addition of a methyl group on cytosine bases, which is observed in most of the organisms at the different evolution levels. In plants, DNA methylation is controlled by several genetic pathways, encoding different methyltransferases which act on different sequence contexts. Targets for cytosine DNA methylation in plant genomes are CG, CHG and CHH (H is A, T, C) sequences. The plant DNMT1-homolog METHYLTRANSFERASE1 (MET1) maintains DNA methylation at CG sites, whereas the DNMT3 homolog DOMAINS REARRANGED METHYLASE 1 and 2 (DRM1 and DRM2) are responsible for the *de novo* methylation in all sequence contexts. In addition, the plant-specific CHROMOMETHYLASE3 (CMT3) is responsible for DNA maintenance methylation at CHG sites, as well as at a subset of CHH sites. In plants DNA methylation is involved in diverse biological processes.

Loss of methylation in the *Arabidopsis thaliana* mutants *met1* and *ddm1 (decrease in DNA methylation 1)* causes several developmental abnormalities. Similarly, combined mutations in the *DRMs* and *CMT3* genes induce pleiotropic defects in plants. Here, we used the *Arabidopsis thaliana* triple mutant *drm1 drm2 cmt3,* defective in DNA methylation to get deeper insight into the correlation between DNA methylation and plant growth. We identified novel developmental defects of the triple mutant dealing with the agravitropic response of the root and an altered differentiation pattern of the leaf which also exhibits a curly shape. Confocal microscopy of mutant transgenic lines expressing *DR5:GFP* reporter gene allowed us to verify that the loss of DNA methylation impacts on the accumulation and distribution of auxin from embryo to adult plant. The expression of auxin-related genes has been also found to be altered in *drm1 drm2 cmt3* mutant. Furthermore, through an optimized and implemented protocol of comparative analysis of genomic methylated regions based on MeDIP-qPCR, we provide evidence about the direct and organ-specific modulation of auxin-related genes through DNA methylation process.

The epigenetic mechanisms interplay with each other rather than work independently to modulate gene function. Accordingly, in our study we provide a novel evidence of the crosstalk between DNA methylation status and histone modification.

Indeed, in the *drm1 drm2 cmt3* mutant the overexpression of *CLF* gene, a component of PCR2 complex that performs trimethylation of histone H3 lysine 27, was accompanied by a high level of histone methylation, as evaluated through ChIP-qPCR analysis, and by a concomitant down-regulation of genes target of PRC2 complex action. Thus, the results obtained in these three years of PhD course are encouraging and may open new perspectives in the study of the DNA methylation in plants.

Abstract

Le modificazioni epigenetiche del DNA contribuiscono al processo di rimodellamento della cromatina ed alla regolazione dell'espressione genica giocando un ruolo rilevante negli eventi di sviluppo degli organismi eucarioti. La metilazione del DNA è un importante tratto epigenetico che consiste nell'aggiunta di un gruppo metilico attraverso la formazione di un legame covalente al carbonio 5 della citosina. Tale meccanismo è stato osservato nella maggior parte degli organismi a diversi livelli della scala evolutiva. In particolare, i contesti di sequenza della metilazione del DNA nelle piante sono: CG, CHG, e CHH (H è A, T, C). I diversi enzimi responsabili del meccanismo di metilazione del DNA sono: i) METHYLTRANSFERASE1 (MET1) omologo di DNMT1 mantiene la metilazione del DNA nei siti CG; ii) DOMAINS REARRANGED METHYLASE 1 and 2 (DRM1 and DRM2), omologhi di DNMT3, sono responsabili della metilazione *de novo* in tutti i contesti di sequenza; iii) CHROMOMETHYLASE3 (CMT3), unica del regno delle piante, è responsabile della metilazione di mantenimento dei siti CHG e di un subset di siti CHH. Nelle piante la metilazione del DNA è coinvolta in diversi processi biologici.

La perdita di metilazione nei mutanti *met1* e *ddm1* (*decrease in DNA methylation 1*) di *Arabidopsis thaliana* causa diverse anomalie nello sviluppo, così come mutazioni combinate dei geni *DRMs* e *CMT3* inducono difetti pleiotropici nelle piante. Nel presente lavoro di Dottorato, è stato utilizzato il triplo mutante *drm1 drm2 cmt3* di *Arabidopsis thaliana,* deficiente nel processo di metilazione del DNA (*de novo* e di mantenimento) per studiare la relazione tra il meccanismo di metilazione e la crescita della pianta. Sono stati identificati nuove alterazioni nello sviluppo del triplo mutante *drm1 drm2 cmt3* come la risposta agravitropica della radice ed un alterato pattern di differenziazione della foglia che esibiva un fenotipo aberrante definito "curly leaf". L'analisi di linee transgeniche, che esprimono il gene reporter *DR5:GFP,* condotta mediante microscopia confocale, ha consentito di verificare che la perdita di metilazione del DNA ha un impatto sull'accumulo e distribuzione dell'auxina dalle prime fasi embrionali fino allo stadio adulto della pianta. Tramite analisi di qRT-PCR è stato dimostrato che nel triplo mutante *drm1 drm2 cmt3* è presente, rispetto alle linee di controllo wild type, un'alterazione dell'espressione dei geni correlati al pathway dell'auxina. Inoltre, attraverso un protocollo ottimizzato di analisi comparativa delle regioni metilate, basato sulla tecnica della MeDIP-qPCR, è stato dimostrato che la

metilazione del DNA esercita una modulazione diretta ed organo-specifica sui geni correlati alla biosintesi dell'auxina.

Nel modulare l'espressione genica i meccanismi epigenetici interagiscono tra di loro piuttosto che agire in modo indipendente. Questo lavoro ha permesso di scoprire una nuova interazione tra lo stato di metilazione del DNA e le modificazioni istoniche. Infatti, nel mutante *drm1 drm2 cmt3* l'over-espressione del gene *CLF,* un componente del complesso PRC2 che effettua tri-metilazione della lisina 27 dell'istone H3, è accompagnata da un alto livello di metilazione istonica, come è stato valutato dall'analisi ChIP-qPCR, e da una concomitante down-regolazione di geni target del complesso PRC2. Pertanto, i risultati ottenuti in questi tre anni di Dottorato sono incoraggianti e aprono nuove prospettive di studio della metilazione del DNA in piante.

LIST OF ABBREVIATIONS

ARP	ASYMMETRIC LEAF1/ROUGH SHEATH2/PHANTASTICA
BR	Brassinosteroids
CDGS	Chromatin-dependent gene silencing
cDNA	Complementary DNA
ChIP	Chromatin DNA Immunoprecipitation
ChIP	Chromatin Immunoprecipitation
Col-0	Columbia-0
CZ	Central Zone
DNA	Deoxyribonucleic acid
dsRNA	Double-stranded RNA
GFP	Green Fluorescent Protein
H3K27me3	Histone 3 Lysine 27 trimethylation
HGI	Horizontal Growth Index
KNOX1	KNOTTED-LIKE HOMEOBOX Class I
LBD	LATERAL ORGAN BOUNDARIES DOMAIN
m^5C	5-methylcytosine
MeDIP	Methylated DNA Immunoprecipitation
MeDIP	Methylated DNA Immunoprecipitation
miRNA	MicroRNAs
mRNA	Messenger RNA
MS	Murashige and Skoog
NAA	1-Naphthaleneacetic acid
NPA	1-N-Naphthylphthalamic acid
piRNA	PIWI-interacting RNA
PTGS	Post-transcriptional gene silencing
PTM	Post-translational modifications
PZ	Peripheral Zone
QC	Quiescent Center
qRT-PCR	Quantitative Reverse Transcriptase Polymerase Chain Reaction
RAM	Root Apical Meristem
RdDM	RNA-directed DNA methylation
RNA	Ribonucleic acid

RNAi	RNA interference
RNAseq	RNA sequencing
SAM	Shoot Apical Meristem
SD	Standard Deviation
siRNA	Short interfering RNA
smRNA	Small RNA
ssRNA	Single-stranded RNA
T-DNA	Transfer DNA
TE	Transposable Element
TGS	Transcriptional gene silencing
TSS	Transcription Starting Site
UTR	Untranslated Region
VGI	Vertical Growth Index

CHAPTER 1: INTRODUCTION

1.1 Epigenetics.

The term *epigenetics* was introduced in the early 1940s by Conrad Waddington (Waddington, 1942). In the original definition, epigenetics referred to all molecular pathways modulating the gene expression that do not involve the DNA sequence itself.

While the field of genetics focuses on the study of inherited genes, the epigenetics is the branch of the biology which studies changes in chromatin structure without alterations in the DNA sequence resulting in stable heritable phenotype (Berger *et al*., 2009). The epigenetic modifications described in current literature generally comprise histone variants, post-translational modifications of amino acids on the amino-terminal tail of histones, covalent modifications of DNA bases and non-coding RNAs including long and short non-coding RNAs (Fig. 1).

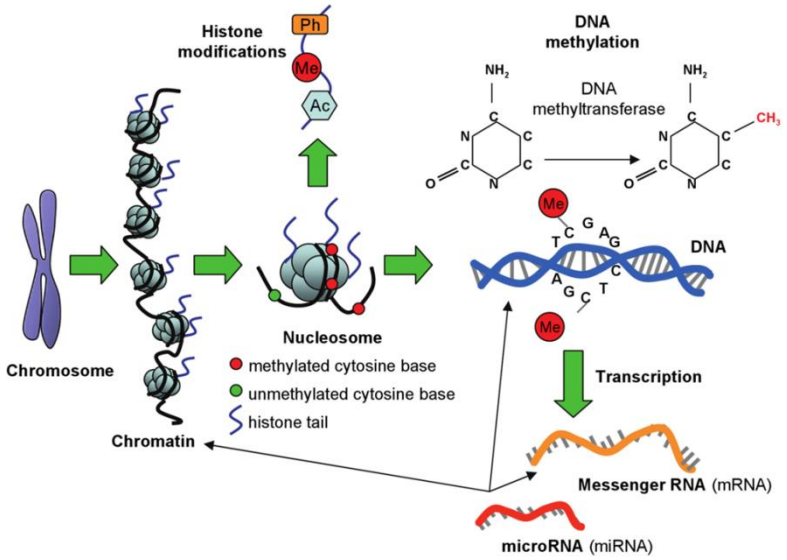

Figure 1. Chromosomes are composed of chromatin, consisting of DNA wrapped around eight histone protein units. Histone tails protruding from histone proteins are decorated with modifications, including phosphorylation (Ph), methylation (Me), and acetylation (Ac). DNA molecules are methylated by the addition of a methyl group to carbon position 5 on cytosine bases. Transcription involves the conversion of DNA to messenger RNA (mRNA). mRNA is translated into a protein product (Relton and Davey Smith, 2010).

Epigenetic marks affect gene expression and have tissue-specific patterns (Eckhardt *et al*., 2006) underlying tissue-specific gene expression (Musco and Peterson, 2008).

Epigenetic processes are essential for development and differentiation, but they can also arise by random change or under the influence of the environment (Issa, 2000).

Indeed, in many studies, environmentally induced changes in gene expression are associated with epigenetic mechanisms. Moreover the epigenetic mechanisms interplay with each other rather than work independently to modulate gene function.

1.1.1 Histone modifications.

As above mentioned, the regulation of gene expression involves an intertwined complex of chromatin modifiers that is connected to post-translational histone modifications (PTM). The chromatin consists of DNA wrapped around a protein complex core that forms chromosomes. The single unit of the chromatin is the nucleosome which is based on a histone octamer that is surrounded by 146 base pairs of DNA. The major proteins of chromatin are the histones, small proteins containing a high proportion of basic amino acids (arginine and lysine) that facilitate binding to the negatively charged DNA molecule. The histones are classified into five types: H1, H2A, H2B, H3 and H4 (Kornberg and Lorch, 1999) and their variants (Ausiò, 2006). Detailed analysis of the nucleosome has shown that the DNA is wrapped 1.65 times around a histone core consisting of two molecules each of H2A, H2B, H3, and H4. To the core histones, there is the linker histone, H1, which contacts the exit/entry of the DNA strand on the nucleosome. Finally, 15-30 residues at the amino terminal of all the histones are unstructured and commonly referred to as tails (Kornberg and Lorch, 1999).

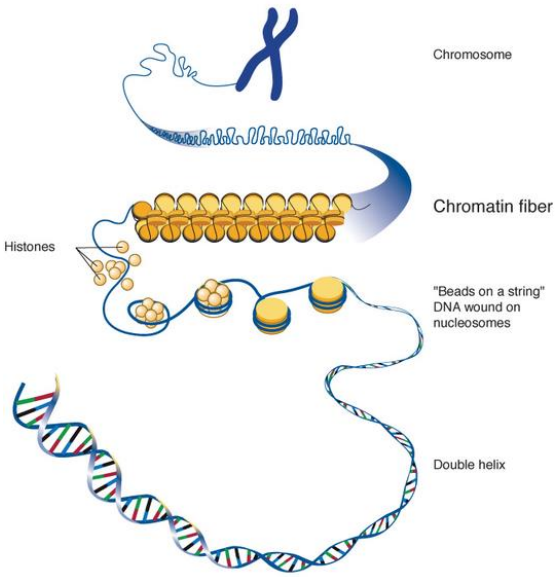

Figure 2. Schematic representation of the organization of the DNA wrapped around the histones to form the nucleosome, which in turn give rise to the chromatin and then the chromosomes.

The chromatin shows a highly dynamic structure with different levels of condensation during the life cycle of the cell. It is commonly divided into euchromatin and heterochromatin. In euchromatic regions, genes are actively transcribed, whereas heterochromatic regions are transcriptionally inactive. Nucleosomes must dynamically change so that DNA binding complexes can access their binding sites. These dynamic changes involve the formation or disruption of interactions within the interfaces between the DNA and histones and are strictly dependent on post-translational modifications of the histone tails. The histone tails are subject to a vast array of post-translational modifications that include: ubiquitination, sumoylation, methylation, acetylation, phosphorylation, ribosylation, glycation, and carbonylation.

Ubiquitin is a polypeptide often associated with proteolysis. Ubiquitination occurs at the histones H2A and H2B where is attached to the lysine residues. H2A ubiquitination is more frequently correlated with gene silencing (Cao and Yan, 2012), while the H2B ubiquitination induces transcriptional activation by promoting other epigenetic marks related to histone methylation (Shukla *et al*., 2006). While DNA methylation is mainly linked to gene silencing, histone methylation represents a mark for transcription activation (Kouzarides, 2002).

A genome-wide analysis of histone methylation marks in plants revealed that trimethylation of histone 3 lysine 4 and di-/trimethylation of histone 3 lysine 36 (H3K4me3 and H3K36me2/me3, respectively) are enriched in actively transcribed gene sequences, whereas H3K27me3 and H3K9me2 are the main gene silencing markers (Zhang *et al*., 2007, Wang *et al*., 2009). A few histone methylations such as H3K27me1, H3K27me2 and H4K20me1 have been found in both transposon regions and heterochromatic regions (Roudier, *et al*., 2011).

Acetylation of core histones have been shown to positively affect gene transcription (Nelissen *et al*., 2007). Histones are acetylated at the lysine residues of the N-terminal tail. The addition of an acetyl group on the lysine residues neutralizes the positive charge of the histone tails and decreases its affinity for DNA. The new conformation facilitates the access of transcriptional regulatory proteins to the chromatin resulting in an increased transcriptional activity (Nelissen *et al*., 2010).

All the histone proteins of the core in the nucleosome are phosphorylated at specific serine and threonine residues. The phosphorylated histones are correlated with

transcriptional activation and often linked to acetylation of H3K9 and H3K14 (Turner, 2000).

Table 1. Post-translational histone modifications in plants.

Residue	Type of modification	Effect on the transcription
Lysine	Acetylation	Activation
Lysine	Methylation	Depends on the histone residue
Lysine	Ubiquitination	Depends on the histone
Serine/Threonine	Phosphorylation	Activation

In the past decade there were many genetic and biochemical studies that explored the relationship between DNA methylation and histone modification, particularly focusing on methylation of histones. It is known that DNA methylation and histone methylation are led by different sets of enzymes in different chemical reactions, but there are evidences that these pathways can be dependent on one another. Histone methylation can help to direct DNA methylation, and DNA methylation might be used as template for some histone modifications (Du *et al*., 2012). In particular, according to Ooi *et al*. (2007) DNA methylation might be mediated through histone modification: methylation of H3K4 (mono, di and trimethylation) might be formed in the embryo before *de novo* DNA methylation.

In addition, a model for heterochromatin assembly that links DNA methylation with histone methylation has been proposed by Soppe *et al*. (2002). By using two hypomethyleted mutants *ddm1* and *met1* they investigated on the relationship between DNA methylation and chromatin organization in *Arabidopsis thaliana*. The decrease in DNA methylation in both hypomethylated mutants occurred in parallel with the reduced methylation of H3K9, so the main cause of reduction of H3K9 methylation should be the reduction in DNA methylation.

Several other studies reported potential functional relationships between DNA methylation and H3K27me3 suggesting that these two epigenetic marks represent major epigenetic silencing mechanisms in plants and in many animal systems. For example H3K27me3 has been suggested to directly target DNA methylation in mammalian cells (Viré *et al*., 2006). By contrast, Zhang *et al*. (2007) suggest that the patterning and function of H3K27me3 in Arabidopsis are independent of DNA methylation.

1.1.2 Small RNA.

Diverse types of RNA ranging from small to long non-coding RNAs are regulators of gene expression beside play a role in genome stability and defence against foreign genetic elements. Indeed, these RNAs are able to modify chromatin and target gene expression via RNA interference (RNAi) pathways and prevent translational process by degradation at post-transcriptional level. These RNAs also play a role in chromatin remodelling and structure through pathways that do not involve RNAi; they seem to contain signals that recruit chromatin-modifying complexes (Rinn and Chang, 2012).

Three classes of small RNA have been identified in eukaryotes. The first two classes, short interfering RNAs (siRNAs) and microRNAs (miRNAs), are 21-25 nucleotides and are generated from longer dsRNA precursors by DICER, a ribonuclease III (RNaseIII) enzyme (Verdel *et al*., 2004). The third class of small RNAs, called PIWI-interacting RNAs (piRNAs), with a larger average size (24-31 nucleotides) than siRNAs and miRNAs, are involved in defence against parasitic DNA elements (Das *et al*., 2008).

Small RNA	Size (nucleotides)	Mechanism of action	Eukaryotes conserved in
siRNA	~21–25	PTGS (RNA degradation or translational arrest) CDGS	Plants, animals, fungi, ciliates
miRNA	~21–25	PTGS (RNA degradation or translational arrest) CDGS (to a lesser extent)	Plants, animals
piRNA	~24–31*	PTGS (RNA degradation) CDGS (to a lesser extent)	Animals

Table 2. Conservation of small-RNA silencing pathways in eukaryotes. All three of the major RNA silencing pathways identified seem to act in both post-transcriptional gene silencing (PTGS) and chromatin-dependent gene silencing (CDGS) pathways (Moazed, 2009).

There are many reports on how RNAi mediate histone or DNA methylation events that repress transcription (Moazed, 2009; Matzke *et al*., 2001). Studies of the flowering plant *Arabidopsis thaliana* demonstrated that one of the post-transcriptional gene silencing pathway was due to the production of small interfering RNAs (siRNAs) and its interaction with DNA methylation through RNA-directed DNA methylation (RdDM) of target loci (Matzke *et al*., 2001).

The pathway in which small RNAs (smRNAs) modulate gene activity is related to the type of ARGONAUTE (AGO) protein, which represents the catalytic component of the RISC (RNA induced silencing complex) which either prevents translational process or degrade target transcript. The association of siRNAs with one of the ten AGO proteins depends on its length and 5′ terminal nucleotide. For instance, AGO1 is associated to the majority smRNAs that are 21 or 22 nucleotide long and carry 5′ uracil, while most of the smRNAs associated with AGO2 are 21 nucleotide long and have 5′adenine (Mallory and Vaucheret 2010). Since smRNAs are of different sizes and contain distinct 5′ terminal nucleotides, they can repress gene expression either at the post-transcriptional level at the chromatin level through TGS depending on which AGO protein they interact.

1.1.3 DNA Methylation.

Nowadays it is known that among the epigenetic modifications DNA methylation, which is a covalent addition of a methyl group to the fifth carbon of the cytosine, has a direct impact on the regulation of gene expression.

Covalent modification of DNA have been described since 1948 (Hotchkiss, 1948), but it was only in 1969 that Griffith and Mahler proposed that gene expression (Fig. 3) may be modulated by these modifications (Griffith and Mahler, 1969).

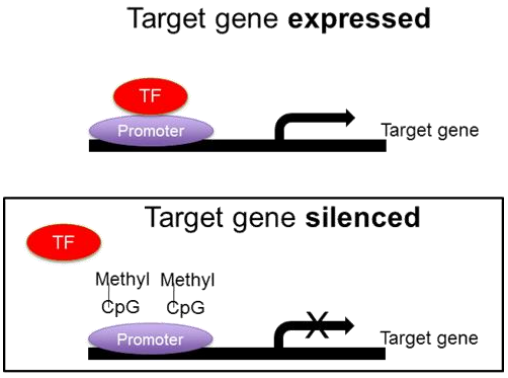

Figure 3. The addition of methyl groups to CG is one mechanism for suppressing (or silencing) gene transcription (Fry, 2011).

This model was supported by additional studies over the next years, targeting the DNA methylation as the responsible for the stable maintenance of a particular gene expression pattern through mitotic cell division (Holliday and Pugh, 1975). The lack of methylation in the promoter region of the genes is usually associated with the

chromatin pattern of actively transcribed genes, as characterized by an opened nucleosome configuration (Tazi and Bird, 1990).

DNA methylation basically is a post-replication event. There are specific enzymes called methyltransferases which catalyze the transfer of methyl groups from S-adenosyl-L-methionine to DNA bases (Fujimoto *et al*., 1965). Although DNA methylation was found in both adenine and cytosine in bacteria and eukaryotes, it has been shown that cytosine methylation is more impactful on regulation in eukaryotes while adenine methylation seems to have mainly regulatory role in bacteria (Bickle and Kruger, 1993).

In animal genomes, cytosine methylation was thought to be restricted largely to the CG dinucleotide. In mammals, DNA methylation is predominantly found in cytosines of the dinucleotide sequence CG. Studies in the past decade have shown that CH (H = A, T, or C) methylation is present in cultured pluripotent stem cells, including embryonic stem cells (Ramsahoye *et al*., 2000), and recently CH methylation was found in the adult mouse cortex and human brain (Lister *et al*., 2013).

There are two basic types of DNA methylation processes known in eukaryotic cells. First is *de novo* methylation which is involved in the rearrangement of methylation pattern during embryogenesis or differentiation processes in adult cells (Razin and Cedar, 1993). The methyltransferases create hemimethylated CG dinucleotides after replication where methylation is found only on the original strand and is absent from the newly synthesized strand (Fig. 4). The second methylation activity in eukaryotic cells is the so-called maintenance methylation which is necessary to preserve DNA methylation after every cellular DNA replication cycle. Hemimethylated CGs attract the maintenance methyltransferases, which methylate the unmethylated strand to restore symmetric DNA methylation (Fig. 4).

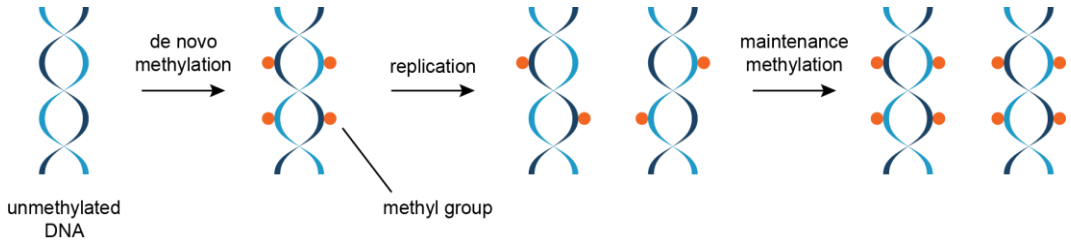

Figure 4. The two types of DNA methylation. Schematic representation of *de novo* methylation and maintenance methylation of DNA. The methyl group is indicated by a red lollipop.

Methyltransferase enzymes involved in DNA methylation belong to different families and subfamilies whose members act on different sequence context and

different processes (i.e. maintenance VS *de novo*). For example, in mammalian genomes DNA methylation is established and maintained by two DNA METHYLTRANSFERASES (DNMTs) families. In particular DNMT1 acts in DNA methylation maintenance (Cheng and Blumenthal, 2008), while members of the DNMT3 family are responsible for *de novo* methylation (Okano *et al*., 1999).

Relevant roles of DNA methylation have been demonstrated in mammalian genomes. One of these is the maintenance of the inactive state of one of the female X chromosomes. X-inactivation is a process by which one of the two X chromosomes present in female mammals is inactivated. The inactive X chromosome is silenced by packaging in a transcriptionally inactive structure, the heterochromatin. By comparing the epigenetic profile of the heterochromatin of the inactive X chromosome with the euchromatin of the active X chromosome, it has been demonstrated that the inactive X chromosome has high levels of DNA methylation. Note that together with increased levels of DNA methylation, X chromosome inactivation shows low levels of histone acetylation, low levels of histone H3 lysine-4 methylation, and high levels of histone H3 lysine-9 and H3 lysine-27 methylation, all of which are strictly linked with gene silencing (Chow *at al*., 2005).

It was also found that DNA methylation is a key molecular mechanism of genomic imprinting. In this epigenetic phenomenon genes could be differently expressed depending on whether they came from the mother or the father (Surani *et al*., 1984). Forms of genomic imprinting have been demonstrated first in mammals and later in plants. There are evidences that, in plants, genes are imprinted primarily in the endosperm and in tissues that surround and nourish embryo during its development. An example is represented by the *Arabidopsis thaliana* gene *MEDEA (MEA)* that regulates cell proliferation by exerting a gametophytic maternal control during seed development (Grossniklaus *et al*., 1998) Several studies report that the majority imprinted genes examined show differences in DNA methylation. Consistently, the maintenance of the genomic imprint at the *MEA* locus is related to its methylation status (Vielle-Calzada *et al*., 1999).

Another relevant role of DNA methylation deals with the inactivation of Transposable Elements (TEs) present in the genomes of higher eukaryotes. Active TEs also known as “jumping genes”, move from one location on the genome to another.

Much of what a TE does depends on where it lands. TE landing inside a gene can result in a mutation. This behavior of TEs might play a causal role in disease development, generate new genes and alter gene regulation and consequently cause

new phenotypes. Not all transposition results in negative effects. In fact, transposons can drive the evolution of genomes by facilitating the translocation of genomic sequences, and the repair of double-stranded breaks (Pray, 2008). TEs have the propensity to increase their representation from one generation to the next by replicating themselves at a higher rate than other genes. Moreover, there is evidence that transposons in all species examined appear to be largely quiescent (Yoder *et al*., 1997). This lack of activity is due to an epigenetic control. Molecular analysis of these elements revealed that inactivation was associated with DNA methylation where addition of a methyl group to cytosine was often associated with silencing.

Finally, it has been proposed that DNA methylation also represents one of the ways for controlling telomere length. Telomere is the region present at each end of a chromosome, formed by repetitive nucleotide sequences, that protects the chromosome end from degradation or fusion with neighboring chromosomes (Chan and Blackburn, 2002). Most adult cells progressively lose telomeres during cell division and tissue renewal, and it has been proposed that this telomere shortening contributes to the development of age-related pathologies, limiting human lifespan (Flores *et al*., 2005). Recent studies have shown that mammalian telomeres and subtelomeric regions are also enriched in epigenetic marks that are characteristic of heterochromatin. Mammalian telomere repeats (TTAGGG) cannot be methylated because they lack CG sequences. However decreases in DNA methylation, at subtelomeric regions, are accompanied by dramatically elongated telomeres (Gonzalo *et. al*., 2006).

In human, disruption of DNA methylation and other epigenetic marks give rise to many diseases. Changes in both DNA methylation and histone modifications have been discovered in many cancer types. There are findings on the association of DNA hypomethylation with tumors suggesting activation of oncogenes as a possible consequence of decrease in DNA methylation (Feinberg and Vogelstein, 1983). Also in mouse alteration in DNA methylation status related the total homozygous knockout of *DNMT1* homologous with its ortholog in human and chicken (Yen *et al*., 1992), was lethal for the embryo (Li *et al*., 1992) suggesting a relevant role in embryo development.

However, despite all this information, the dynamic status of DNA methylation during development and across generations, as well as the related role, remains poorly understood and mainly in plants (Lisch, 2009).

1.2 DNA methylation in plants.

The occurrence of DNA methylation in plants was firstly assessed in 1950s by establishing that higher plant DNA contains 5-methylcytosine (m^5C) in addition to four ordinary bases (G, A, T, C) (Wyatt, 1950).

Since then, significant progress has been made and in the past decade plant research has improved our knowledge on the distribution and function of plant DNA methylation at a genome-wide scale. A very recent study provides a comparative DNA methylation profile of 34 different flowering plants (Niederhuth *et al*., 2016).

1.2.1 Sequence context and methylation pathways.

In plant genomes DNA methylation is more extensive and affects a wider sequence diversity than in animals. Plants have relatively high concentrations of 5-methylcytosine (m^5C) compared to non-plant species because cytosine methylation occurs in three sequence contexts: symmetric CG, CHG, and asymmetric CHH (in which H= A, T or C) (Henderson and Jacobsen, 2007).

Like in animals, different families of DNA methyltransferases with distinct substrate specificity and different modes of action account for DNA methylation in plants: METHYLTRANSFERASE (MET) family, DOMAINS REARRANGED METHYLTRANSFERASES (DRMs) family and the CHROMOMETHYLASES (CMTs) plant specific family (Table 3).

In details, DNA methylation in CG context is maintained by MET1, the homolog of mammalian DNMT1, which is recruited to hemi-methylated CG sites and methylates the opposing strand (Finnegan *et al*., 1996), whereas CHG methylation is maintained by CMT3 (Lindroth *et al*., 2001).

The maintenance of methylation at CHG sites does not seem to depend on the palindromic symmetry of the sequence. The CMT3 activity is strongly associated with dimethylation of lysine 9 on histone 3 where the dual recognition of H3K9me2 by BAH (Bromo Adjacent Homology) and CHROMO domains of CMT3 leads the methylation of CHG sites (Du *et al*., 2012). In more detail, it has been demonstrated that KRYPTONITE (KYP) is capable of binding methylated mCHH or mCHG of the DNA through its SRA (SET and RING-associated) domain (Jackson *et al*., 2002). CMT3 is recruited by H3K9me and

further methylates CHG of the DNA to create binding sites for KYP, resulting in a self-reinforcing feedback loop (Law and Jacobsen, 2010).

In addition to CMT3, other members of the CMT family are present in *Arabidopsis thaliana* genome. *CMT1* is expressed at low levels and is truncated in many Arabidopsis ecotypes (Henikoff and Comai, 1998). CMT2, establishes and maintains asymmetrical methylation of CHH sites (Stroud *et al*., 2014). Recent studies on whole-genome methylation profile of *cmt2* mutant showed loss of CHH methylation predominantly at TEs in the heterochromatic fraction (Zemach *et al*. 2013).

DRM1 and DRM2, homologue of the mammalian *de novo* DNA methyltransferase DNMT3, mediate *de novo* methylation of cytosines in all classes of sequence contexts (CG, CHG and CHH) (Law *et al*., 2010) (Table 3). Both enzymes are targeted by small interfering RNAs through a pathway termed RNA-directed DNA methylation (RdDM),

Table 3. Plant DNA methyltransferases.

Gene Name	Target Sequence	Effect on Chromatin/Transcription	Effects of Mutation
METHYLTRANSFERASE1 (*MET1*)	CG	Maintains the global methylation	Inability to establish CG methylation
CHROMOMETHYLASE2 (*CMT2*)	CHH	Maintains the DNA methylation	Loss of CHH methylation
CHROMOMETHYLASE3 (*CMT3*)	CHG	Maintains the DNA methylation	Loss of CHG methylation
DOMAIN REARRANGED METHYLTRANSFERASES (*DRM1, DRM2*)	CG, CHG and CHH	*De novo* methylation of asymmetric sites; DRM2 is involved in *de novo* methylation in the RdDM pathway	Loss of *de novo* DNA methylation

RdDM pathway is under the control of a specialized mechanism which depends on two plant-specific RNA polymerase called Pol IV and Pol V. Pol IV transcribes a single-stranded RNA (ssRNA) at its target loci. The ssRNA is copied into a double-stranded RNA (dsRNA) by the RNA-Dependent RNA polymerase 2 (RDR2) with the assistance of the chromatin remodeller CLASSY 1 (CLSY1). The dsRNA is processed by DICER-LIKE 3 (DCL3) into 24‑nucleotide siRNAs that are methylated at their 3‘ ends by HUA ENHANCER 1

(HEN1) and incorporated into ARGONAUTE 4 (AGO4). Pol V transcribes a scaffold RNA that base-pairs with AGO4‑bound siRNAs. A key role is played by RNA-DIRECTED DNA METHYLATION 1 (RDM1) the only protein that interacts with both AGO4 and DRM2 thus creating a bridge between them (Gao *et al*., 2010). These nucleoprotein complexes target chromatin-associated scaffold transcripts in a sequence-specific manner. The chromatin-bound complexes then recruit DRM1 and DRM2 which methylate DNA in CG, CHG, and CHH sequence contexts (Haag *et al*., 2011)(Fig. 5).

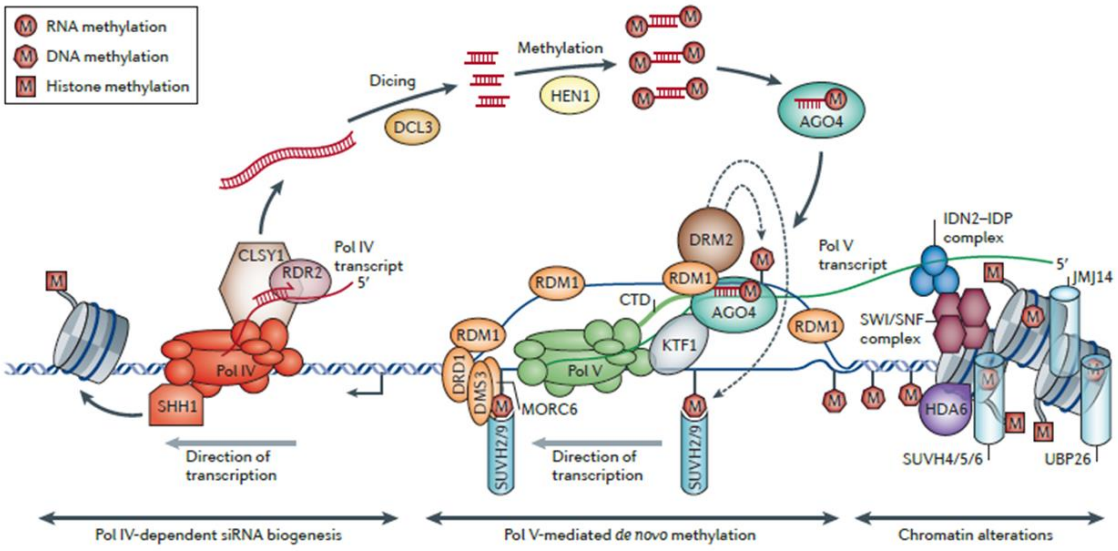

Figure 5. Canonical RNA-directed DNA methylation (RdDM) pathway (Matzke and Mosher, 2014).

1.2.2 DNA Methylation landscape of the Arabidopsis genome.

Most of the studies on DNA methylation in plants have been performed on the model plant *Arabidopsis thaliana* due to the high-quality sequence of its genome.

Several studies report DNA methylation to be conspicuously dense in the pericentromeric regions of nuclear chromosomes (Zhang *et al*., 2006; Zilberman *et al*., 2007; Lister *et al*., 2009) where CHG methylation results in higher levels likely due to its preference for transposon-related sequences. In contrast, to the dense methylation in pericentromeric regions, CG and CHH methylated sequences are widely distributed throughout the arms of all five chromosomes. Moreover, each methylation sequence is

distributed in distinct profiles over the Arabidopsis genome showing highest fraction in CG context. Indeed the CG methylation represents more than half of the methylated fraction of the DNA, whereas CHG and CHH represent an equally lower fraction (Lister *et al*., 2008).

Methylation of genes has been extensively studied in Arabidopsis (Chan *et al*., 2005). Genome-wide analysis of DNA methylation revealed that more than 60% of the 27000 *Arabidopsis thaliana* genes are entirely unmethylated. A large number of genes (about 30%) are methylated within transcribed regions but not within their promoter, and a restricted 5% of the Arabidopsis expressed genes is methylated upstream of the transcription start site (Zhang *et al*., 2006).

DNA methylation of promoters is known to block transcription initiation, gene-body methylation has been hypothesized to interfere with elongation within active genes in Arabidopsis, especially if the methylation is close to the 5' end (Hohn *et al*., 1996).

DNA methylation can inhibit transcriptional activity or make silent chromatin in two different ways. First, DNA methylation can physically impede the binding of transcription factors to the gene making them inaccessible to the transcription machinery. Second, methylated DNA may recruit methyl-cytosine binding proteins which in turn may recruit additional protein complexes, such as histone deacetylases and other chromatin remodeling protein that can modify the structure, resulting in inactive and silent chromatin (Boyes and Bird, 1991).

1.2.3 Methods to identify DNA methylation.

DNA samples are usually derived from a collection of cells, which might be variable in their methylation pattern. For this reason analysis of DNA methylation is complicated. Conventional techniques such as cytosine hybridization-based are not able to distinguish 5-methyl-cytosine from unmethylated cytosine. Furthermore DNA methyltransferases are not present during PCR or in biological cloning systems so DNA methylation information is lost during amplification. To maintain DNA methylation during PCR it would require a thermostable enzyme with no *de novo* methyltransferase activity, but it has not been discovered to date (Laird, 2010). Currently, methylation dependent pre-treatments of DNA are employed to reveal the presence or absence of

the methyl group at cytosine residues. There are three main approaches used to identify DNA methylation.

First, restriction endonucleases are such powerful tools in molecular biology. They are dependent on the presence of specific recognition sequences and some of them are inhibited by the methyl group on the cytosine. Endonuclease activity followed by hybridization can provide information on DNA methylation pattern. The major issue with this technique is about the location of the methyl-cytosines and therefore the precise sequence of the methylation is not identifiable. The method of methylation-sensitive restriction digestion followed by PCR amplification across the restriction site is a very sensitive technique that is still used today. However, it can give false-positive results caused by incomplete digestion for reasons not connected to DNA methylation (Tompa *et al*., 2002).

Similarly to chromatin immunoprecipitation (ChIP) assay used in determination of enriched histone modifications, methylated genomic regions can be detected using antibodies specific for 5 methyl-cytosines or using methyl-binding proteins with affinity for methylated DNA. A specific antibody for methylated cytosine is employed to detect enrichment of methylated regions by immunoprecipitation of denatured genomic DNA, followed by hybridization (MeDIP-chip), sequencing (MeDIP-seq) or amplification (MeDIP-qPCR).

These techniques have been widely used to explore the methylomes of plant (Zhang *et al*., 2006), mouse (Mukhopadhyay *et al*., 2004) and human (Irizarry *et al*., 2008). However, these techniques are subject to limitations such as low resolution of detection.

Bisulfite conversion provides high-resolution detection of DNA methylation. Chemical treatment of genomic DNA with sodium bisulfite converts cytosines residues, much more rapidly than methylated cytosines, into uracil via a sulfonation, deamination, desulfonation reaction (Hayatsu, 2008). Subsequently the use of direct sequencing determines the locations of unmethylated cytosines and 5-methyl-cytosines at single-nucleotide resolution. Over the past decade, Sanger sequencing after bisulfite modification has represented a key role in the study of DNA methylation. Today, by coupling bisulfite conversion to NGS (Next Generation Sequencing) technology it is possible to map the sites of DNA methylation at single-base resolution throughout an entire genome with very high quality and sensitivity.

1.2.4 DNA methylation in the context of plant development.

The development of a multicellular organism requires the spatially coordinated acquisition of numerous cell identities. Therefore a spatio-temporal regulation of gene expression is required. On the other hand to generate the body pattern the cells of the developing organism have to exchange and respond to information about their relative position. In such positional signaling endogenous hormones play a relevant role (Swarup *et al*., 2001; Davies, 2010; Zažímalová *et al*., 2014).

In higher plants, the apical-basal axis that determine the future growth direction of the organism is precociously established during embryogenesis and is driven by the shoot and root apical meristems (SAM and RAM) positioning. The radial pattern is made of concentric layers of the main tissue types. The normal apical-basal axis formation in embryo is determined by the correct distribution of auxin which is under the control of the PIN family proteins that are expressed in embryo in different places and at different time during development. *PIN7* and *PIN1* are the earliest *PIN* genes expressed in the embryo. PIN7 protein is found at the apical membrane of the basal cell in the two-cell embryo and at the apical membrane in suspensor cells until the 32 cell stage suggesting a role for PIN7 in transporting auxin from the basal cell to the apical cell. PIN1 protein is localized throughout the embryo, from the single-cell stage until the 32-cell stage. PIN4 protein begins to accumulate in the hypophyseal lineage and suspensor. *PIN3* mRNA expression is detected at the root pole of the heart-stage embryo (Friml *et al*., 2002; Friml *et al*., 2003).

Both SAM and RAM are maintained during the postembryonic phase and are essential for plant growth and development because they features as stem cell niche where cells continuously divide and produce progeny cells which undergo different fate, while self-renewing (Bitonti and Chiappetta, 2010; Petricka *et al*., 2012; Zažímalová *et al*., 2014; Pfeiffer *et al*., 2016; Soyars *et al*., 2016).

In such a way, SAM continuously produces stems and lateral organs (leaves and floral organs). Leaf initiation occurs at specific positions at the periphery of the SAM (Reinhardt *et al*., 2000) which is organized in zones with different rates of cell division and different functions (Medford *et al*., 1992). The dome-shaped structure can be generally divided into three distinct zones: the Central Zone (CZ) at the surface of the dome, surrounding its apex which maintains indeterminate growth and produce daughter cells for the neighboring peripheral and rib zones; the Peripheral Zone (PZ), also on the surface contributes to the formation of new organs; the Rib Zone (Rib),

deeper within the dome, below the central zone. The majority of cell division occurs in the peripheral zone and rib meristem, with slower division occurring in the central zone. SAM is also subdivided into distinct cell layers termed L1, L2, and L3 (Satina *et al*., 1940). The L1 and L2 each form single cell sheet because of anticlinal cell division patterns. When the cells in the L1 layer differentiate they produce pavement cells, guard cells and trichomes. The cells of the L2 layer give rise to mesophyll cells (photosynthetic tissue) in the leaf. In developing anthers L2 layer cells differentiate into microsporocytes and tapetum, the latter nourishes the developing pollens. Similarly, in ovules the L2 cell layer is responsible for megasporocytes development. The cells in the L3 undergo both anticlinal and periclinal cell division patterns to form the inner core of the meristems where cells later on differentiate into vascular bundles and pith cells and form the stem tissue.

The SAM has properties of a self-regulatory system in which the interactions between the genes *WUSCHEL* (*WUS*) and *CLAVATA* (*CLV*) establish a feedback loop between the stem cells and the underlying organizing center. The *WUSCHEL* (*WUS*) gene is required for stem cell identity (Pfeiffer *et al*., 2016; Soyars *et al*., 2016). The *CLAVATA* (*CLV1, CLV2, CLV3*) genes, which encode for components of a signaling pathway that limits the size of the SAM, promote the progression of meristem cells toward organ initiation. The function of the *CLV* genes is antagonized by the *SHOOTMERISTEMLESS* (*STM*) gene, a transcription factors belonging to the class *1 KNOTTED-LIKE HOMEOBOX* (*KNOX1*) gene family (Clark *et al*., 1996). *STM*, indeed, promotes meristem formation and maintenance. The repression of the gene *STM* and the activation of the gene *ASYMMETRIC LEAVES1* (*AS1*) are also crucial for leaf initiation (Byrne *et al*., 2000). Notably, an interaction between these genetic network and different hormone classes has been largely demonstrated (Gray, 2004).

The RAM assures the growth and development of root system (Bitonti and Chiappetta, 2010; Petricka *et al*., 2012). The primary root, or radicle, is the first organ to appear when a seed germinates. It grows downward into the soil, anchoring the seedling and enhancing water uptake. The RAM dome is located subterminally and is covered by the root cap, which protects the apical meristem, produces mucilage to facilitate a passage for the growing root, and serves as a gravity perceiving tissue. The RAM pattern consists of concentrically arrayed stem cells that extend the radial pattern in the growing root, the four cells of the quiescent center (QC), which divide only infrequently, and most distally, the initials of the central root cap (columella). Several network of genes are involved in the establishment and maintenance of the RAM. One of them

deals with the *PLETHORA* (*PLT*) gene family that plays a key role in the acquisition of the QC fate (Aida *et al*.,2004). These genes are required for stem cell specification and maintenance in the RAM and act in parallel with *SHORT-ROOT (SHR)* and *SCARECROW (SCR)* to define QC and stem cell position. *SHR* is transcribed exclusively in the provascular tissue from embryogenesis onward, but the protein moves outwards to the surrounding cell layers including the QC and promotes *SCR* expression in these cells (Nakajima *et al*., 2001). *SCR* is required for QC identity, which in turn promotes the activity of surrounding stem cells (Sabatini *et al*., 2003).

The proper expression of *PLT1* and *PLT2* relies on the establishment of an auxin response maximum (Blilou *et al*., 2005). It is known that auxin is transported in a directional manner by membrane spanning proteins that mediate the influx and efflux of this signaling molecule into and out of cells. The localization of members of the PINFORMED (PIN) family of auxin efflux facilitators within cells reflects the direction of auxin transport (Petrásek *et al*., 2006). In particular PIN1 is localized at the basal (root apex-facing) side of the root vasculature; PIN2 at the basal side of the cortical cells and at the apical (shoot apex-facing) side of the protoderm and root cap cells; PIN3 in the columella cells of the root; PIN4 at the basal side of cells in the central root meristem and in the cells of the quiescent center; and PIN7 at the basal side of the stele cells and in the columella cells (Feraru and Friml, 2008). Moreover, the auxin effects on the transcription of genes involved in root patterning are mediated by members of the AUXIN RESPONSE FACTORS (*ARF*) family (Aida *et al*.,2004). The *MONOPTEROS (MP*) gene encodes a member of the *ARFs* that can bind to promoter elements of auxin-inducible genes which is required for embryonic root formation and RAM maintenance.

The development of plant leaves follows a common basic program. Leaves initiate at the flanks of the SAM and then develop into a flat blade of variable size and form. This process is regulated by several plant hormones and transcriptional regulators (Bar and Ori, 2014). Leaf development can be divided in two three main processes: i) initiation of the leaf primordium, ii) establishment of dorsiventrality and iii) development of a marginal meristem which lead to lamina growth. So far, several aspects of the hormonal and genetic network that control leaf development have been clarified in recent developmental and molecular genetic studies of Arabidopsis (Bar and Ori, 2014). In more details, it has been demonstrated that the hormone auxin is a central regulator of leaf initiation and points of auxin accumulation have been found to precede organ initiation. These are created by auxin biosynthesis in the SAM and by directional auxin transport generated by PIN1 auxin transporter (Bar and Ori, 2014). Moreover leaf

initiation is tightly correlated with vasculature development which involves changes in PINs polarization, from a polarization towards the outermost cell layer (L1) of primordium to a basal localization towards the future vasculature (Scarpella *et al*., 2006).

Specification of the leaf primordium domain depends also on differential expression of genes that regulate the balance between undeterminated vs committed cell fates. In particular this balance is mainly controlled by (i) KNOX1 transcription factors, which are expressed in the SAM central dome, where promote meristematic state, and are downregulated at the site of organ initiation (Hay and Tsiantis,2010); (ii) ARP [ASYMMETRIC LEAVES1 (AS1), ROUGH SHEATH2 (RS2), PHANTASTICA] transcription factors and the LBD (LATERAL ORGAN BOUNDARIES DOMAIN) protein AS2 which are expressed at the site of leaf initiation and, together with LBD protein AS2 repress *KNOX1* thus specifying leaf initiation domain (Barkoulas *et al*., 2007; Bar and Ori 2014). To more KNOX genes *KNAT2* and *KNAT6* are also negatively regulated by *AS1* but their inter-relationship is less understood. Interestingly, recent studies demonstrated a role for chromatin remodeling factors in the repression of *KNOX1* genes by AS1-AS2 in Arabidopsis. For example, AS1 interacts with the histone deacetylase HDA6 and increased acetylation of *KNOX1* genes has been detected in *hda6* mutants (Luo *et al*., 2012). In addition, it has recently been shown that the AS1-AS2 complex recruits POLYCOMB-REPRESSIVE COMPLEX 2 (PRC2), a complex involved in chromatin structure modification, to the promoters of two *KNOX1* genes, likely determining their repression at later stages of leaf development (Lodha *et al*., 2013).

Following initiation, the leaf primordium undergoes lamina growth, morphogenesis and differentiation associated to a precocious establishment of leaf dorsiventrality (i.e. the juxtaposition of abaxial and adaxial tissues). The establishment of leaf dorsiventrality which involves the commitment of abaxial and adaxial cell fate and underpins functional specialization of the upper and lower side of the leaf. Many genes are involved in this commitment working in both cooperative and antagonistic way. For example, a relevant role is played by *AS1* and *AS2* genes that are expressed through the leaf primordium at early stage when the leaf develops. AS2 localizes to the adaxial side while AS1 is confined to the inner regions between the adaxial and abaxial domains. Both promote adaxial fate by repressing the abaxial promoting factors. Moreover, a balance between transient cell proliferation, which underlies growth and morphogenesis and differentiation, which requires repression of meristematic status, is

essential during leaf blade formation. An overlapping set of genes and antagonistic transcription factors are involved in controlling also these processes (Bar and Ori, 2014).

Therefore, very complex genetic frameworks and signaling machinery are at the base of plant development which requires a precise temporal and spatial regulation of regulatory genes. Moreover, the plants are sessile organisms, constantly exposed to the environmental cues. Therefore, a rapid modulation of gene expression is also essential to adapt themselves to environmental changes. In this context, epigenetic mechanisms which act at the transcriptional or post-transcriptional level can play a relevant role.

Accordingly, there are evidences that DNA methylation, together with other epigenetic marks, is involved in the regulation of gene transcriptional activity in response to both endogenous developmental factors and external stimuli (Finnegan *et al*., 1993 ; Dennis *et al*., 1998; Bitonti *et al*., 2002; Fojtova *et al*., 2003; Greco *et al*., 2012). Moreover, through novel dissection methods, such as laser-capture microscopy (Kerk *et al*., 2003; Nakazono *et al*., 2003) combined with highly sensitive detection of DNA or chromatin modifications at target loci, it has been demonstrated that the root and shoot tissues of Arabidopsis accumulate significant epigenetic changes which accompany the transcriptional reprogramming associated with the development of roots and shoots. A recent comparative analysis about DNA methylation in shoot and root revealed that sites that are differentially methylated are preferentially hypermethylated in shoots compared with roots (Widman *et al*., 2013). Hence, epigenetic differences between shoots and roots in Arabidopsis reveals tissue-specific regulation.

1.2.5 DNA methylation-defective mutants of *Arabidopsis thaliana.*

During the past decade, the most widely used and easy experimental organism for studies in molecular genetics, has been the small *Arabidopsis thaliana.* Despite, Arabidopsis is not an economically important plant, it has been a model to study a broad range of problems in development, metabolism, genetics, environmental adaptation, pathogen interactions, and many other areas.

Arabidopsis thaliana is a member of the Cruciferae (family Brassicaceae, Capparales). The genus *Arabidopsis* contains about ten species that are native to

Eurasia, North Africa and North America (Mitchell-Olds, 2001). World map showing the geographical distribution (longitude, latitude, elevation) of more than 30 Arabidopsis ecotypes (Fig. 6).

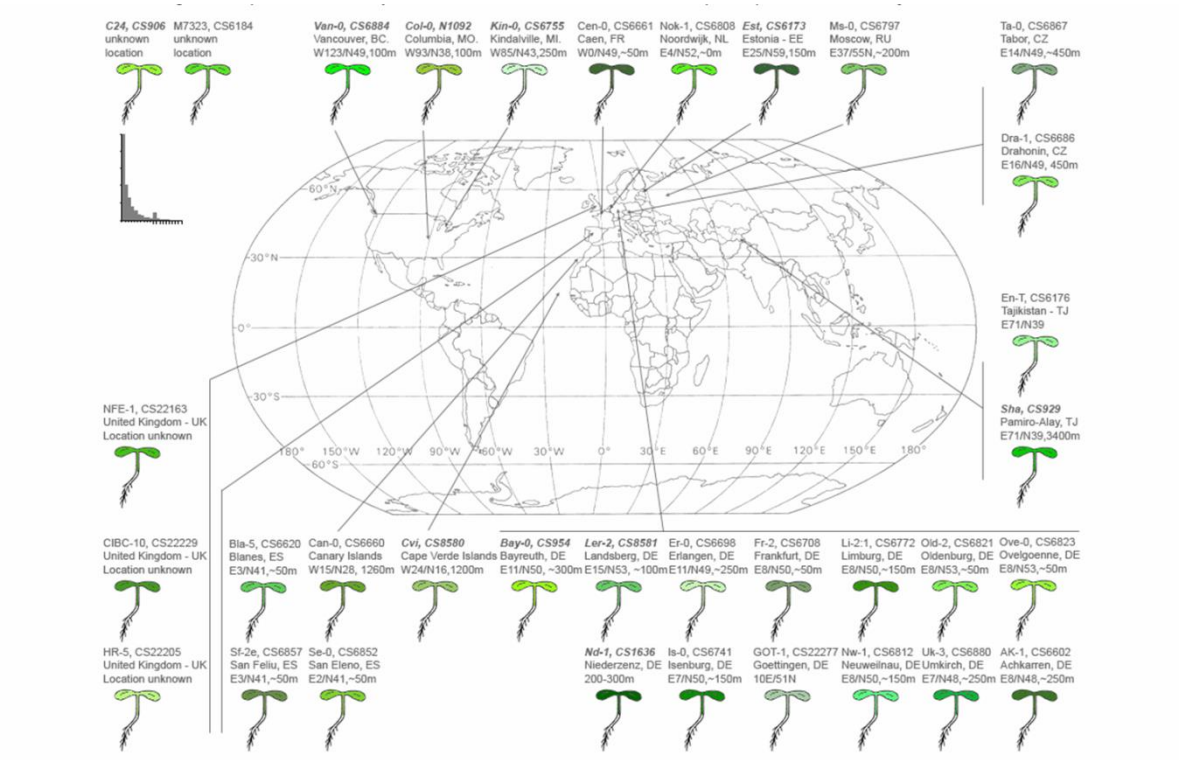

Figure 6. Image of worldwide distribution of *Arabidopsis thaliana* (Jonathan Clarke, 1993).

Arabidopsis thaliana has been for many plant scientist the organism of choice as model system presenting many advantages: it is easily manipulated indeed, it can be grown in confined laboratory environments; it has a rapid life cycle of about 6 weeks from germination to mature seed and a very prolific seed production. Furthermore one advantage offered to the plant researcher by Arabidopsis is its relatively small genome size (135 Mb approximately divided in five chromosomes). It is know that the large crop genomes pose challenges to the researcher, including difficulty in sequencing as well as in isolation and cloning of mutant loci. The entire Arabidopsis genome has been completely sequenced and it represents a powerful tool for studying the function and the identity of more than 27000 protein coding genes. Arabidopsis plants are found to be easily transformable with the current technologies. Finally, the large collections of *Arabidopsis thaliana* mutant alleles are the most important resource for in vivo characterization of gene function.

This large collection includes mutants affected in the establishment, maintenance or removal of DNA methylation. The plant research community has employed, for long time, these mutants in order to provide information about the functional aspect of this epigenetic modification in the plant genome. One of these mutant is the loss-of-function *met1* mutant. As above mentioned, MET1 protein is responsible for maintaining cytosine methylation throughout the Arabidopsis genome. In the *met1* mutants a reduction of global cytosine methylation levels, particularly at CG sites, was observed (Finnegan *et al*. 1996; Ronemus *et al*. 1996) together with developmental abnormalities in both vegetative and reproductive structures. Seedlings from the T2 and subsequent generations had decreased stature, smaller rounded leaves, leaves with margins curled toward the upper leaf surface, decreased fertility, reduced apical dominance and shorter roots (Finnegan *et al*. 1996). A large class of endogenous genes has been described with CG methylation in their ORFs and promoter region. The promoter of *FLOWERING WAGENINGEN* (*FWA*) is normally methylated within two direct repeats causing *FWA* expression to be silenced. It has been verified that the *met1* mutation causes *FWA* demethylation and missexpression resulting in a dominant late-flowering phenotype (Soppe *et al*., 2000). Similar abnormalities were observed in methylation-deficient Arabidopsis lines with defects in either the *SWI2/SNF2*chromatin remodeling factor-related gene *DDM1* (Kakutani *et al*., 1996) or the Dnmt1-related *MET1* gene (Finnegan *et al*., 1996; Ronemus *et al*., 1996).

Other loss-of-function mutants, *drm1* and *drm2*, deals with *DRM1* and *DRM2* genes whose encoded product may be responsible for methylation of cytosines in inverted repeat transgenes at both CHG and CHH sites (Cao and Jacobsen, 2002a) and together with CMT3 maintains the non-CG methylation in Arabidopsis. Additional mutant are *cmt2* and *cmt3*. Actually, the Arabidopsis genome contains three CMT-encoding genes. *CMT1* is preferentially expressed in flowers and the extraordinarily low presence of its mRNA in *Arabidopsis thaliana* plants made it impractical to obtain full-length cDNA using standard protocols. Molecular characterization of *CMT1* genomic and cDNA sequences revealed that CMT1 protein is truncated in several Arabidopsis ecotypes (Henikoff and Comai, 1998). *CMT2* is expressed and is a putative DNA methyltransferase. Recently a whole-genome methylation profiling in *cmt2* mutant showed loss of CHH methylation predominantly at large TEs that were heterochromatic (Stroud *et al*., 2014). CMT3 is the main methyltransferase of the CMT family and is involved in CHG DNA methylation. *Cmt3* loss-of function mutants showed a genome-wide loss of CHG methylation (Lindroth *et al*., 2001).

The *drm1*, *drm2* and *cmt3* single mutants did not show any apparent phenotypes, as well as *drm1 drm2* double homozygotes showed a morphology similar to the wild-type WS strain, even after five generations of inbreeding (Cao and Jacobsen, 2002a, 2002b). Whereas the triple *drm1 drm2 cmt3* mutant evidenced pleiotropic phenotypic abnormalities, dealing with plant size, leaf shape and seed production (Cao and Jacobsen, 2002a; Chan *et al*., 2006; Bruno *et al*., unpublished data)

1.3 Aim of the work.

The overall aim of this thesis was to extend the knowledge about the DNA methylation and its role in the modulation of the plant growth and development.

As already mentioned plant development relies on very complex signaling machinery and genetic networks which requires a temporal and spatial regulation of regulatory genes. Moreover, since plants are sessile organisms, they developed a surprising growth plasticity to achieve adaptive traits under environmental pressure.

In this context, DNA methylation, which controls gene expression together with other epigenetic events, may represent a dynamic mechanism of adaptation, through a rapid and simultaneous modulation of genetic pathways.

The main objective of the present PhD project was to identify genetic networks and metabolic pathways that are affected as consequence of the altered DNA methylation pattern taking advantage DNA methylation-defective mutants of *Arabidopsis thaliana*.

Preliminary data, obtained through visual and microscopic observations carried out by the Plant Biology group at the University of Calabria, indicated the *drm1 drm2 cmt3* triple DNA methylation mutant, defective in three genes that encode for methyltransferases, was the most interesting subject to bring our attention because conversely than the single mutants *drm1*, *drm2*, *cmt3* and the double mutant *drm1 drm2* it showed visible developmental defects compared to the wild type.

Starting from these assumptions, in this project we wanted to investigate about novel growth disorders in DNA methylation triple mutant and elucidate the correlation between DNA methylation status and specific genetic and/or hormonal pathways.

CHAPTER 2: MATERIALS AND METHODS

2.1 Plant lines.

A triple DNA methylation mutant of *Arabidopsis thaliana*, created by crossing (as reported in Henderson and Jacobsen, 2008) single T-DNA homozygous mutant lines of *drm1-2* (SALK_021316; At5g15380), *drm2-2* (SALK_150863; At5g14620) and *cmt3-11* (SALK_148381; At1g69770), was purchased from Nottingham Arabidopsis Seed collection (http://arabidopsis.info) and it was a pure mutant line for each locus where the T-DNA was inserted as reported in the paragraph 3.4 of the result chapter. *drm1 drm2 cmt3* *drm1 drm2 cmt3* triple mutant is in Columbia (Col-0) background. Seedlings of Col-0 were used as control for the comparison.

2.2 Seeds sterilization and *In vitro* plant growth conditions.

Arabidopsis thaliana ecotype Columbia-0 and the mutant seeds were sterilized separately in 70% Ethanol (EtOH) for 2 minutes then in 5% bleach and 0.05% Tween20 for 10 minutes and washed in water for five times for 5 minutes. After sterilization seeds were sown in Petri dishes containing growth medium. In this study MS medium (Murashige and Skoog, 1962) was used including vitamins (Glycine 2 mg/l, myo-Inositol 100 mg/l, Nicotinic acid 0,5 mg/l, Pyridoxine HCl 0,5 mg/l, Thiamine HCl 0,1 g/l), 1% sucrose, 0,1 g/l myo-inositol, 0,5g/l 2-N-morpholine ethane sulphonic acid (MES), 8 g/l agar. The pH was set to 5,7 with KOH 1N.

After 2 days of stratification at 4 °C Petri dishes were transferred in the growth chamber in 16h/8 (day/night) with white light (neon fluorescent tubes “Radium NL Spectralux, cool white”), 100 µmoles m^{-1} s^{-1} light intensity, and 21°C, and 50% relative humidity.

For germination experiments the seeds were sterilized, sown in Petri dishes on MS medium, stratified and transferred in the growth chamber as described above. One-hundred seeds of Col-0 and one-hundred seeds of *drm1 drm2 cmt3* from different batches were sown in the same Petri dish. Observations were performed every day to check the germination status of the seeds. The results are from three independent repeats.

For exogenous IAA treatment seeds of Col-0 and mutant were sterilized and sown in Petri dishes containing growth medium (see materials and methods paragraph 2.2) supplemented with 0.02, 0.2, 1 µM IAA concentration. After 2 days of stratification at 4 °C Petri dishes were transferred in the growth chamber in 16h/8 (day/night) with white light (neon fluorescent tubes, cool white), 100 µmoles m^{-1} s^{-1} light intensity, and 21°C, and 50% relative humidity. Six days old seedlings were photographed and imaging analysis was carried out by Image J software (https://imagej.nih.gov/ij/). The obtained data of three biological replicates (n=30) were used for statistical analysis of the mean and standard deviation and Student's t-test.

The study of aerial part of the plant was carried out on 15 days old seedlings transferred from MS medium to Jiffy-7 Pellets and grown in growth chamber in the same conditions as above. Observations were performed periodically and every stage was photographed in order to catch difference between wild type and mutant.

2.3 Molecular characterization of T-DNA insertion mutant in the *DRM1*, *DRM2* and *CMT3* genes in the triple mutant.

Wild type ecotype Columbia-0 and *drm1 drm2 cmt3* insertion T-DNA line were obtained from the European Arabidopsis Stock Centre (NASC). Triple mutant generated by crossing *drm1* (SALK_021316), *drm2* (SALK_150863) and *cmt3* (SALK_148381) plants; individual mutants are confirmed lines isolated from original SALK lines and are homozygous for the insertion. To screen for homozygous insertion alleles in *drm1 drm2 cmt3* triple mutant, primers were designed following the instructions of the Salk institute genomic analysis laboratory (http://signal.salk.edu/tdnaprimers.2.html). PCR were performed by using complementary primers to the region flanking the T-DNA insertions site in *DRM1*, *DRM2* and *CMT3* genes and a primer (LBb1.3) complementary to the T-DNA sequence (Tab. 1) in order to detect the insertion within the gene. For general PCR the Taq DNA polymerase (Promega) was used. The reaction mixes were prepared in a sterile nuclease-free 0,2 ml microcentrifuge tubes with following components:

5x Reaction Buffer (1,25 mM $MgCl_2$)	**10 µl**
10 mM dNTPmix	1 µl
10 µM Primer forward	1 µl
10 µM Primer backward	1 µl
5U/µl DNA Polymarase	0,25 µl
50 ng totDNA	X µl
nuclease-free water	To 50 µl

PCR was performed on a Primus 96 Plus Thermal Cycler (MWG Biotech) using the following program:

	Step 1	**Step 2**			**Step 3**	**Step 4**
Temperature	95°C	95°C	55-60°C	72°C	72°C	4°C
Time	2 min	40 sec	40 sec	1-3 min	5 min	∞
Cycles	1x	35x			1x	

Table 4: List of primers and PCR conditions used for genotyping.

Locus	**Name**	**Sequence**
	LBb1.3	5'-ATTTTGCCGATTTCGGAAC-3'
AT5G15380	SALK_021316(DRM1)LP	5'-GAGCCGTCTCATCAAACTGAC-3'
AT5G15380	SALK_021316(DRM1)RP	5'-TTGCAGGAGCAAATATGGAAC-3'
AT5G14620	SALK_150863(DRM2)LP	5'-AGATCGCTTCCAGAGTTAGCC-3'
AT5G14620	SALK_150863(DRM2)RP	5'-TTGTCGCAAAAAGCAAAAGAG-3'
AT1G69770	SALK_148381(CMT3)LP	5'-CCCTCAACAATTAACTGACGC-3'
AT1G69770	SALK_148381(CMT3)RP	5'-ATAAGAGAAGGAGCTGCTGCC-3'

2.4 Root analysis.

For root analysis seeds of wild type (Col-0) and *drm1 drm2 cmt3* triple mutant were sterilized and sown together (4 seeds Col-0 and 4 seeds triple mutant) on MS medium in square plates (12 x 12 cm). After 2 days of stratification the plates were placed in vertical position in the growth chamber under continuous light condition with

white light (neon fluorescent tubes "Radium NL Spectralux, cool white"), 100 µmoles m^{-1} s^{-1} light intensity, and 21°C, and 50% relative humidity. Four seeds of Col-0 and four seeds of *drm1 drm2 cmt3* from different batches were sown in the same Petri dish (in total 12 plates). Primary root length was marked every 2 days for 12 days, the plates were randomized in the incubator and images of the plates have been acquired by scanner.

Root length was determined with Image J software by calculating the distance between successive marks along the root axis. The obtained data of three biological replicates (n=45) were used for statistical analysis of the mean and standard deviation and Student's t-test.

Lateral root investigations were carried out in 12 days old seedlings grown in square plates (12 x 12 cm) in vertical position under continuous light condition as previously described. Single plants were observed by stereomicroscope (Leica IC80 HD), the number of lateral roots were counted and the images of the plates have been acquired by scanner. Primary root length was measured with Image J software. Lateral root density was calculated by dividing the number of lateral roots by the primary root length for each root. The obtained data of three biological replicates (n=45) were used for statistical analysis of mean, standard deviation and t-test.

2.5 Morphometric analysis of the primary root.

Seedlings (n=45) were grown in square plates (120 x 120 mm) in vertical position on MS medium and growth conditions as previously described. After 6 days the plates were scanned and primary root length was measured as already mentioned above. Root deviation angle (β), horizontal growth index (HGI), vertical growth index (VGI) and straightness (Grabov *et al*., 2005) were measured. The obtained data were used for statistical analysis of mean, standard deviation and two-tailed t-test.

$$HGI = \frac{Lx}{L}$$

$$VGI = \frac{Ly}{L}$$

$$Straightness = \frac{length\ of\ chord\ connecting\ base\ and\ apex\ of\ primary\ root}{L}$$

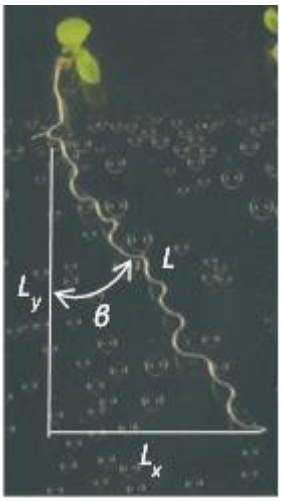

2.6 RNA extraction.

Six seedlings of Columbia-0 and six of *drm1 drm2 cmt3* were grown in round Petri dishes (140 x 20 mm) for 21 days in long day condition, light intensity, temperature and humidity as already described.

Whole seedlings of the same genotype were pooled, frozen with liquid nitrogen and grinded with mortar and pestle. About 100 mg of tissue powder were transferred in 2 ml microcentrifuge tube for RNA isolation by using Kit RNeasy Plant Mini Kit (RNA isolation and cleanup) (QIAGEN). 450 µl of RLT buffer (extraction buffer provided by Qiagen kit) were added in the 2 ml microcentrifuge tube and vortexed vigorously. Previously 10 µl of β-mercaptoethanol were added at each ml of RLT buffer used. The lysate was transferred in QIAshredder spin column (lilac) placed in a 2 ml collection tube and centrifuged at 14.000 rpm (full speed) for 2 minutes. The supernatant of the flow-through was transferred in a new microcentrifuge tube without disturbing the cell-debris pellet in the collection tube. The supernatant was precipitated by adding 0,5 volume of ethanol (96–100%) and mixed immediately by pipetting. The sample (usually 650 µl), including any precipitate that may have formed, was transferred to an RNeasy spin column (pink) placed in a 2 ml collection tube (supplied in the kit) and centrifuged at 10.000 rpm for 15 seconds. To wash the spin column membrane 350 µl Buffer RW1 were added and then the sample was centrifuged at 10.000 rpm for 15 seconds. To

eliminate DNA contamination on column DNase digestion (RQ1 RNase-Free Dnase, Cat. Nr. M6101) was performed. A mix containing 8 µl of RQ1 buffer, 8 µl DNase (8 unit) and 64 µl of RNase free water previously prepared, was added directly on the membrane of the RNeasy spin column (pink) and incubate at room temperature for 15 minutes. To wash the spin column membrane 350 µl Buffer RW1 were added and then the sample was centrifuged at 10.000 rpm for 15 seconds. To purify the RNA 500 µl Buffer RPE were added and then the sample was centrifuged at 10.000 rpm for 15 seconds. Three additional washing with 500 µl, 350 µl and 300 µl were carried out. In order to remove residual ethanol which may interfere with downstream reactions a centrifugation at full speed for 1 minute was applied. The RNeasy spin column was transferred into a new 1,5 ml collection tube (supplied) and 30 µl RNase-free water were added directly on the spin column membrane and the sample was centrifuged at 10,000 rpm for 1 minute to elute the RNA. The integrity of extracted RNA was assayed through electrophoresis on agarose gel (1%) and the concentration was determined by Nanodrop (ND-1000).

2.7 Single strand cDNA synthesis.

First-strand cDNA synthesis was performed by SuperScript™ III Invitrogen USA. A reaction mix containing 1 µg of total RNA, 1 µl of oligo$(DT)_{20}$ (50 µM), 1 µl of 10 mM dNTPmix and DEPC-treated water up to 10 µl was incubated at 65 °C for 5 minutes and then on ice for at least 1 minute. The following cDNA Synthesis mix containing 2 µl 10x RT buffer, 4 µl 25 mM $MgCl_2$, 2 µl 0,1 M DDT, 1 µl RNaseOUT (40 U/µl) and 1 µl SuperScript™ III RT (200 U/µl) was added to the previous reaction mix and incubated at 50 °C for 50 minutes. The reaction was terminated at 85 °C for 5 minutes then the sample was chilled on ice. Any residual RNA was digested by adding 1 µl of RNase H and incubate at 37 °C for 20 minutes.

2.8 Quantitative Reverse Transcriptase Polymerase Chain Reaction (qRT-PCR).

Specific primers complementary to the coding sequence of selected genes were designed by using Primer-BLAST (http://www.ncbi.nlm.nih.gov/tools/primer-blast/index.cgi?LINK_LOC=BlastHome). The reaction mix were prepared by JANUS

Automated Workstation (Perkin Elmer) in 384-well plates with 2,5 µl Power SYBR® Green PCR Master Mix (Roche), 0,5 µl of cDNA and 2 µl each primer (0,2 µM). The reactions were run in a LightCycler 480 machine (Roche Diagnostics) and the conditions of the PCR were: 95°C for 10 minutes followed by 40 cycles at 95°C for 10 seconds and 60°C for 30 seconds. The results of three biological replicates and three technical replicates, were analyzed using the qBase PLUS software (Hellemans *et al*., 2007).

In this study we used for statistical analysis the "Comparative Ct method" also known as the ΔΔCt method, where ΔΔCt = ΔCt [sample]-ΔCt [reference] (Rao *et al*.,2013). In a qRT-PCR assay a positive reaction is detected by accumulation of a fluorescent signal. The Ct (Cycle threshold) is defined as the number of cycles required for the fluorescent signal to cross the threshold. Ct levels are inversely proportional to the amount of target nucleic acid in the sample.

Before the analysis of the data, in qBase PLUS were selected specified parameters such as the reaction efficiency 2,0 and the sample used as control. The expression levels were normalized with CT values obtained using the reference gene *SAND* and *GAPDH* previously tested (Table 9) using the standard curve.

Table 5: Primers used to detect transcripts in different organs of Col-0.

Locus	Name	Primer	Sequence
AT5G15380	DRM1	Forward	5'-AGGGAACTCGTTTCAGGTTGA-3'
AT5G15380	DRM1	Reverse	5'-CCGTACTCGTCCATAAGCCG-3'
AT5G14620	DRM2	Forward	5'-AGCCGAGTTGGTCTTGAAGG-3'
AT5G14620	DRM2	Reverse	5'-CTCTCATCCTCGCACGTACC-3'
AT1G69770	CMT3	Forward	5'-AAACTCTTTGGCCCACCCAA-3'
AT1G69770	CMT3	Reverse	5'-TCTTTCCCAACTGCGAGTCC-3'

Table 6: Primers used to detect transcripts up-stream and down-stream of the T-DNA insertion in the mutant and wild type.

Locus	Name	Primer	Sequence
AT5G15380	DRM1 upstream	Forward	5'-CGGCAAGCACTGAAGCTAGT-3'
AT5G15380	DRM1 upstream	Reverse	5'-GCATTCGTGATCTCTCCCACA-3'
AT5G15380	DRM1 downstream	Forward	5'- AGCGTTGATCAAAATGGGCT -3'
AT5G15380	DRM1 downstream	Reverse	5'- TGCCATCTGAGCTGCACAA -3'
AT5G14620	DRM2 upstream	Forward	5'-GGGTAAAAACAAAGCTGCCCC-3'
AT5G14620	DRM2 upstream	Reverse	5'-CGCTCAGTTCTACTCATGCC-3'
AT5G14620	DRM2 downstream	Forward	5'-AGCCGAGTTGGTCTTGAAGG-3'
AT5G14620	DRM2 downstream	Reverse	5'-CTCTCATCCTCGCACGTACC-3'
AT1G69770	CMT3 upstream	Forward	5'-GAGCTGCTGCCATATCAGAGA-3'
AT1G69770	CMT3 upstream	Reverse	5'-CACAGCCGGAGTAAAGGTCA-3'
AT1G69770	CMT3 downstream	Forward	5'-AAACTCTTTGGCCCACCCAA-3'
AT1G69770	CMT3 downstream	Reverse	5'-TCTTTCCCAACTGCGAGTCC-3'

Table 7: Primers used in qRT-PCR for auxin related genes.

Locus	Name	Primer	Sequence
AT1G73590	PIN1	Forward	5’-CTTCTTATGCCGTTGGCCTC-3’
AT1G73590	PIN1	Reverse	5’-CACCGCAGTGCTAAGAATGTC-3’
AT5G57090	PIN2	Forward	5’- CGTGCGGAAAATCAGTAGCAG-3’
AT5G57090	PIN2	Reverse	5’- TTCCTTGAGGAAGAGCAGCC-3’
AT1G70940	PIN3	Forward	5’-GTTTGCCATGGCGGTTAGGT-3’
AT1G70940	PIN3	Reverse	5’-CGCAAACACAAAGGGCACAA-3’
AT2G01420	PIN4	Forward	5’-GCGACCTTCTCCGTATAGCC-3’
AT2G01420	PIN4	Reverse	5’-ACCCCAGTGCTTAGAATCGTG-3’
AT1G23080	PIN7	Forward	5’- ATTGCGTGTGGCCATTGTTC-3’
AT1G23080	PIN7	Reverse	5’- CCTGTACTCAAGATTGCGGGA-3’
AT5G20730	ARF7	Forward	5’- GATCTAGCGCGCATGTTTGG-3’
AT5G20730	ARF7	Reverse	5’- TTCTTCCCATGGATCATCGC-3’
AT2G21050	LAX2	Forward	5’- GACTGGGGCATTCACGATCA
AT2G21050	LAX2	Reverse	5’- GGTGAAGAGGCCAAAGGTGT-3’
AT1G77690	LAX3	Forward	5’- ATTCGTAGTTGGGTTCGGGT-3’
AT1G77690	LAX3	Reverse	5’- CATGGCTTGTGAGGAGGGC-3’
AT5G20820	SAUR76	Forward	5’- GCCGAACACGGAGGACATA-3’
AT5G20820	SAUR76	Reverse	5’- CAAGACAACTTCGCACGACA-3’
AT1G23160	GH3	Forward	5’- TAAAAGTGGTGCGTCAAGGG-3’
AT1G23160	GH3	Reverse	5’- TGTGGCTACCACATTTTCCTCT-3’
AT3G23030	IAA2	Forward	5’- AAGGATCTGGATTTGTACCAACA-3’
AT3G23030	IAA2	Reverse	5’- GAGTCTAGAGCAGGAGCGTC-3’
AT1G04240	IAA3	Forward	5’- TGTTCAAATTCTCTGTGGGAGA-3’
AT1G04240	IAA3	Reverse	5’- CCATGGAACATCACCAATGAGC-3’
AT4G32540	YUCCA1	Forward	5’- TCCTAACGGCTGGAGAGGAG-3’
AT4G32540	YUCCA1	Reverse	5’- CCTGGTGGACCCCTTGATTT-3’
AT4G13260	YUCCA2	Forward	5’-GGCGAAAGCGGATTGTATGC-3’
AT4G13260	YUCCA2	Reverse	5’- ACAATGTTGAGGACGAGCCAA-3’
AT1G70560	TAA1	Forward	5’- TGGCTAGGGACGAAGGAAGA-3’
AT1G70560	TAA1	Reverse	5’- GCTGACTCGGACATGCTTCT-3’

Table 8: Primers used in qRT-PCR for leaf development genes.

Locus	Name	Primer	Sequence
AT2G37630	AS1	Forward	5’-AGGGGGACTTGTGTTAGGGA-3’
AT2G37630	AS1	Reverse	5’-GTGCCCTTCCTCCAACTCTC-3’
AT1G65620	AS2	Forward	5’-TACGACGGTGGGATTCTTGC-3’
AT1G65620	AS2	Reverse	5’-GATCAACAGTACGGCGACCA-3’
AT1G62360	STM	Forward	5’-CTTGATTGGTGGAGCCGTCA-3’
AT1G62360	STM	Reverse	5’-ATCTGTTTCTGGTCCAGCCC-3’
AT1G26770	EXP10	Forward	5’-CGGCGATCAAGGGTTCAAGA-3’
AT1G26770	EXP10	Reverse	5’-TCGCTGGTGGTGACCTTAAA-3’
AT2G23380	CLF	Forward	5’-TTGCTGCAGATCGGGAATGT-3’
AT2G23380	CLF	Reverse	5’-TATCGCCTCTTTGGCTTGGG-3’
AT4G08150	KNAT1	Forward	5’-TTCTCACGTGGTGGGAGTTG-3’
AT4G08150	KNAT1	Reverse	5’-GTTGATTCCGCCAACGCTAC-3’

AT1G70510	KNAT2	Forward	5'-ATGACCGCGATCTGAAGGAC-3'
AT1G70510	KNAT2	Reverse	5'-GCAACGCTTGTCTTGCTTCT-3'
AT1G23380	KNAT6	Forward	5'-ACGAGGAACTGAGTGGAGGT-3'
AT1G23380	KNAT6	Reverse	5'-AGGTCCCGGTCTTCACATCT-3'
AT4G18390	TCP2	Forward	5'-CATCAGGTGGTGGCTTCAGT-3'
AT4G18390	TCP2	Reverse	5'-AACTGTGGACCTCCTCCACT-3'
AT3G15030	TCP4	Forward	5'-TACAGGAAACGGAGGAGGGT-3'
AT3G15030	TCP4	Reverse	5'-GCCAAGAACTGGCTGAAACG-3'
AT1G19270	DA1	Forward	5'-GGCAATGTGAAGTTACCGCC-3'
AT1G19270	DA1	Reverse	5'-TTTGAGCCTCATCCACGCAT-3'
AT1G14920	DELLA	Forward	5'-GGTCCTCCTGTTTTCCGGTT-3'
AT1G14920	DELLA	Reverse	5'-GAGCCAGCTTACACCCAACT-3'
AT4G29040	RPT2a	Forward	5'-CACTCAGGAGGTGAACGTGA-3'
AT4G29040	RPT2a	Reverse	5'-AATCCGTCCAGGTCGAAGC-3'
AT1G25540	MED25	Forward	5'-TTTCGGGCCATGAGTCAACA-3'
AT1G25540	MED25	Reverse	5'-AGAAGCGTCTGTGATGGCAA-3'
AT2G45210	SAUR36	Forward	5'-GGCCAACGTCTCAAGCAAAG-3'
AT2G45210	SAUR36	Reverse	5'-CAGTCGCCGTCTTTTTGACC-3'

Fourteen possible reference genes were tested (table 9) (Czechowski *et al*., 2005) and among them *SAND (MONENSIN SENSITIVITY1*) and *GAPDH (GLYCERALDEHYDE-3-PHOSPHATE DEHYDROGENASE)* were selected to normalize the results obtained by qBasePLUS.

Table 9: Primers list of reference genes in qRT-PCR.

Locus	Name	Primer	Sequence
AT5G08290	YLS8	Forward	5'-TTACTGTTTCGGTTGTTCTCCATTT-3'
AT5G08290	YLS8	Reverse	5'-CACTGAATCATGTTCGAAGCAAGT-3'
AT3G53090	UBQT	Forward	5'-TTCAAATACTTGCAGCCAACCTT-3'
AT3G53090	UBQT	Reverse	5'-CCCAAAGAGAGGTATCACAAGAGACT-3'
AT4G34270	TIP41	Forward	5'-GTGAAAACTGTTGGAGAGAAGCAA-3'
AT4G34270	TIP41	Reverse	5'-TCAACTGGATACCCTTTCGCA-3'
AT2G28390	SAND	Forward	5'-AACTCTATGCAGCATTTGATCCACT-3'
AT2G28390	SAND	Reverse	5'-TGATTGCATATCTTTATCGCCATC-3'
AT3G01150	PTBP	Forward	5'-GATCTGAATGTTAAGGCTTTTAGCG-3'
AT3G01150	PTBP	Reverse	5'-GGCTTAGATCAGGAAGTGTATAGTCTCTG-3'
AT1G62930	PPR	Forward	5'-AAGACAGTGAAGGTGCAACCTTACT-3'
AT1G62930	PPR	Reverse	5'-AGTTTTTGAGTTGTATTTGTCAGAGAAAG-3'
AT1G13320	PP2A	Forward	5'-TAACGTGGCCAAAATGATGC-3'
AT1G13320	PP2A	Reverse	5'-GTTCTCCACAACCGCTTGGT-3'
AT1G13440	GAPDH	Forward	5'-TTGGTGACAACAGGTCAAGCA-3'
AT1G13440	GAPDH	Reverse	5'-AAACTTGTCGCTCAATGCAATC-3'
AT5G15710	FBOX	Forward	5'-TTTCGGCTGAGAGGTTCGAGT-3'
AT5G15710	FBOX	Reverse	5'-GATTCCAAGACGTAAAGCAGATCAA-3'
AT5G46630	CA	Forward	5'-TCGATTGCTTGGTTTGGAAGAT-3'
AT5G46630	CA	Reverse	5'-GCACTTAGCGTGGACTCTGTTTGATC-3'

AT4G26410	AT4G26410	Forward	5'-GAGCTGAAGTGGCTTCCATGAC-3'
AT4G26410	AT4G26410	Reverse	5'-GGTCCGACATACCCATGATCC-3'
AT4G33380	AT4G33380	Forward	5'-TTGAAAATTGGAGTACCGTACCAA-3'
AT4G33380	AT4G33380	Reverse	5'-TCCCTCGTATACATCTGGCCA-3'
AT5G12240	AT5G12240	Forward	5'-AGCGGCTGCTGAGAAGAAGT-3'
AT5G12240	AT5G12240	Reverse	5'-TCTCGAAAGCCTTGCAAAATCT-3'
AT2G32170	AT2G32170	Forward	5'-ATCGAGCTAAGTTTGGAGGATGTAA-3'
AT2G32170	AT2G32170	Reverse	5'-TCTCGATCACAAACCCAAAATG-3'

2.9 Rosette area and leaf series.

Rosette area was obtained in 21 days old plants (n=39) grown on MS medium prepared as above in round Petri dishes (140 x 20 mm), in long day condition. The plates were photographed and the rosette area of 35 seedlings per genotype (Col-0 and *drm1 drm2 cmt3*) was measured with Image J software.

Fifteen seedlings from the same plates were selected for leaf series. Leaves of mutant and wild type were placed on large square plates containing 1% plant tissue agar in distilled water and incisions were made to make the leaves fully expanded when necessary. The plates were photographed and the area was measured with Image J software.

All the measurements were subjected to statistical analysis of the mean, standard deviation and two-tailed t-test.

2.10 Epidermal cell analysis.

For epidermal cell analysis the leaves were clarified with 100% ethanol overnight at room temperature, then were fixed in 90% lactic acid and mounted on microscope slide. The epidermal cells and stomata of the upper side of the leaves were drawn with a "Leica DMLB microscope" equipped with a drawing tube and differential interference contrast objectives. The cell area was measured with Image J software. Epidermal cell density (a), stomatal density (b), stomatal index (c) and number of cells per leaf (d) were calculated (Hara *et al.*, 2009).

$$(a) \quad epidermal\ cell\ density = \frac{number\ of cells}{total\ area\ measured}$$

$$(b) \quad stomatal\ density = \frac{number\ of\ stomata}{total\ area\ measured}$$

$$(c) \quad stomatal\ index = \frac{stomatal\ density}{stomatal\ density + epidermal\ cells\ density}$$

$$(d) \quad number\ of\ cells\ per\ leaf = \frac{leaf\ area}{average\ cell\ area}$$

The obtained data of fifteen seedlings from each genotype were used for statistical analysis of mean, standard deviation and two-tailed t-test.

2.11 Confocal microscopy analysis.

Seedlings for confocal microscopy analysis were grown in MS medium as already described above. For root meristem analysis, six days old seedlings were fixed in a solution of 50% methanol and 10% acetic acid at 4°C for at least 12 hours. Next tissue were rinsed with water and incubated in 1% of periodic acid at room temperature for 40 minutes. Seedlings were again rinsed with water and incubated in Schiff reagent with propidium iodide (100 mM sodium metabisulphite and 0,15 N HCl; propidium iodide to a final concentration of 100 mg/ml was freshly added) for 1 to 2 hours or until plants were visibly stained. The samples were then transferred onto microscope slides and covered with a chloral hydrate solution (4 g chloral hydrate, 1 ml glycerol, and 2 ml water). Slides were left undisturbed at least 24 hours to allow the mounting solution to set (Truernit *et al.*, 2008).

For pro*DR5:GFP* analysis, embryo harvested from green siliques at different time points after fertilization, four days old seedlings and rosette leaf number three from thirteen days old plants were fixed in paraformaldehyde 4% for 5 minutes. The samples were then transferred onto microscope slides and covered with PBS 1x buffer (NaCl 137 mM, KCl 2,7 mM, Na_2Hpo_4 10 mM, KH_2PO_4 1,8 mM, pH 7,4) and glycerol 1:1.

Confocal visualization samples were imaged using a Leica inverted TCS SP8 confocal scanning laser microscope with a 40x oil immersion objective. The detection of Green Fluorescence Protein (excitation peak centered at about 488 nm, emission peak

wavelength of 509 nm) was performed by combining the settings indicated in the sequential scanning facility of the microscope.

2.12 Methylated DNA Immunoprecipitation (MeDIP).

MeDIP is an immunocapturing approach to enrich DNA that is methylated. The principle is that genomic DNA is randomly sheared by sonication and immunoprecipitated with an antibody that specifically recognizes 5-methylcytidine (5mC).

In this study we used a modified version of the protocol described by Weber and Schübeler (2007) that we optimized.

Seedlings of Col-0 and *drm1 drm2 cmt3* were grown on soil in independent pots under long day light regime. Temperature and humidity conditions are already described above in the paragraph number 2 of this chapter.

Fifteen 13 days old plants of the same genotype were selected and the third and fourth leaf were harvested and pooled, frozen in liquid nitrogen and ground by using mortar and pestle. About 100 mg of tissue powder were transferred in 2 ml microcentrifuge tube for DNA isolation and 500 µl of TE buffer (10 mM Tris-HCl pH 8,0; 1 mM EDTA) were added in the tube. One volume of lysis buffer (20 mM Tris-HCl pH 8,0; 4 mM EDTA; 20 mM NaCl; 1% SDS) containing 33 µl of proteinase K (0,45 mg/ml) was added in the tube and incubated at 55°C for 5 hours inverting the tube now and then. One volume phenol was added and mixed by inverting the tube which was centrifuged at 10.000 rpm for 5 minutes at 4°C. The supernatant was transferred in a new 2 ml microcentrifuge tube. One volume of chloroform was added and mixed by inverting the tube which was centrifuged at 10.000 rpm for 5 minutes at 4°C. The supernatant was transferred in a new 2 ml microcentrifuge tube and 1/10 of the volume of sodium acetate (3 M pH 5,2) and two volumes of Et-OH 100% were added in the tube. After mix by inverting, the tube was stored at -20°C overnight.

The tube was centrifuged at 14.000 rpm for 20 minutes at 4°C. The supernatant was poured off and the residual ethanol was removed by pipet. The pellet was dissolved in 30 µl of TE buffer containing 20 mg/ml RNase A and the tube was incubated one hour at 37°C. After quantification of the DNA concentration by Nanodrop (ND-1000), about 20 µg of gDNA (genomic DNA) were diluted in 400 µl TE buffer and sonicated in SONICS Vibra-cell sonicator with four 15 seconds pulses at 20% amplitude. Twenty µl of

sonicated gDNA, non-sonicated gDNA and 1 Kb Plus DNA Ladder (Invitrogen, Catalog number: 10787018) were loaded on the same 1% agarose gel to assess the quality of the sonication step. The fragments of the sonicated DNA had a mean size between 200 and 1000 base pairs.

The remaining sonicated gDNA was precipitated with 400 mM NaCl, 0,2 mg of glycogen, two volume of Et-OH 100% and stored at -20°C overnight.

The tube was centrifuged at 14.000 rpm for 40 minutes at 4°C. The supernatant was poured off and the residual ethanol was removed by pipet. The pellet was dissolved in 30 µl of water and the DNA concentration was quantified by Nanodop. Four µg of sonicated gDNA were diluted in 900 µl of TE buffer and 45 µl of them (5%) were stored and used as Input sample. The remaining volume was split in two different 1,5 ml microcentrifuge tubes. The sonicated gDNA was denatured for 10 minutes in boiling water and immediately cooled on ice for 10 minutes. Forty-eight µl of 10x IP buffer (100 mM Na-Phosphate pH 7,0; 1,4 M NaCl; 0,5% Triton X-100) were added in the tubes.

One sample is used for immunoprecipitation (IP sample) where the antibody is added. The second sample is the mock sample which does not contain antibody and it is used as the control to account for the unspecific DNA binding (Fig. 7).

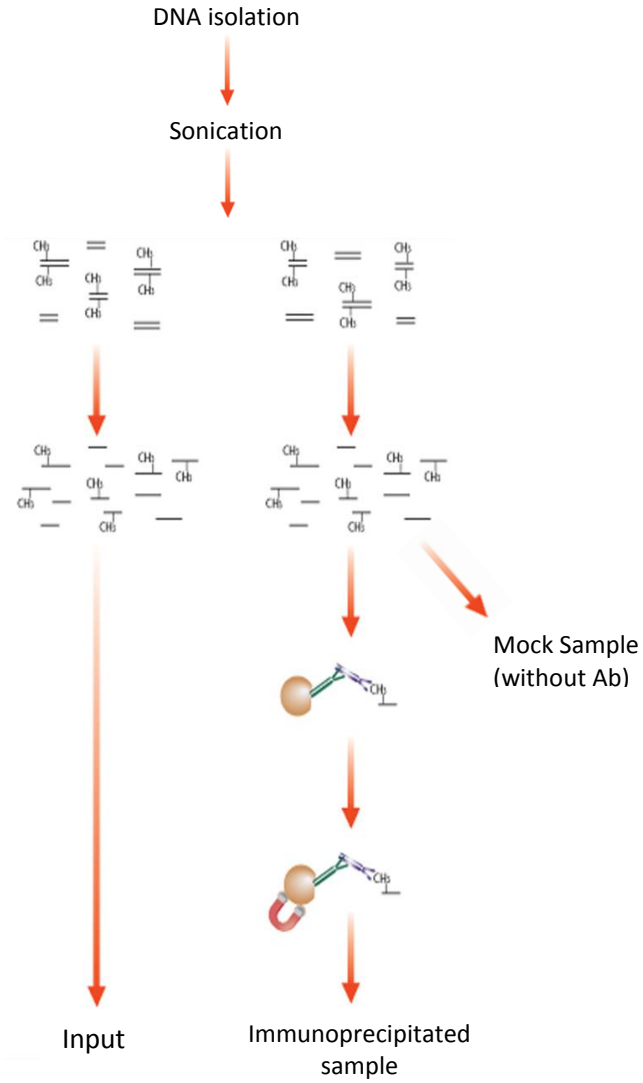

Figure 7: After gDNA isolation and sonication for every gDNA sample there are three samples to analyse: Input, Immunoprecipitated and Mock

In the IP sample were added 2 µl of 5mC Antibody (#BI-MECY 1000 Eurogentec). All the tubes were incubated for 2 hours at 4°C with overhead shaking.

Separately, 40 µl of beads (Dynabeads M-280 Sheep anti-mouse IgG - Dynal Biotech #112.01) were pre-washed with 800 µl of PBS-BSA 0,1% (9 ml PBS; 1 ml BSA 10 mg/ml) for 5 minutes at room temperature with shaking. To collect the beads a magnetic rack was used and an additional washing was carried out. The beads were dissolved in 40 µl of 1x IP buffer and then added to the IP and mock samples which were incubated for 2 hours at 4°C with overhead shaking.

By using the magnetic rack the beads were collected from IP and mock samples and washed with 700 µl of 1x IP buffer for 10 minutes at room temperature with shacking. This washing was repeated for two times.

The beads were dissolved in 250 µl of proteinase K digestion buffer (50 mM Tris-HCl pH 8,0; 10 mM EDTA; 0,5% SDS; 7 µl proteinase K 10 mg/ml) and incubated for 30 minutes at 50°C.

Methylated DNA isolation was carried out by adding 1 volume of phenol and mixing by inverting the tube. The samples were centrifuged at 10.000 rpm for 5 minutes at 4°C. The supernatants were transferred in a new 1,5 ml microcentrifuge tube. One volume of chloroform was added and mixed by inverting the tube which was centrifuged at 10.000 rpm for 5 minutes at 4°C. The supernatants were transferred in a new 2 ml microcentrifuge tube precipitate with 400 mM of NaCl, 0,2 mg of glycogen and two volumes of Et-OH 100%.

The tube was centrifuged at 14.000 rpm for 40 minutes at 4°C. The supernatant was poured off and the residual ethanol was removed by pipet. The pellet was dissolved in 30 µl of sterile water and stored at -20°C until qPCR analysis. To perform the qPCR specific primers were designed complementary to the promoter region and coding region of a set of genes selected for our experiments.

The concentration of each MeDIP sample was measured by Qubit® 2.0 Fluorometer Invitrogen, and analyzed by real-time PCR (Roche LC480). The qPCR was used to compare the amount of immunoprecipitated DNA fragments (methylated) between the IP samples of control and mutant line. To account for differences in the starting material we normalize versus Input samples and to account for differences in

DNA concentration we normalize versus *ACT7 (ACTIN 7)* reference gene which is unmethylated in control and in the triple mutant (Zhang *et al*., 2006). The mock samples is used to check if there is any unspecific binding of DNA to the beads. If the conditions of the experiment are well optimized such unspecific binding does not occur and signals from all mock samples are very low and comparable to background.

To perform the qPCR the specific primers were designed homologous to the promoter region and coding region of a set of genes selected for our experiments.

Table 10: List of primers used for MeDIP assay in the whole plant.

Locus	Name	Primer	Sequence
AT1G53490	HEI10	Forward	5'-GCCCGGGATCGATAGGATCT-3'
AT1G53490	HEI10	Reverse	5'-CTTCGTCAGTCTCTTCGCGG-3'
AT5G09810	ACT7	Forward	5'-CGTTTCGCTTTCCTTAGTGTTA-3'
AT5G09810	ACT7	Reverse	5'-AGCGAACGGATCTAGAGACTC-3'
AT5G57090	PIN2-I	Forward	5'-CCACGAGACAGAAGGTAAACCA-3'
AT5G57090	PIN2-I	Reverse	5'-CCTCGGCATTTTGTGAATGGA-3'
AT5G57090	PIN2-II	Forward	5'-GGTCAACGAGTGGAGCAAGT-3'
AT5G57090	PIN2-II	Reverse	5'-TAGCGAGGTTGTCGTGAGGA-3'
AT5G57090	PIN2-III	Forward	5'-TGGAAATGGACCAAGACGGT-3'
AT5G57090	PIN2-III	Reverse	5'-AGAGACAAGGGACCAAGCAA-3'
AT5G57090	PIN2-IV	Forward	5'-AGTAGCAGGGTTTGCGATGG-3'
AT5G57090	PIN2-IV	Reverse	5'-ACGATGGCGATATGGAGGAG-3'
AT1G23160	GH3-I	Forward	5'-TGTACCTCAATAATGTTTGCGACT-3'
AT1G23160	GH3-I	Reverse	5'-TCCTCGGATCCTCCGAATCA-3'
AT1G23160	GH3-II	Forward	5'-TTCGGAGGATCCGAGGAATTT-3'
AT1G23160	GH3-II	Reverse	5'-TATTGGGAAACGTGTGAAACGA-3'
AT1G23160	GH3-III	Forward	5'-TGGTGCAGTATGTTCCCACA-3'
AT1G23160	GH3-III	Reverse	5'-GTAGGACACGTTGGGCATGA-3'
AT1G23160	GH3-IV	Forward	5'-GGAGACATTCTAGTGGTGACTGG-3'
AT1G23160	GH3-IV	Reverse	5'-GTGTCCCGGGATAGTGGAGA-3'
AT1G23160	GH3-V	Forward	5'-AGACAAGAAGAGCAAAAAGCACA-3'
AT1G23160	GH3-V	Reverse	5'-GTCCCTTGACGCACCACTTT-3'

Table 11: List of primers used for MeDIP assay in leaf.

Locus	Name	Primer	Sequence
AT4G13260	YUCCA2-I	Forward	5'-GGGGCACACGAAAACACTTT-3'
AT4G13260	YUCCA2-I	Reverse	5'-ATCATGCAGGGTCACGTTTT-3'
AT4G13260	YUCCA2-II	Forward	5'-TCGGGTTGGCTAAATTTGGTC-3'
AT4G13260	YUCCA2-II	Reverse	5'-GGATAGGTAGTGGGATGGGC-3'
AT4G13260	YUCCA2-III	Forward	5'-GCCCATCCCACTACCTATCC-3'

AT4G13260	YUCCA2-III	Reverse	5'-TTGGGGAGAGAGAAGCAACT-3'
AT4G13260	YUCCA2-IV	Forward	5'-CAATCATTGTCGGTTCCGGG-3'
AT4G13260	YUCCA2-IV	Reverse	5'-TTTGTGCTGCCATAGTGACG-3'
AT1G70560	TAA1-I	Forward	5'-AGTATACCACAGCTCACCGG-3'
AT1G70560	TAA1-I	Reverse	5'-AGCAAGAAAGTGAAGAGGTTTGT-3'
AT1G70560	TAA1-II	Forward	5'-ATATCGGTCATCAACTCTTCAGT-3'
AT1G70560	TAA1-II	Reverse	5'-TTTCTCGCTACCAAATGCGG-3'
AT1G70560	TAA1-III	Forward	5'-ACACTTCGACCTACACTATTCTC-3'
AT1G70560	TAA1-III	Reverse	5'-ACATGGGGATGTTCTTGTTCG-3'
AT5G20730	ARF7-I	Forward	5'-AATCGTGGCCAGTTTGCTAG -3'
AT5G20730	ARF7-I	Reverse	5'- AAAGGGATGATCAGCGACCA -3'
AT5G20730	ARF7-II	Forward	5'- TCGATTGTCCTTGGTCATCC -3'
AT5G20730	ARF7-II	Reverse	5'- CCGGAGAGACAAACAAAGCA -3'
AT5G20730	ARF7-III	Forward	5'- GTTGAGTGATCATGAAAGCTCCT -3'
AT5G20730	ARF7-III	Reverse	5'- TTCAGGTTCTCAAATCCAGCA -3'

2.13 Chromatin Immunoprecipitation (ChIP).

Chromatin immunoprecipitation (ChIP) is a powerful method for studying interactions between specific proteins and a genomic DNA region. ChIP is often used to determine whether a transcription factor interacts with a candidate target gene and is used to monitor the presence of post-translational modifications at specific genomic locations of the histones. We used this technique to evaluate the H3K27me3 levels in genes that are target of CLF (CURLY LEAF), which has histone methyltransferase activity. This technique was performed by making some changes to protocol of Bowler *et al*. (2004).

Third and fourth leaf from 13 days old seedlings, grown on soil in independent pots in long day photoperiod, were harvested fixed in 1% formaldehyde for 10 minutes (cross-linking) and neutralized by 0,125 M glycine for 5 minutes using the vacuum infiltrations under room temperature. After cross-linking the leaves were washed with cold sterile water, put in liquid nitrogen and ground with mortar and pestle. The sample was incubated in cold Extraction buffer 1 (0,4 M Sucrose; 10mM Tris-HCl pH 8,0; 5 mM β-mercaptoethanol; 0,1 mM PMSF; protease inhibitors (Roche) [2 tablet/100 ml]) on ice for 30 minutes. The sample was filtered in a new falcon tube and centrifuged at 2880xg for 20 minutes at 4°C. The pellet was dissolved in 1 ml of Extraction buffer 2 (0,25 M Sucrose; 10mM Tris-HCl pH 8,0; 10 mM of $MgCl_2$; 1% Triton X-100; 5 mM β-mercaptoethanol; 0,1 mM PMSF; protease inhibitors (Roche) [1 tablet/50 ml]) and

centrifuged at 12.000xg for 10 minutes at 4°C. The pellet was dissolved in 300 µl of Extraction buffer 3 (1,7 M Sucrose; 10mM Tris-HCl pH 8,0; 2 mM of MgCl2; 0,15% Triton X-100; 5 mM β-mercaptoethanol; 0,1 mM PMSF; protease inhibitors Roche [1 tablet/50 ml]). The sample was than overlaid on 300 µl of clean Extraction buffer 3 and centrifuged at 16.000xg for 1 hour at 4°C. The pellet was dissolved in 300 µl of Nuclei Lysis buffer (50mM Tris-HCl pH 8,0; 10 mM EDTA; 1% SDS; 0,1 mM PMSF). A volume of 10 µl has been saved for electrophoresis test (non-sonicated sample). The sample was sonicated in SONICS Vibra-cell sonicator with four 15 seconds pulses at 20% amplitude and stored on ice in cold room. A volume of 30 µl has been used in the following steps for electrophoresis sonication test (sonicated sample). A volume of 500 µl of Eluition buffer (1% SDS; 0,1 M $NaHCO_3$) and 20 µl of 5 M NaCl were added (sonicated and non-sonicated samples) before incubation overnight at 65°C (de-crosslinking step).

Next day a volume of 10 µl 0,5 M EDTA, 40 µl 0,5 M Tris-HCl pH 6,5 and 1 µl of proteinase K (20 mg/ml) was added to the samples before incubation at 45°C for 1 hour. The samples was purified using MINelute PCR Product Purification Kit (Qiagen) according to the manufacturer's protocol. After the purification the samples were loaded on 1% agarose gel to check the proper size comprises between 200 and 1000 base pairs of the sonicated chromatin. A volume of 10 µl of the sonicated DNA has been saved for the Input control.

In parallel, 80 µl of protein A agarose beads (Millipore, 16-157) were washed 3 times with 1 ml of Chip Dilution buffer (1,1% Triton X-100; 10 mM EDTA; 16,7 mM Tris-HCl pH 8,0; 167 mM NaCl; 0,1 mM PMSF; protease inhibitors Roche [1 tablet/50 ml]) and centrifuged at 3800xg for 1 minute at room temperature.

The samples (stored on ice in the cold room) were centrifuged at 16.000xg for 5 minutes at 4°C and the supernatant was transferred to a new tube (low adhesion). Then each sample was divided in two aliquots.

A volume of 900 µl of Chip Dilution buffer and 40 µl of beads were added to the sonicated sample (previously stored on ice in the cold room) and incubated for 1 hour on the rotation wheel at 4°C. The samples were centrifuged at 3800xg for 1 minute, the supernatants of each genotype were transferred in a new tube, they were mixed and then divided in two tubes (2 x 1000 µl in low adhesion tubes). 1000 µl were used for immunoprecipitation (ChIP sample) where 3 µl of Antibody anti H3K27me3 (Millipore, 07-449) were added. The remaining 1000 µl were the mock control (without antibody). The Chip and mock samples were left on the rotation wheel at 4°C, overnight.

Next day 40 µl of beads were washed as described above, added to the ChIP and mock samples and incubated at 4°C on the rotation wheel for 2 hours. The sample was centrifuged at 3800xg for 1 minute at room temperature and the pellet was washed for 10 minute with each solution at 4°C on the rotation wheel using 1 ml of the following solution:

- 1x Low salt buffer (150 mM NaCl; 0,1% SDS; 1% Triton X-100; 2 mM EDTA; 20 mM Tris-HCl pH 8,0);
- 1x High salt buffer (500 mM NaCl; 0,1% SDS; 1% Triton X-100; 2 mM EDTA; 20 mM Tris-HCl pH 8,0)
- 1x LiCl buffer (0,25 LiCl; 1% NP-40; 1% sodium deoxycholate; 1 mM EDTA; 10 mM Tris-HCl pH 8,0);
- 2x TE buffer (10 mM Tris-HCl pH 8,0; 1 mM EDTA).

The pellet was dissolved in 250 µl elution buffer and incubated at 65°C for 15 minutes with agitation. The samples were briefly centrifuged and the supernatant was transferred in a new tube. The elution was repeated once again and the two eluates were combined in the same tube (final volume 500 µl) . To the input sample were added 500 µl of Eution buffer. A volume of 20 µl of 5 M NaCl were added to input, ChIP and mock samples and they were incubated overnight at 65°C.

Next day a volume of 10 µl 0,5 M EDTA, 40 µl 0,5 M Tris-HCl pH 6,5 and 1 µl of proteinase K (20 mg/ml) was added to the samples before incubation at 45°C for 1 hour. DNA was purified using MINelute PCR Product Purification Kit (Qiagen) according to the manufacturer's protocol. Final elution was carried out in 20 µl of elution buffer containing RNaseA (10 µg/ml).

The DNA concentration of each ChIP sample was measured by Qubit® 2.0 Fluorometer Invitrogen, and analyzed by real-time PCR (Roche LC480). The qPCR was used to compare the amount of immunoprecipitated DNA fragments (H3K27me3 enrichment) between the IP samples of control and mutant line. To account for differences in the starting material we normalize versus Input samples and to account for differences in DNA concentration we normalize versus *ACT2* reference gene. The mock samples is used to check if there is any unspecific binding of DNA to the beads. If the conditions of the experiment are well optimized such unspecific binding does not occur and signals from all mock samples are very low and comparable to background.

To perform the qPCR the specific primers were designed homologous to the promoter region and coding region of a set of genes selected for our experiments.

Table 12: List of primers used for ChIP assay.

Locus	Name	Primer	Sequence
AT3G18780	ACT2	Forward	5’-GGCTGAGGCTGATGATATTC-3’
AT3G18780	ACT2	Reverse	5’-CCATGATGTCTTGGCCTACC-3’
AT1G23380	KNAT6-I	Forward	5’-GATGGGTCAATCAACCTGTC-3’
AT1G23380	KNAT6-I	Reverse	5’-ATGAGTTTAGTGCTTCGAAAC-3’
AT1G23380	KNAT6-II	Forward	5’-GTATGTATCAGCTCACTAGTTG-3’
AT1G23380	KNAT6-II	Reverse	5’-GAAGTCGCATATCAGAAGATA-3’
AT1G23380	KNAT6-III	Forward	5’-TACCATCTAAGTGTATTGTCG-3’
AT1G23380	KNAT6-III	Reverse	5’-AGGTCCAAGGCTGTGTTATGA-3’
AT1G23380	KNAT6-IV	Forward	5’-TCTCTCTACACACTCCCATAG-3’
AT1G23380	KNAT6-IV	Reverse	5’-GTATAAGATCTCCGGTAAGAAC-3’
AT1G23380	KNAT6-V	Forward	5’-GCGATTTAGAAGACGGAGGA-3’
AT1G23380	KNAT6-V	Forward	5’-GAATAATCACCGGCCGAAT-3’
AT1G23380	KNAT6-VI	Reverse	5’-GTGGTTAGTTCTGAATGATT-3’
AT1G23380	KNAT6-VI	Forward	5’-CTATCAACAAGCTACCAATC-3’
AT1G23380	KNAT6-VII	Reverse	5’-TGACTAAGCACGGTTGCTTG-3’
AT1G23380	KNAT6-VII	Forward	5’-ACGACTCTACTGACCCACTTA-3’
AT1G23380	KNAT6-VIII	Reverse	5’-CTCTTTAGCCACTTAGCCGT-3’
AT1G23380	KNAT6-VIII	Forward	5’-GACATCAAAGACAGAGAATGGT-3’
AT1G65620	AS2-I	Reverse	5’-TCCATACGCATTCCAACTAC-3’
AT1G65620	AS2-I	Forward	5’-GGTAACTAGACCTAAGAGTC-3’
AT1G65620	AS2-II	Reverse	5’-GTGTGTGTGTAGTGTATGTGCA-3’
AT1G65620	AS2-II	Forward	5’-AAGCTGCTATTTGGGGTTGC-3’
AT1G65620	AS2-III	Forward	5’-GCAACCCCAAATAGCAGCTT-3’
AT1G65620	AS2-III	Reverse	5’-AGAAAGCTTTTACCTGCGAGT-3’
AT1G65620	AS2-IV	Forward	5’-TTTTCAATGGCGGCTTTGTG-3’
AT1G65620	AS2-IV	Reverse	5’-CATTCCGGTTGACATTTTCG-3’
AT1G65620	AS2-V	Forward	5’-GTATTCGCGCCCTATTTCCC-3’
AT1G65620	AS2-V	Reverse	5’-GTGAAGGGTGAAGCTCGTTG-3’
AT1G65620	AS2-VI	Forward	5’-GAGCTTCACCCTTCACAACG-3’
AT1G65620	AS2-VI	Reverse	5’-ACGAAGCTGATGTTGGAGGA-3’
AT1G65620	AS2-VII	Forward	5’-ACCAAAGCCTCGGTATCCTC-3’
AT1G65620	AS2-VII	Reverse	5’-CTGGTGGTGGTGATAGTGGT-3’
AT1G65620	AS2-VIII	Forward	5’-ACAACTACGACGGTGGGATT-3’
AT1G65620	AS2-VIII	Forward	5’-CGACGAAGATGAACACCACC-3’
AT4G18390	TCP2-I	Reverse	5’- GCCCTCCATTGATAATCGCT-3’
AT4G18390	TCP2-I	Forward	5’-TCGTGATTAAAGAAGAAGGAGCT-3’
AT4G18390	TCP2-II	Reverse	5’-TGTTATTGCAGGCTTGTGGTTA-3’
AT4G18390	TCP2-II	Forward	5’-AAAGTCAGTAGATACAGCTTCGT-3’
AT4G18390	TCP2-III	Reverse	5’-CCTCTGAGGGTATTCATCATCAA-3’
AT4G18390	TCP2-III	Forward	5’-AACTTTAGGGTTGGTTTGGGA-3’
AT4G18390	TCP2-IV	Reverse	5’-ATGGCGACGTTGTGGATAAC-3’
AT4G18390	TCP2-IV	Forward	5’-GCTGTGTCGATCTTTACCACC-3’
AT4G18390	TCP2-V	Reverse	5’- CGATGACGAGAATCACCAGA -3’
AT4G18390	TCP2-V	Forward	5’- TTGCTCGTGTCTGAATTGCT -3’
AT4G18390	TCP2-VI	Reverse	5’- GGTTCAGATCCGGTTAACTCA -3’
AT4G18390	TCP2-VI	Forward	5’- TGACCCGACCCGAGAATTAA -3’

CHAPTER 3: RESULTS

3.1 Organ-specific expression of *DRM1*, *DRM2* and *CMT3* genes in Arabidopsis wild type plant.

Firstly, we analyzed through qRT-PCRs (Reverse Transcriptase quantitative Polymerase Chain Reaction) the expression pattern of *DRM1, DRM2* and *CMT3* in the different organs of *Arabidopsis* wild type (Col-0) by using custom made primers with complementary sequences to the coding regions of each gene. In particular we analyzed young roots sampled from one week old seedlings, cotyledons and Shoot Apical Meristem (SAM), first and second leaves sampled from two weeks old seedlings, mature leaves and opened flowers from adult plants.

qRT-PCR data analysis revealed that transcript levels of *DRM1* and *CMT3* were very high in flower tissue compared with the others tissues tested (Fig. 8 A and C). This is in line with previous data indicating a role of DRM1 and CMT3 in sexual reproduction (Jullien *et al*., 2012). Transcript levels of *DRM1* and *CMT3* were much lower in roots, shoot apices, young leaves and extremely low in expanded leaves, which indicated they have a major function in young tissues during development compared to fully differentiated tissues. Strikingly, *DRM2* expression despite some little differences between root and leaves in flowers was quite comparable to all other tissues which suggested its minor role in flower development (Fig. 8 B).

It is known that *de novo* and maintenance DNA methylation, together with 24-nt small interfering RNAs (siRNAs) drive RNA-directed DNA methylation (RdDM) (Cao *et al*., 2003) might have an important function to maintain genome stability targeting loci like transposons, keeping them silenced. This mechanism is compatible with the stable maintenance of epialleles across generations and fits with the global major involvement of analyzed gene in flower development.

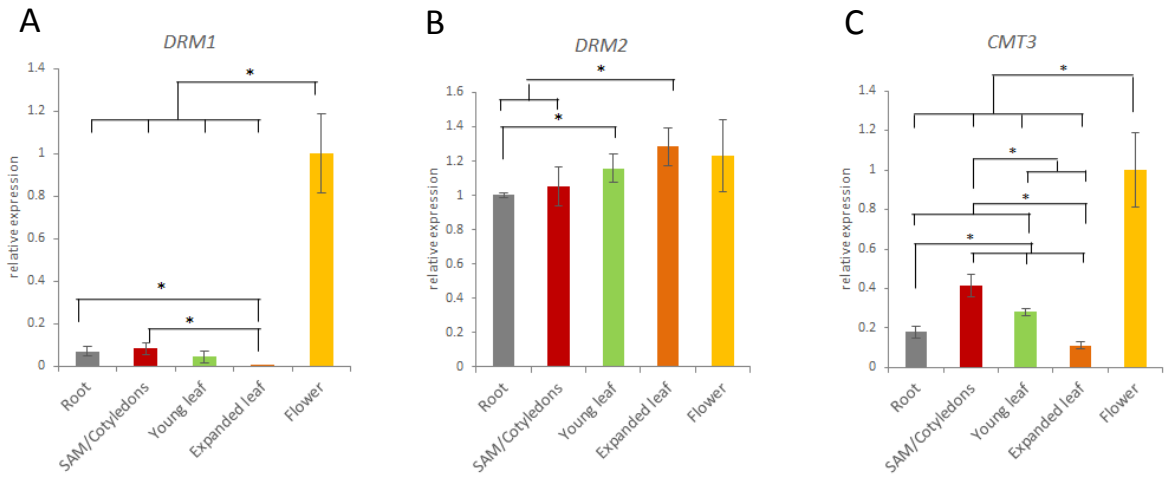

Figure 8. Gene expression levels of methyltransferases *DRM1*(**A**), *DRM2*(**B**) and *CMT3*(**C**) in root, SAM/cotyledons, young leaves, expanded leaves and flowers in wild type plant *Arabidopsis* (Col-0). The qRT-PCR data were normalized using *SAND* and *GAPDH* as housekeeping genes and analyzed by qBasePLUS software. The results represent the mean value (± standard deviation) of three independent biological replicates. Asterisks indicate significant pairwise differences using Student's t-test ($p \leq 0.05$).

3.2 *In silico* methyltransferases gene expression.

qRT-PCR analysis of methyltransferases gene expression was integrated with an *in silico* study. Software analysis is often used to find how strongly a certain gene is expressed in different organs and tissues. With Genevestigator a heat map was created in order to identify at which stage of development the methyltransferases *DRM1, DRM2, CMT3* and *MET1* are expressed. Genevestigator software is a high performance search engine for gene expression, which integrates public microarray and RNAseq experiments, including Arabidopsis, showing gene expression in different biological context such as development, hormonal treatment and environmental stimuli (light, cold), in mutant background. (Hruz *et al*., 2008). In particular 127 different anatomical parts of Arabidopsis wild type were included in this study. A general overview of the heat map shows how some methyltransferase is mainly expressed in floral tissue (embryo, ovule, anther, pollen, pistil) affecting the architecture in both male and female organs (Fig. 9).

Figure 9. Heat map of methyltransferases expressed in 127 different anatomical parts of Arabidopsis. The anatomical parts were collected from the dataset in Genevestigator. The colors are normalized to the expression potential of a gene which represents the top percentile of all expression values for a given probe.

In response to external stimuli the plants can change their gene expression. A gene that is sensitive to perturbations suggests that it has a role in the related pathway. A heat map was created using Genevestigator software in order to check which kind of perturbations affects the expression of genes that encode for DNA methyltransferases *DRM1, DRM2, CMT3* and *MET1* of *Arabidopsis thaliana.*

First analysis of the heat map shows that DNA methyltransferases *DRM1* and *DRM2* behave similarly in almost all the stress conditions analyzed as well as the more inducible *CMT3* and *MET1* suggesting that their regulation is connected with their role in *de novo* or in maintenance DNA methylation, respectively (Fig. 10).

Through the *in silico* analysis we also observed that the maintenance DNA methyltransferase as *CMT3* and *MET1* are up-regulated in germination process likely due to a high mitotic activity with intense DNA replication during the transition stage from seed to seedling as well as in callus formation where an unorganized growth of cells occurs. *CMT3* and *MET1* also were overexpressed upon exogenous application of 1-Naphthaleneacetic acid (NAA) and 1-N-Naphthylphthalamic acid (NPA), *CMT3* and *MET1* were up-regulated suggesting a possible involvement in methylation of auxin related genes.

Moreover, down-regulation of these maintenance methyltransferases occurred under light perturbations affecting the synchronization of the circadian rhythm, as well as abscisic acid treatments. *DRM2* methyltransferase was moderately up or down-regulated in several stress conditions indicating a marginal role of *de novo* DNA methylation in response to stress.

Finally, the most marked up-regulation for *DRM1 de novo* methyltransferase as well as *MET1* was following 5-Azacytidine treatment. 5-Azacytidine works as inhibitor of DNA methylation and likely induces some of the methyltransferase in order to restore DNA methylation levels. These data might indicate that *DRM1* and *MET1* are themselves repressed by DNA methylation.

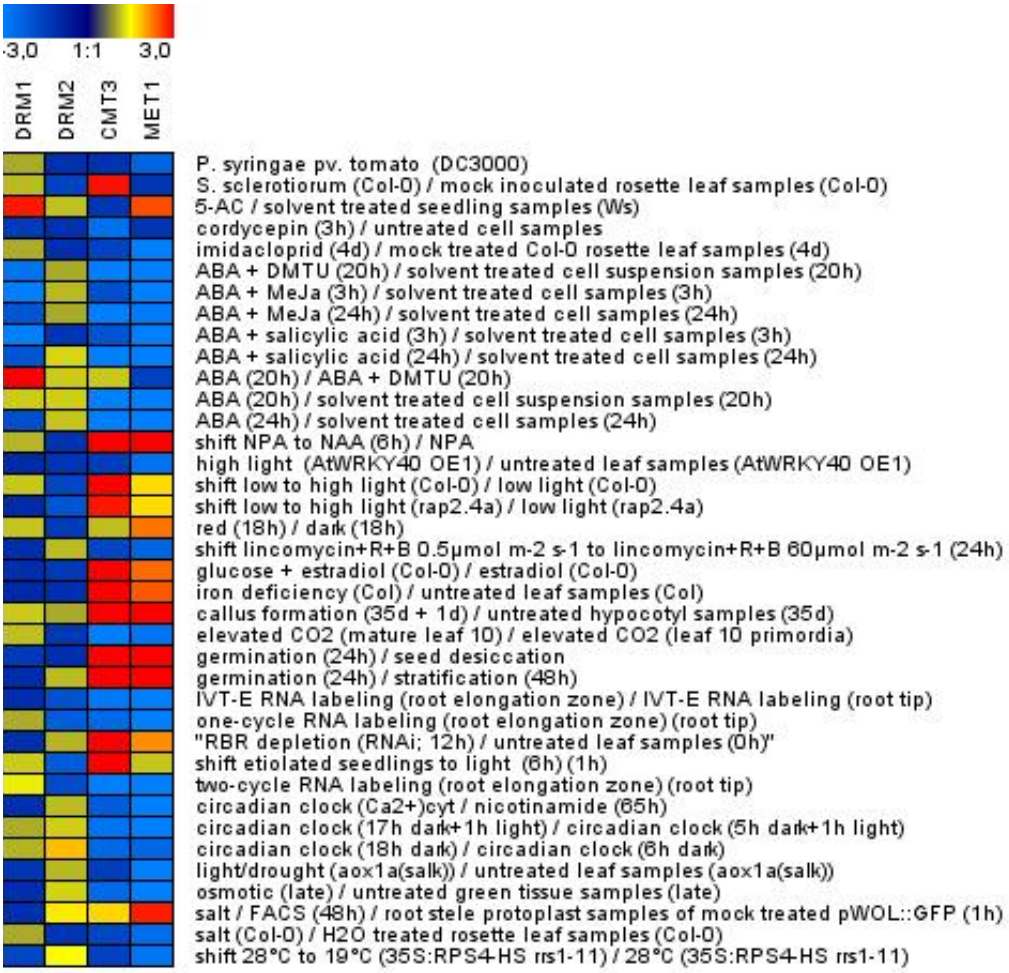

Figure 10. Heat map of Arabidopsis methyltransferases response to different perturbations. The perturbations were collected from the dataset in Genevestigator. Blue and red represent up- and down-regulation and a fold-change between -3.0 and 3.0, respectively.

3.3 *DRM1, DRM2* and *CMT3* expression during flower development in Arabidopsis wild type plant.

The higher expression of *DRM1* and *CMT3* in flower tissues compared with the other selected organs of Arabidopsis wild type, verified through both qRT-PCR and *in silico* analysis, strongly supported a role of DNA methylation during reproduction phase of the plant.

Some effect of DNA methylation on flower phenotype was already known as in the case of the *FWA* epiallele. It has been demonstrated that in *met1* mutant the loss of

CpG DNA methylation leads to overexpression of *FWA* transcription factor causing dominant and heritable late-flowering phenotype (Soppe *et al*., 2000). Moreover, Arabidopsis plants transformed with a *MET1* antisense construct showed a reduced level of DNA methylation resulting in a higher number of stamen and unfused carpels (Finnegan *et al*., 1996).

To clarify the function of DNA methylation in flower formation, the expression levels of *DRM1*, *DRM2* and *CMT3* were monitored at four different stages of flower development in the wild type plant by using qRT-PCR. Sampling of flower developmental stages was performed according to the "Arabidopsis: An Atlas of Morphology and Development" (Bowman, 1994) (Fig. 11).

The first stage corresponds to the age before gamete formation. In the second stage the microspore mother cell in the anthers undergos meiosis and elongation of stamen occurs while megasporogenesis takes place within the ovary. In the third stage the developing flowers are open, long anthers extend above the stigma leaving pollen and fertilization can occur. In the fourth stage the stigma extends above long anthers, petals and sepals withering, and zygote formation and embryo development take place (Fig. 11).

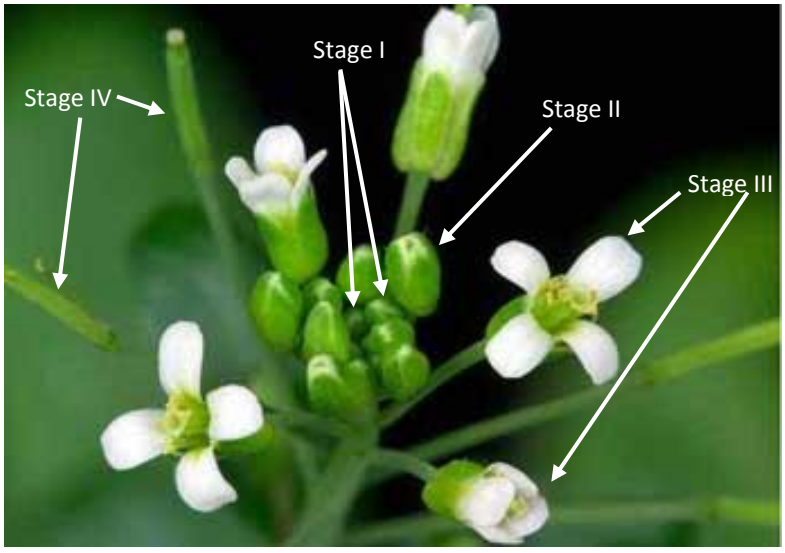

Figure 11. Different developmental stages of the Arabidopsis flower used for sampling.

No big differences in the transcript abundance of the methyltransferases *DRM2* were found among the four stages assayed, conversely than expected. Differences in *DRM1* expression , consisting into a lower transcript level, were detected only in the third stage which is related to the fertilization process. By contrast, a decrease of *CMT3* transcription was found to start earlier already in the second stage (Fig. 12).

All together these results suggest that DNA methylation might play a role in the regulation of processes like gamete formation, fertilization or embryo development rather than in floral organ formation.

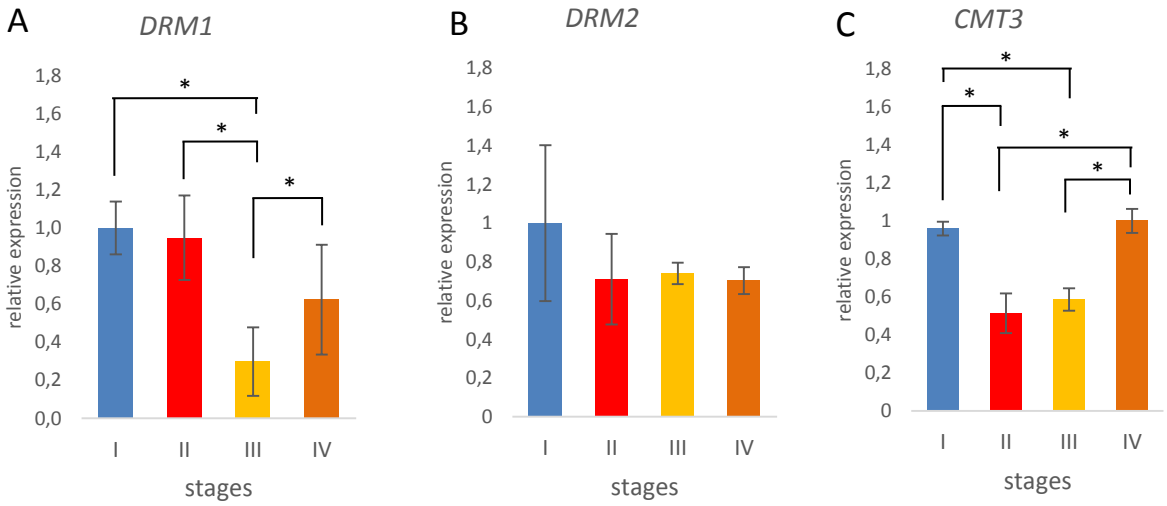

Figure 12. Expression levels of methyltransferases *DRM1* (**A**), *DRM2* (**B**) and *CMT3* (**C**) analyzed by qRT-PCR in four flower developmental stages. The data were normalized using *SAND* and *GAPDH* as housekeeping genes and analyzed by qBasePLUS software. The results represent the mean value (± standard deviation) of three independent biological replicates. Asterisks indicate significant difference between different stages using Student's t-test ($p \leq 0.05$). Every stages represents as follows: stage I = before gamete formation; stage II = gamete formation; stage III = fertilization; stage IV = embryo development.

3.4 Molecular characterization of T-DNA insertion in the *DRM1, DRM2* and *CMT3* genes in the Arabidopsis *drm1 drm2 cmt3* triple mutant.

Insertional mutagenesis is one of the ways of disrupting gene function and is based on the insertion of foreign DNA into the gene of interest. The triple mutant *drm1 drm2 cmt3* (Columbia background) of *Arabidopsis thaliana* that we used in our study, combines *drm1* (SALK_021316) with T-DNA insertion in the sixth exon, *drm2* (SALK_150863) with T-DNA insertion in the last exon, and *cmt3* (SALK_148381) with T-DNA insertion in the eighth intron.

In order to confirm the T-DNA insertion in all three genes in the homozygous mutant line *drm1 drm2 cmt3* of Arabidopsis, PCRs were performed by using complementary primers (right primer [RP] and left primer [LP]) to the region flanking the

T-DNA insertions site in *DRM1, DRM2* and *CMT3* genes and a primer (LBb1.3) complementary to the T-DNA sequence (Tab. 4).

A single PCR product was obtained by the amplification with RP (Right Primer) and LBb1.3 primers indicating the T-DNA insertion in the sixth and tenth exon in *DRM1* and *DRM2* genes, respectively (Fig. 13 A and B; Fig 14 A and B).

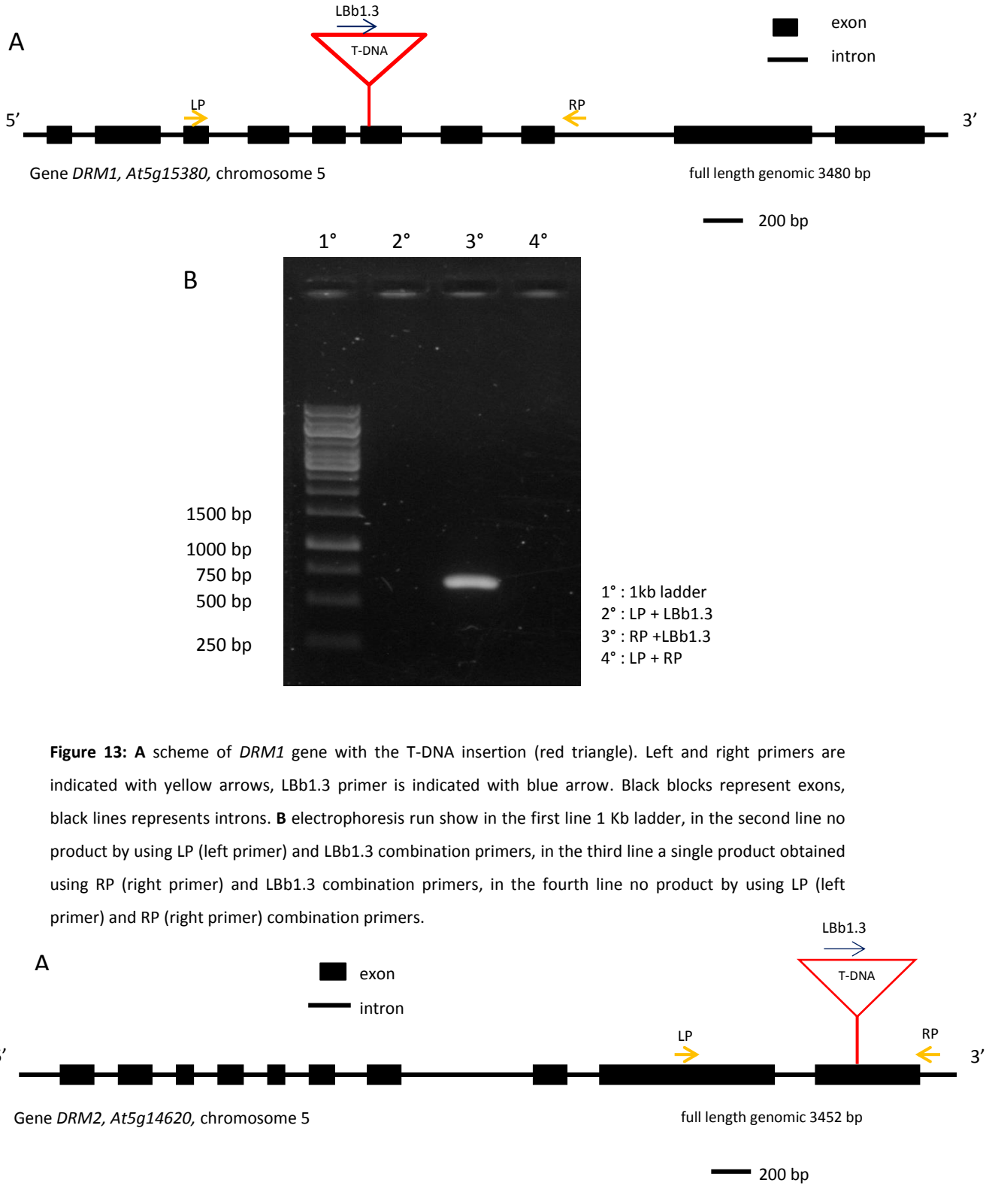

Figure 13: A scheme of *DRM1* gene with the T-DNA insertion (red triangle). Left and right primers are indicated with yellow arrows, LBb1.3 primer is indicated with blue arrow. Black blocks represent exons, black lines represents introns. **B** electrophoresis run show in the first line 1 Kb ladder, in the second line no product by using LP (left primer) and LBb1.3 combination primers, in the third line a single product obtained using RP (right primer) and LBb1.3 combination primers, in the fourth line no product by using LP (left primer) and RP (right primer) combination primers.

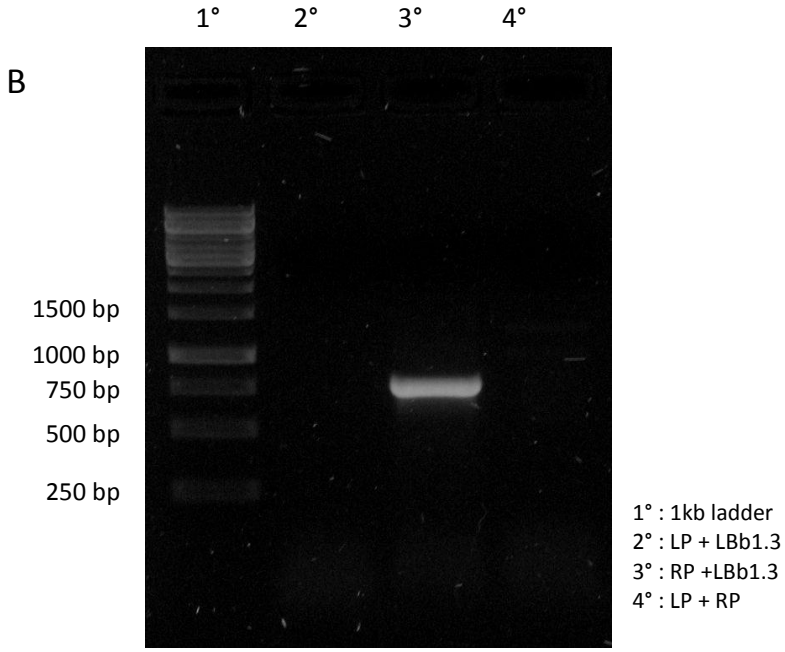

Figure 14: A scheme of *DRM2* gene with the T-DNA insertion (red triangle). Left and right primers are indicated with yellow arrows, LBb1.3 primer is indicated with blue arrow. Black blocks represent exons, black lines represents introns. **B** electrophoresis run show in the first line 1 Kb ladder, in the second line no product by using LP (left primer) and LBb1.3 combination primers, in the third line a single product obtained using RP (right primer) and LBb1.3 combination primers, in the fourth line no product by using LP (left primer) and RP (right primer) combination primers.

In *CMT3* two different PCR fragments were detected by using both pairs of primers combinations: LP with LBb1.3 and RP with LBb1.3. This result likely is due to presence of an inverted repeat of the T-DNA generated by the replication machinery during the integration process (Fig. 15 A and B). All these results confirm that *drm1 drm2 cmt3* is a T-DNA homozygous mutant line.

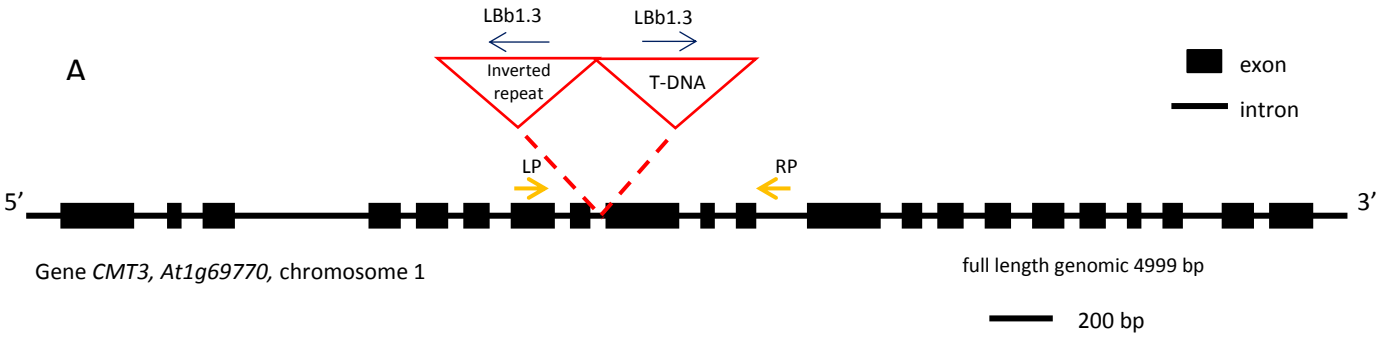

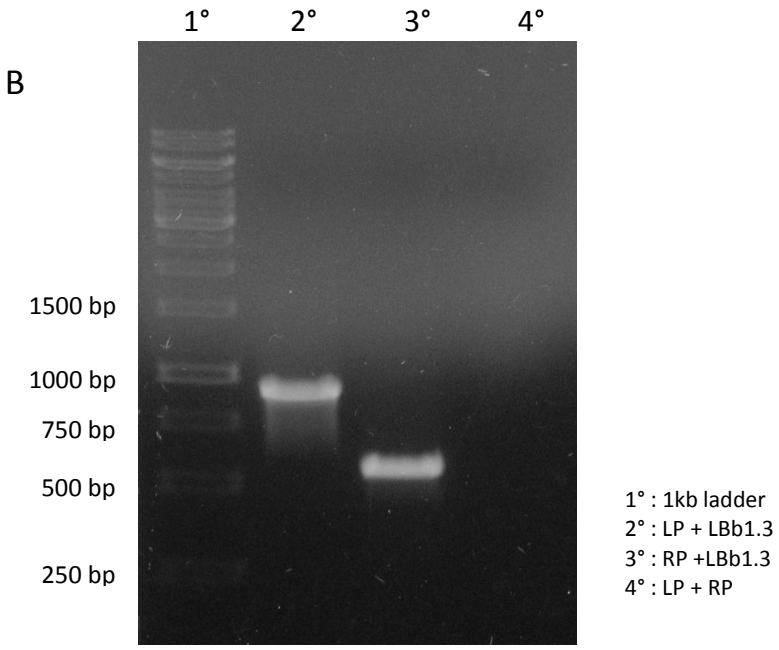

Figure 15: A scheme of *CMT3* gene with the T-DNA insertion and inverted repeat (red triangles). Left and right primers are indicated with yellow arrows, LBb1.3 primer is indicated with blue arrows. Black blocks represent exons, black lines represents introns. **B** electrophoresis run show in the first line 1 Kb ladder, in the second line a single product obtained using LP (left primer) and LBb1.3 combination primers, in the third line a single product obtained using RP (right primer) and LBb1.3 combination primers, in the fourth line no product by using LP (left primer) and RP (right primer) combination primers.

3.5 Expression levels of *DRM1*, *DRM2* and *CMT3* in *drm1 drm2 cmt3* T-DNA insertion line of Arabidopsis.

When a T-DNA is inserted into an Arabidopsis gene, it is expected that no message or an unstable or truncated message will be formed (Krysan *et al*., 1999).

Genotyping experiment above described confirmed the insertion of a T-DNA in the sixth exon, last exon and eighth intron that disrupted the coding sequence of the *DRM1*, *DRM2* and *CMT3*, respectively, of the triple DNA methylation mutant *drm1 drm2 cmt3.*

In order to determine if the T-DNA insertions gives rise to partial transcripts in the *drm1 drm2 cmt3* mutant, qRT-PCR experiments were performed. Two pairs of primers were designed complementary to regions located upstream and downstream of the T-DNA insertion in every gene (Fig. 16 A). Very weak signals of partial transcripts downstream of the T-DNA insertion of *DRM1* were detected in *drm1 drm2 cmt3* which showed it is knock-out mutant (Fig. 16 B). Whereas, despite T-DNA insertion interrupting

DRM2 and *CMT3* genes, the qRT-PCR data evidenced the existence of some transcript downstream of the insertion (Fig. 16 C and D).

It is known that T-DNA mutagenesis of Arabidopsis does not always disrupt gene expression (Krysan *et al*., 1999). However any truncated messages produced from the region downstream of the insertion sites have reduced stability giving rise to nonfunctional protein. Therefore, our conclusion is that *DRM1* gene is a knock-out and the *DRM2* and *cmt3* are knock-down.

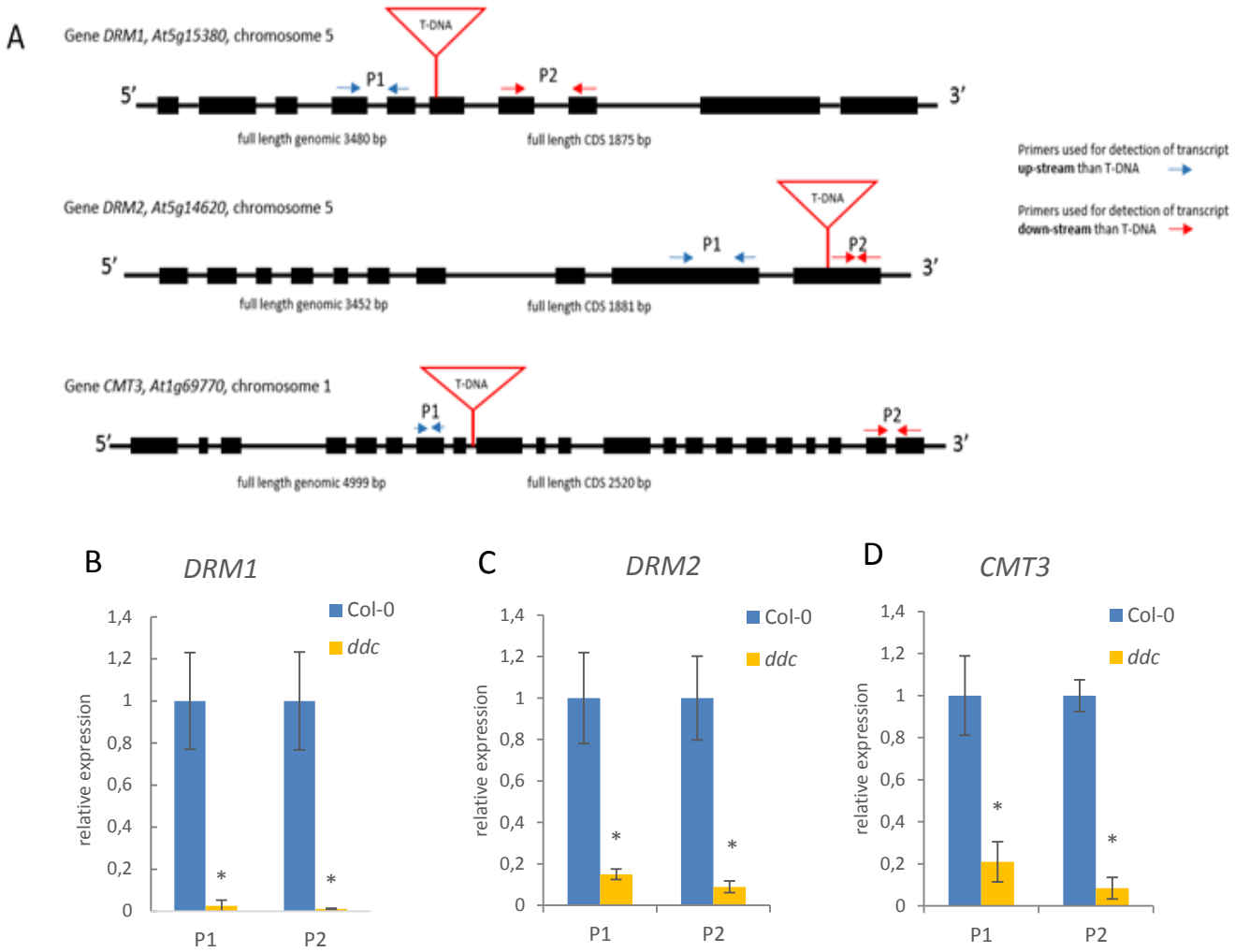

Figure 16. (A) Scheme of the *DRM1*, *DRM2* and *CMT3* genes shows the position of the primer pairs designed upstream (blue arrows) and downstream (red arrows) of the T-DNA (red triangle) insertion. Expression of transcripts upstream and downstream of the T-DNA insertion site of *DRM1* (**B**), *DRM2* (**C**) and *CMT3* (**D**) in wild type (Col-0) and mutant *drm1 drm2 cmt3* plants. P1 and P2 pairs of primers amplified upstream and downstream T-DNA insertion region, respectively. The RT-qPCR data were normalized using *SAND* and *GAPDH* as housekeeping genes and analyzed by qBasePLUS software. The results represent the mean value (± standard deviation) of three independent biological replicates. Asterisks indicate significant pairwise differences using Student's t-test ($p \leq 0.05$).

3.6 Phenotypic analysis and growth parameters of *drm1 drm2 cmt3.*

Phenotypic characteristics of the *drm1 drm2 cmt3* mutant were analyzed by visual and microscopic observations. Seedlings of *Arabidopsis thaliana* Columbia (Col-0) were used as control.

3.6.1 Seed germination and root growth.

In order to check the viability of the seeds, germination rate assay was performed. At day 1 after sowing, the germination rate of Col-0 and *drm1 drm2 cmt3* genotypes was about 95% and 80% respectively. At the end of the observation (5 days after sowing) the germination rate was nearly 100% for Col-0 and 84% for *drm1 drm2 cmt3,* respectively (Fig. 17).

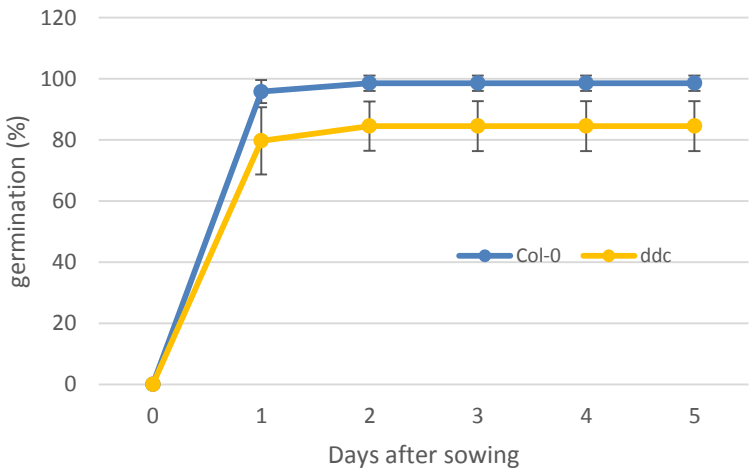

Figure 17. Germination rate of Col-0 and *drm1 drm2 cmt3* seeds plated on MS medium and put to germinate in long day light regime. The results represent the mean value (± standard deviation) of three independent biological replicates (n = 100).

Primary root length and lateral root density (= lateral root number / root length) were also analyzed (Fig. 18) . It was evident that *drm1 drm2 cmt3* roots were shorter than those of wild type (Fig. 18 A). No difference in lateral root density between mutant and wild type was observed, at least in 12 days old seedlings (Fig. 18 B).

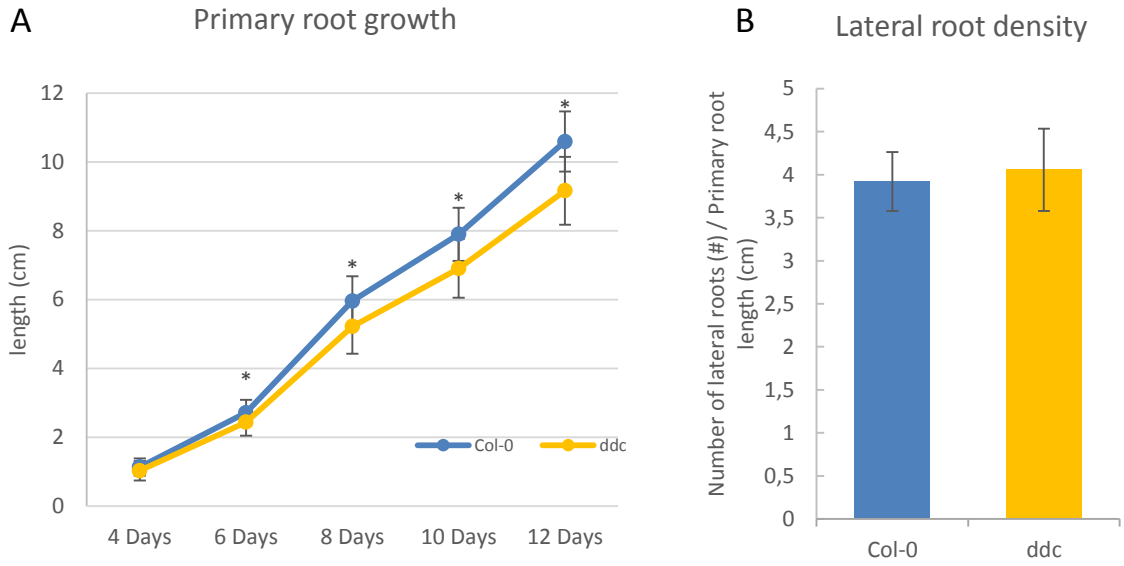

Figure 18. Root analysis: A Kinetics of the primary root growth in continuous light condition (n=45); **B** lateral roots density in 12 days old plant grown in continuous light condition (n=45). The results represent the mean value (± standard deviation) of three independent biological replicates. Asterisks indicate significant pairwise differences using Student's t-test ($p \leq 0.05$).

In order to check whether shorter roots in the triple mutant were due to the altered organization of the root apical meristem (RAM) , evaluation of root-meristem size was also carried out in in 6 days old seedlings of *drm1 drm2 cmt3* mutant VS wild type plants. Meristem size was expressed as the number of cortex cells in a files proximal to the quiescent center to the first elongated cell (Casamitjana-Martinez *et al.*, 2003). The number of the cortex cells per file was counted and meristem length was measured with ImageJ software. No difference in number of cells and size were found (Fig. 19 A and B). These results suggested that the shorter root observed in the triple mutant was likely due either to different proliferation rate or/and different proliferative cell fraction as well as to difference in the cell elongation rate in differentiation zone rather than to meristem size (Sabatini *et al.*, 2003).

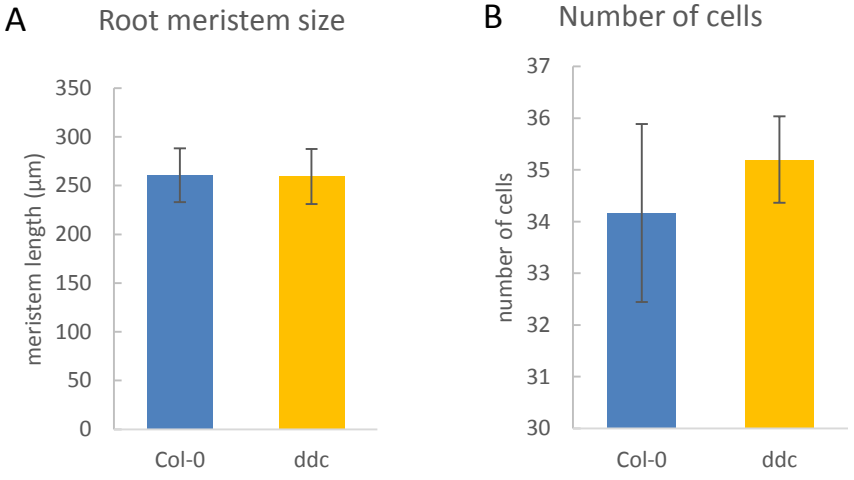

Figure 19. Root meristem analysis: (**A**) root meristem length; (**B**) number of cells in the meristem zone in Col-0 and *drm1 drm2 cmt3.* The results represent the mean value ± standard deviation.

Very interestingly, starting from 6 days after sowing triple mutant primary root showed an agravitropic growth behavior (Fig. 20 A and B). According to Grabov *et al*. (2004) it was quantified taking into account the following parameters: root deviation angle, horizontal growth index (HGI), vertical growth index (VGI) and straightness (Fig. 20 C-F). It was evident a two folds higher deviation angle and HGI and a lower VGI and straightness in the triple mutant compared to wild type seedlings.

Some similarity in the dynamics of gravitropic behaviour was found in auxin mutants (Lusching *et al*., 1998; Müller *et al*., 1998).

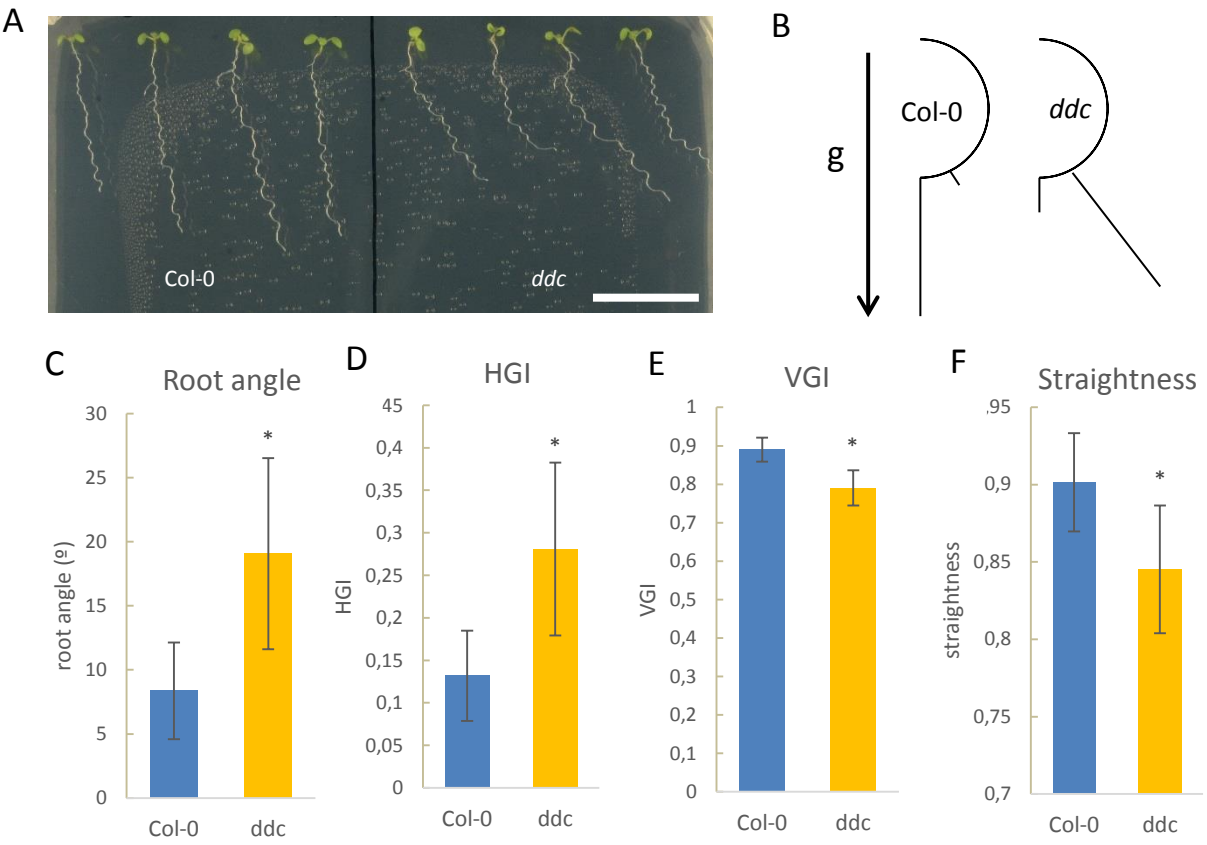

Figure 20. (A) Agravitropic root phenotype of *drm1 drm2 cmt3* in 6 days old seedlings grown in vertical position in continuous light condition; White bar in photograph corresponds to 2 cm. (**B**) Gravitropic growth in seedlings 6 DAG in vertical position (n=45). Bars give percentages of roots at specific orientations; g is the gravity vector. (**C**) Root Angle indicating deviation from perpendicular growth; (**D**) Horizontal Growth Index (HGI); (**E**) Vertical Growth Index (VGI); (**F**) Straightness. The results represent the mean value (± standard

deviation) of three independent biological replicates. Asterisks indicate significant pairwise differences using Student's t-test ($p \leq 0.05$).

3.6.2 Shoot vegetative growth.

Shoot vegetative growth was also compared by measuring rosette and leaf area in three weeks old plants grown *in vitro* in long day condition. Significantly smaller rosette area was observed in the mutant compared with Col-0 (Fig. 21 A and B). Significantly reduced leaf area of the mutant was observed in all expanded leaves of series, with the exception of leaf 8 which was a cauline leaf (Fig. 21 C and D).

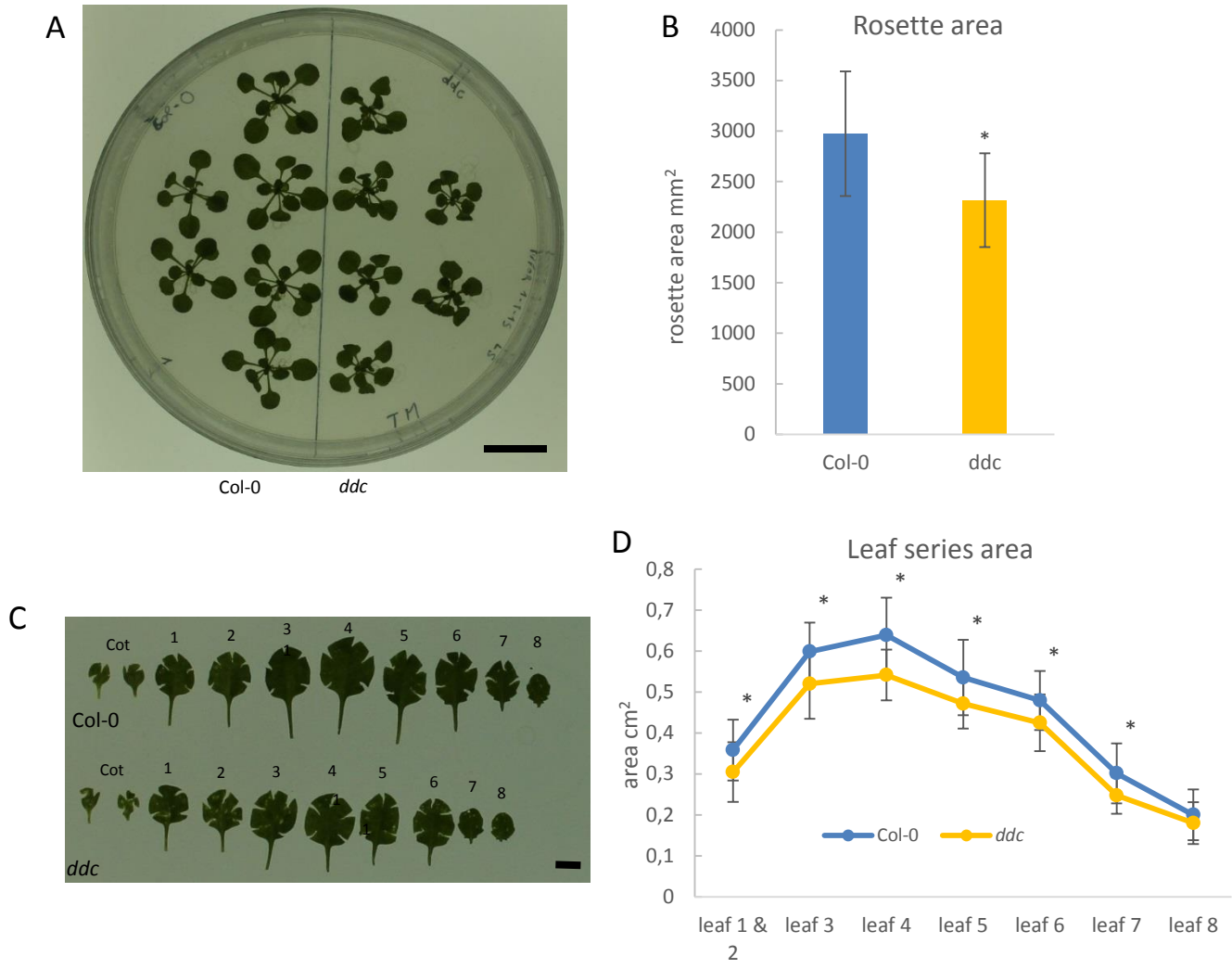

Figure 21. Rosette and leaves analysis: A and **B** mean rosette area (n=39)**; C** and **D** mean leaf area of three weeks old plants of Col-0 and *drm1 drm2 cmt3* grown on MS medium in long day condition. The results represent the mean value (± standard deviation) (n=15). Asterisks indicate significant pairwise differences using Student's t-test ($p \leq 0.05$). Black bars in photographs correspond to 2 cm (A) and to 0,5 cm (C), respectively.

Biggest difference between mutant and wild type was observed in the leaf number 4, that was selected for further analysis.

In particular, we focused our attention only on the upper epidermal cells because it was the fastest way to find out differences in leaf size (Andriankaja *et al.*, 2012). Imaging coupled with microscopic analysis of the upper epidermis of leaf 4 revealed that the cell area was significantly reduced in *drm1 drm2 cmt3,* whereas epidermal cell density did not significantly differ (Fig. 22 A and B). The number of cells calculated per leaf (see materials and methods) was not significantly reduced (Fig. 22 C), therefore the smaller size of the *drm1 drm2 cmt3* leaf was due only to the reduced cell area.

Moreover, despite the similar cell number, the stomatal density, defined as the number of stomata per square millimeter, was significantly increased in the mutant as well as the stomatal index (= stomatal density / stomatal +epidermal cell density) (Fig. 22 D and E). This higher presence of stomata in the mutant could account for the comparable cell density detected in the two samples.

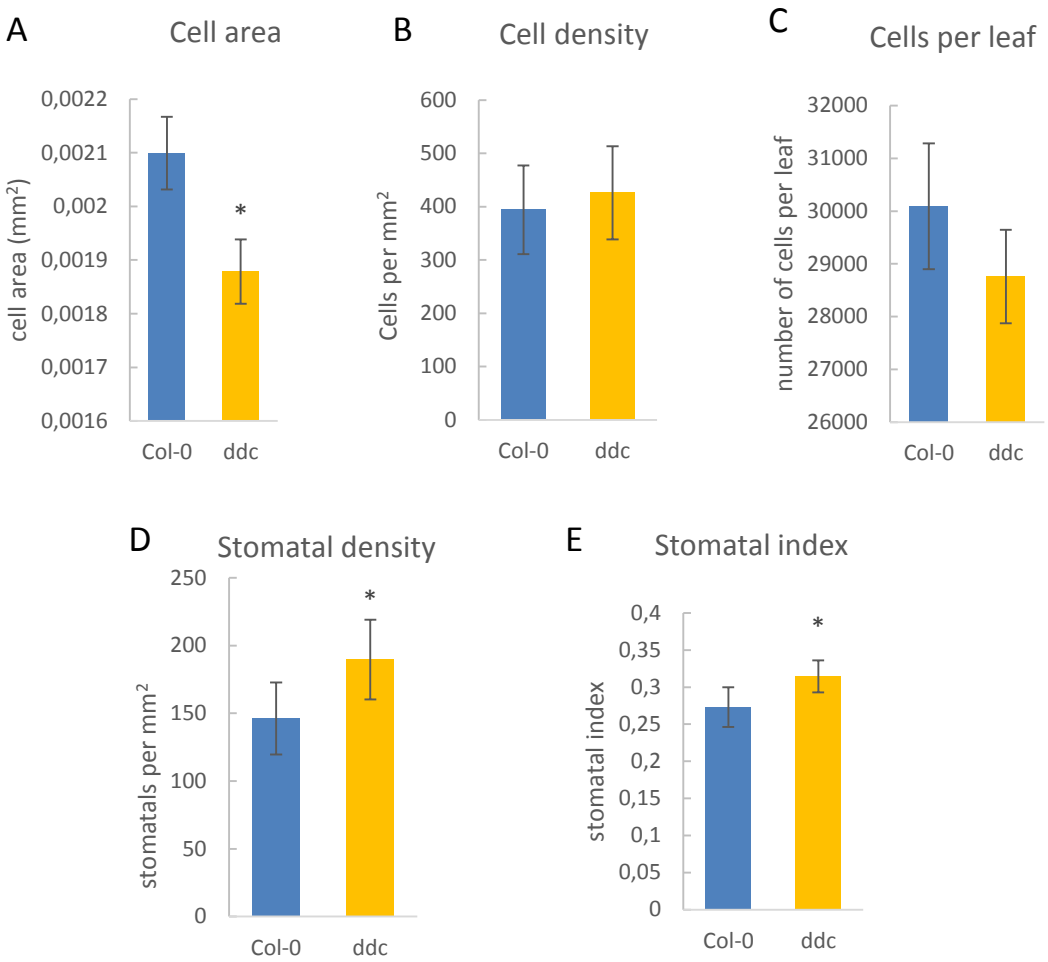

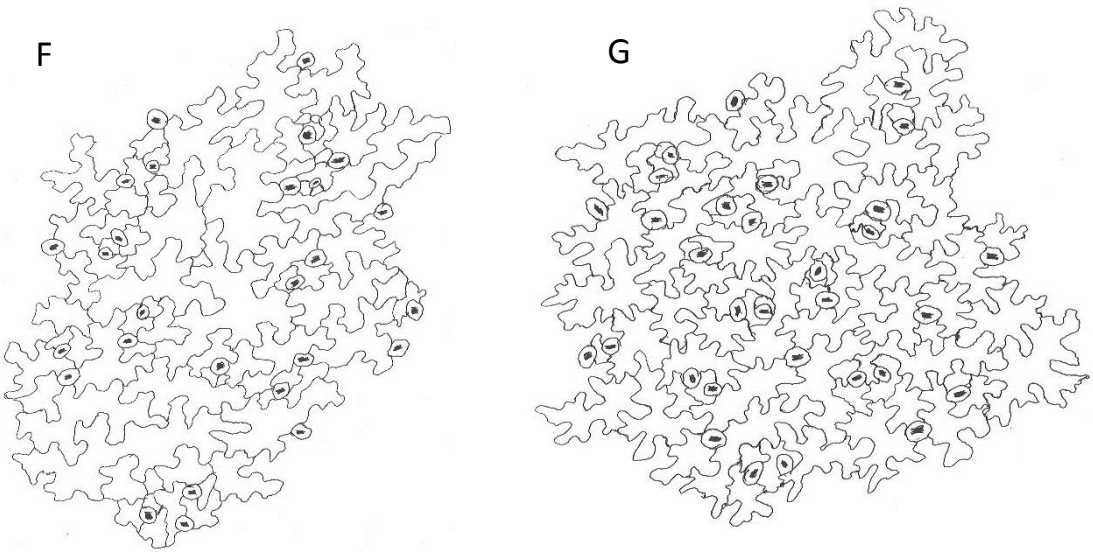

Figure 22. Epidermal cells analysis on leaf 4: **A** epidermal cell area; **B** epidermal cell density; **C** number of cells per leaf; **D** stomatal density; **E** stomatal index. Drawing of epidermal cells and stomata on the adaxial side of leaf 4 in Col-0 (**F**) and *drm1 drm2 cmt3* (**G**) The results represent the mean value (± standard deviation) (n=13-15). Asterisks indicate significant pairwise differences using Student's t-test ($p \leq 0.05$).

Another peculiar feature of leaf morphology in *drm1 drm2 cmt3* mutant deals with the occurrence of a curly phenotype (i.e. downward twisted leaf) with a reduced petiole length (Fig. 23 A and B). Finally, adult plants showed a short stature phenotype (Fig. 23 C and D)

3.6.3 Reproductive growth.

Concerning reproductive phase, our observation allowed us to verify that flowering time of the triple mutant was similar to that of the wild type.

However *drm1 drm2 cmt3* mutant produced shorter siliques with a reduced seed density compared to wild type (Fig. 23 E-G) (Chan *et al.*, 2006). The reduced seed density in *drm1 drm2 cmt3* siliques may be due to defects in fertilization process and embryo development, further supporting the role of the related methyltransferase during the reproductive phase.

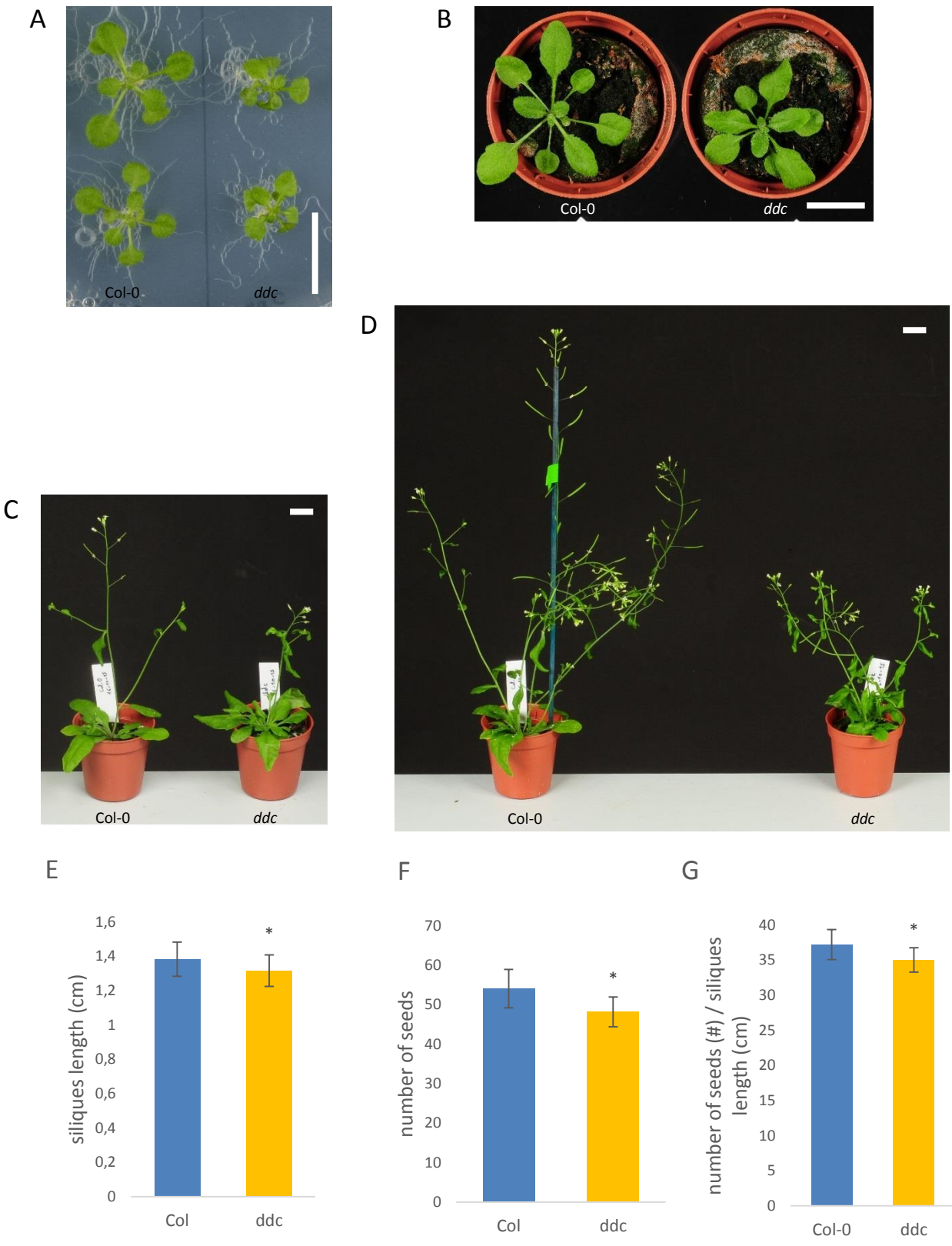

Figure 23. Three weeks old plants of Col-0 and *drm1 drm2 cmt3* grown in soil (**A**) and MS medium (**B**) in long day condition. Five (**C**) and six (**D**) weeks old plants of Col-0 and *drm1 drm2 cmt3* grown on soil in long day condition. Siliques length (**E**), number of seeds per silique (**F**), seed density (**G**) in adult plant of Col-0 and *drm1 drm2 cmt3.* The results represent the mean value (± standard deviation). Asterisks indicate significant pairwise differences using Student's t-test ($p \leq 0.05$). White bars in photographs correspond to 2 cm.

3.7 Auxin distribution in Arabidopsis *drm1 drm2 cmt3*.

As previously discussed hormone responses are fundamental to the development and growth of plants (Davies, 2010). Among the different hormone classes, auxin is one of the most relevant and its gradient play key roles in many distinct and overlapping processes throughout the life cycle of plants, from embryonal to the adult phase (Davies 2010; Zažímalová *et al*., 2014).

Auxin distribution in the plant can be investigated through the construct *DR5:GFP.* The *DR5* is an auxin-inducible synthetic promoter that represents a suitable molecular marker for monitoring changes in auxin distribution. By molecular biology approach the *DR5* promoter is fused with the reporter gene of the *Green Fluorescent Protein* (GFP). Reporter assay are a common molecular tool used to evaluate promoter or gene expression of a particular gene by fusing it to another reporter gene. The expression of the reporter gene should reflect the expression of the promoter/gene of interest.

Notably, some defects observed in *drm1 drm2 cmt3* mutant, such as the reduced and agravitropic root growth, the curly leaf phenotype and the alteration in stomatal density and index either resemble auxin-mutant features or involve processes known to be under auxin control (Trewavas, 1981). These observations prompted us to verify whether in the triple mutant the loss of DNA methylation could be associated to alteration in auxin distribution. At this aim the construct *DR5:GFP* was introduced in both *drm1 drm2 cmt3* and wild type genomes through crosses.

Attention was firstly focused on embryo, where auxin gradient plays a critical role in determining embryo polarity (Zažímalová *et al*., 2014). Analysis through confocal microscopy confirmed a normal distribution in suspensor in early stages of *drm1 drm2 cmt3* embryo (Fig. 24 A). At this stage indeed auxin flow moves from suspensor upward to embryo proper (Jenik and Barton, 2005). In triple mutant heart stage embryo an ectopic auxin accumulation was observed at the basal adaxial region of developing cotyledons precursors, while normally it is distributed mainly at the cotyledon's tip and flows to radicle (Fig. 24 B).

Auxin distribution was investigated also on primary root of 6 days old seedlings. In line with the reduce root growth, a very weak fluorescent signal in *drm1 drm2 cmt3* root tip suggested a lower auxin accumulation compared with Col-0 where a clear and visible fluorescence occurred in the quiescent center, in the columella cells and in the

stele (Fig. 25). The very weak auxin signal in the root of *drm1 drm2 cmt3* impeded a clear definition of its distribution in the root elongation zone responsible of growth direction. Thus our results allow us to relate the agravitropic root growth of the mutant only to the very low presence of auxin at the level of calyptra which is the gravity sensing tissues.

By contrast, a higher auxin accumulation was verified in the leaf of *drm1 drm2 cmt3* mutant compared to the wild type (Fig. 27).

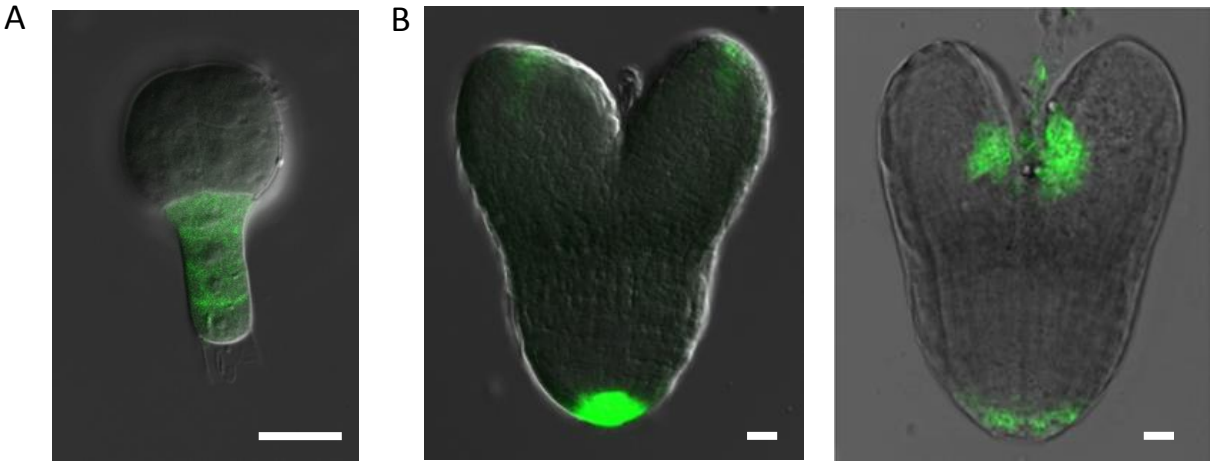

Figure 24. *DR5::GFP* reporter gene activity. **(A)** *drm1 drm2 cmt3* embryo at globular stage. **(B)** heart stage embryo of wild type (left) and *drm1 drm2 cmt3* (right) (n=10). White bars represent 10 µm.

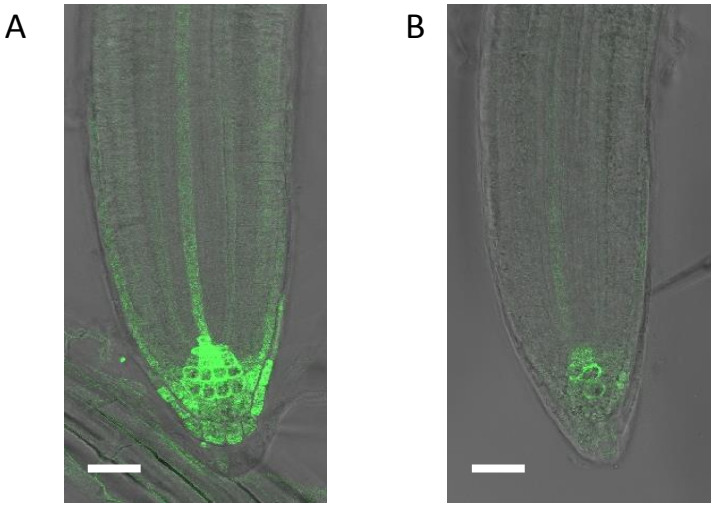

Figure 25. *DR5::GFP* reporter gene activity. Col-0 (**A**) and *drm1 drm2 cmt3* (**B**) root tip (n=40). White bars represent 50 µm.

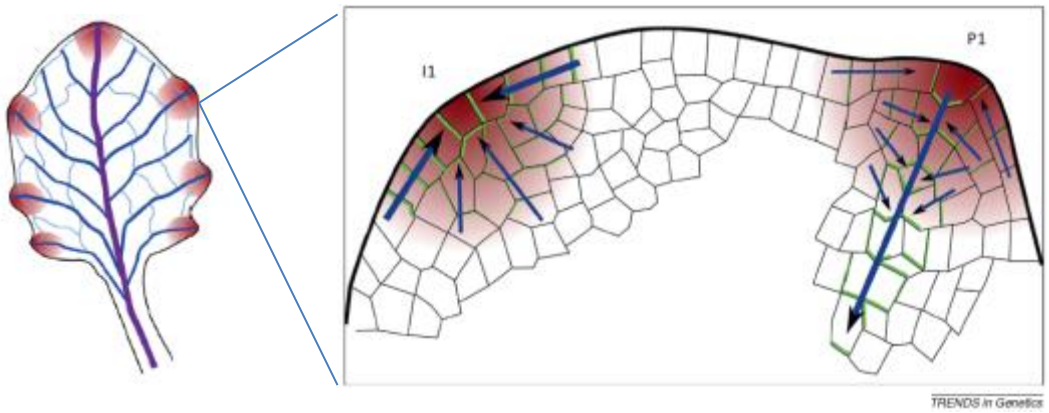

Figure 26. Schematic showing vascular patterning in an Arabidopsis leaf. The midvein (purple) forms first and joins the leaf to the main vascular bundles in the stem. First-order veins (dark blue) directly connect to the midvein at the edge of the leaf. Lower-order veins (light blue) connect first-order veins together to form a highly connective reticulate network that very efficiently serves the whole organ (Bennet *et al.*, 2014).

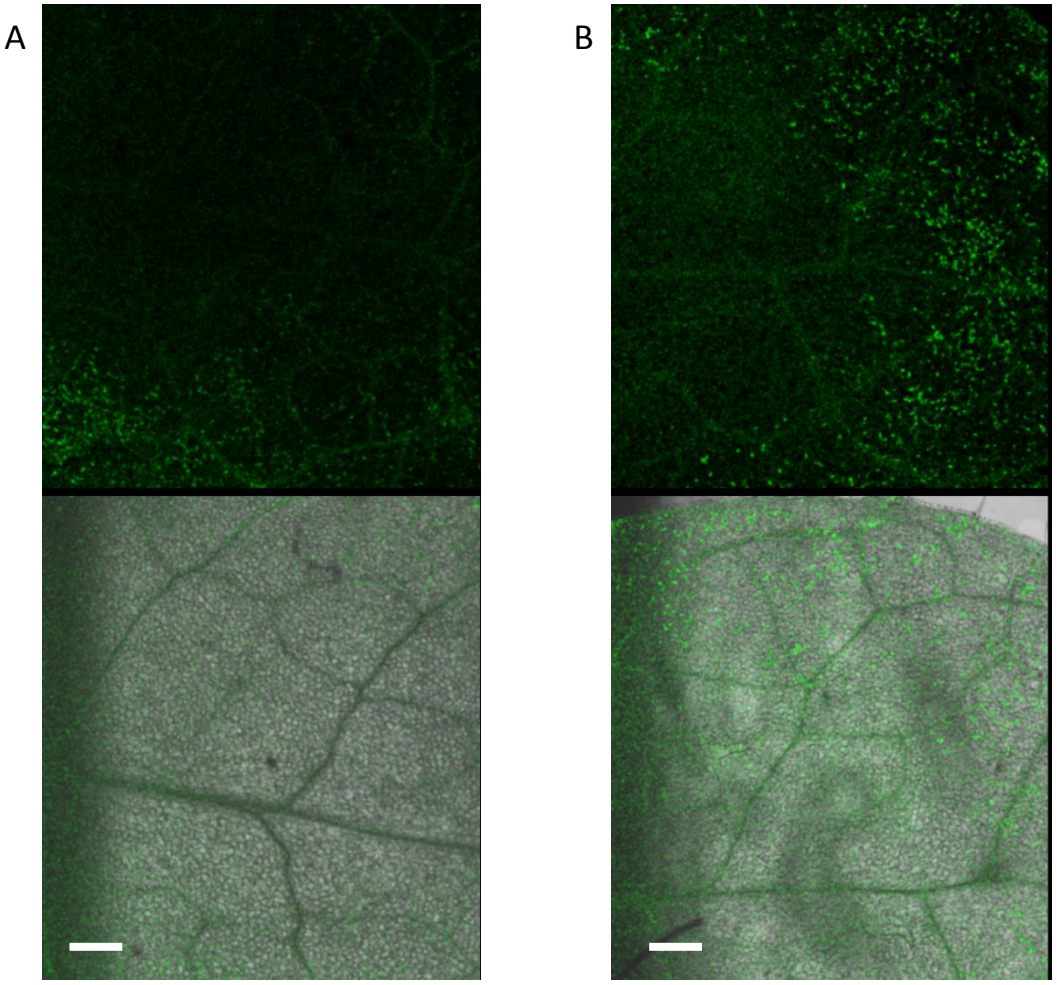

Figure 27. Col-0 (**A**) and *drm1 drm2 cmt3* (**B**) leaf. The upper frame represents the images with the signal of the *DR5:GFP* fluorescence; the lower frame represents the merged of fluorescent and transmission confocal microscopy images. White bars represent 500 µm.

3.8 Expression levels of auxin related genes in the whole plants of Arabidopsis *drm1 drm2 cmt3* mutant.

Studies of Arabidopsis mutants with defects in auxin related pathway, such as *yuc1* and *pin1* (Cheng *et al*., 2007), have contributed substantially to our understanding of hormone function, perception and signal transduction. Moreover, there is evidence that chromatin remodeling events such as histone modification play a role in the transcriptional regulation of genes in response to auxin signaling (Nelissen *et al*., 2007). All together these results highlight an interplay between auxin and epigenetic mechanism in the control of plant development.

Therefore we thought to investigate the expression pattern of a panel of genes controlling auxin pathway from synthesis to transport and signaling (Table 13). Gene expression level was evaluated by qRT-PCR in the whole plant of both mutant and Col-0, by using three weeks old whole plant Arabidopsis. The obtained data revealed that *ARF7* (*AUXIN RESPONSE FACTOR 7*), *PIN2* (*PIN-FORMED 2*) and *GH3 (auxin responsive GH3 family protein)* respectively involved in signaling, transport and metabolism of auxin were significantly up-regulated while *SAUR76 (Small Auxin Up-RNA76)* and *PIN7* respectively involved in signaling and transport were down-regulated in triple DNA methylation mutant (Fig. 28).

Gene	Pathway	Gene	Pathway
YUCCA1	Auxin biosynthetic pathway	***LAX2***	Auxin transport
YUCCA2	Auxin biosynthetic pathway	***LAX3***	Auxin transport
TAA1	Auxin biosynthetic pathway	***PIN1***	Auxin transport
ARF7	Auxin signaling	***PIN2***	Auxin transport
GH3	Auxin signaling	***PIN3***	Auxin transport
IAA3	Auxin signaling	***PIN4***	Auxin transport
SAUR76	Auxin signaling	***PIN7***	Auxin transport

Table 13. Auxin-related genes and the pathway where they work.

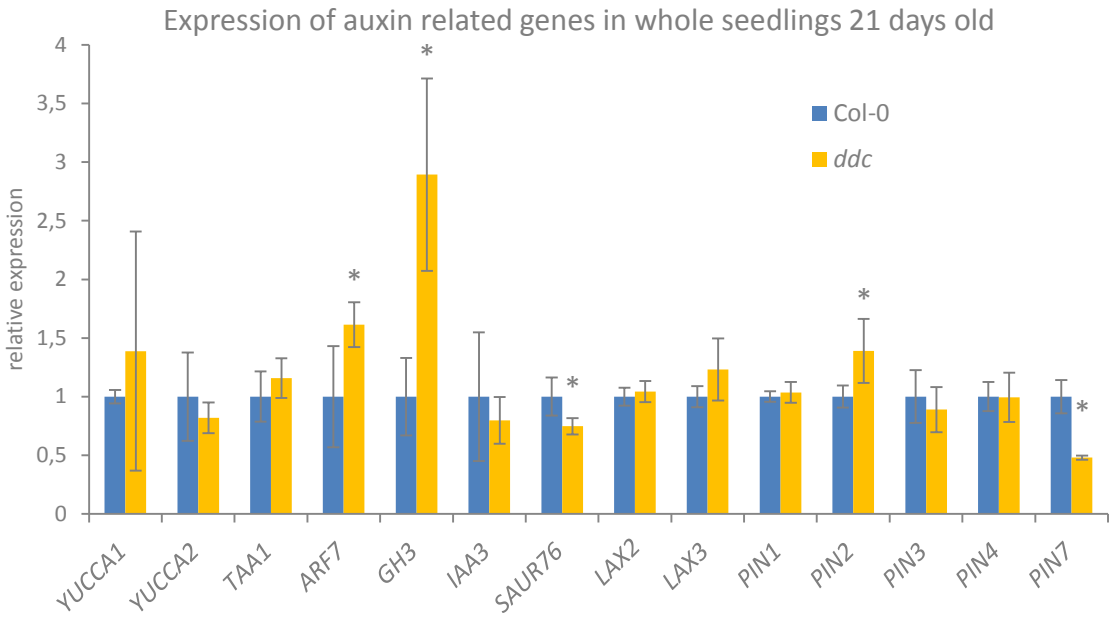

Figure 28. Expression analysis by qRT-PCR of auxin related genes in three weeks old seedlings grown on MS medium in long lay condition. The qRT-PCR data were normalized using *SAND* and *GAPDH* as housekeeping genes and analyzed by qBasePLUS software. The results represent the mean value (± standard deviation) of three independent biological replicates. Asterisks indicate significant pairwise differences using Student's t-test ($p \leq 0.05$).

3.9 Expression levels of auxin related genes in the primary root of Arabidopsis *drm1 drm2 cmt3* mutant.

It is largely known that auxin is a master regulator in root growth and that both auxin and genes encoding factors involved in auxin pathway are required for patterning of the root stem cell niche (Aida *et al*., 2004). Moreover, the root phenotype of *drm1 drm2 cmt3* triple mutant strongly resembles the phenotype of auxin-related mutants in that they exhibited reduced and agravitropic root growth (Fig. 20 A).

Therefore, in order to deeply dissect the interaction between methylation status, auxin pathway and developmental alterations at the single organ level, the expression pattern of the above used panel of auxin related genes was specifically analyzed in root tissues. Surprisingly, only for the *SAUR76* signaling factor the down regulation was confirmed in *drm1 drm2 cmt3* (Fig. 29).

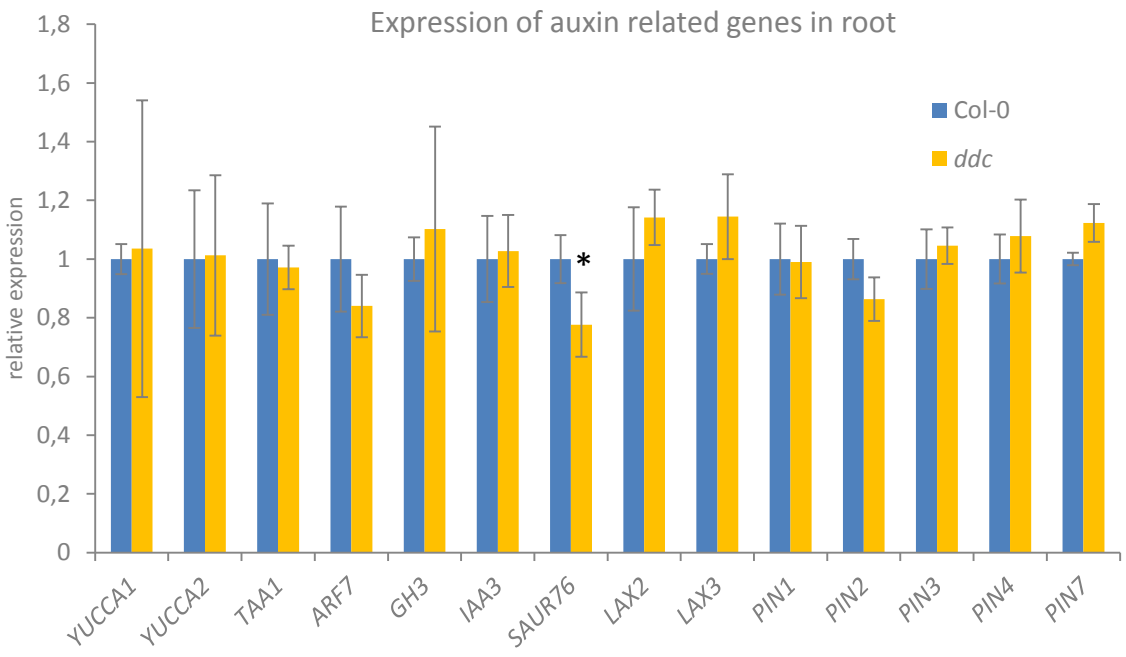

Figure 29. Expression analysis by RT-qPCR of auxin related genes in roots from 18 days old seedlings grown on MS medium in long lay condition. The RT-qPCR data were normalized using *SAND* and *GAPDH* as housekeeping genes and analyzed by qBasePLUS software. The results represent the mean value (± standard deviation) of three independent biological replicates. Asterisks indicate significant pairwise differences using Student's t-test ($p \leq 0.05$).

3.10 Expression levels of auxin- and growth-related genes in leaves of drm1 drm2 cmt3 Arabidopsis mutant.

Thereafter the expression level of the same panel of auxin-related genes (Table 14) was evaluated in leaf tissues. In the last decade several key factors involved in the regulation of leaf growth in *Arabidopsis thaliana* have been identified. Among them, hormone balance plays an extremely important role and several studies have demonstrated that the auxin has a key role in both initiation and elaboration of final morphology leaves and vascular networks (Benkova *et al*., 2003; Braybrook and Kuhlemeier, 2010).

To perform qRT-PCR analysis of gene expression we selected the third and fourth rosette leaves because they showed more clearly differences in size than other rosette leaves. Intriguingly, a lot of genes tested were differentially expressed in leaf tissue. Transcript levels of genes involved in the auxin transport as *PIN1, PIN3* and *PIN4*

were lower in the mutant compared with wild type as well as *SAUR76* which works in the signaling pathway (Fig 30).

Conversely, two genes implicated in auxin biosynthesis such as *YUCCA2* and *TAA1* (*TRYPTOPHAN AMINOTRANSFERASE OF ARABIDOPSIS 1*) were up-regulated more than two fold in *drm1 drm2 cmt3*. The auxin response factor *ARF7* also showed significant overexpression in the leaf mutant (Fig 30).

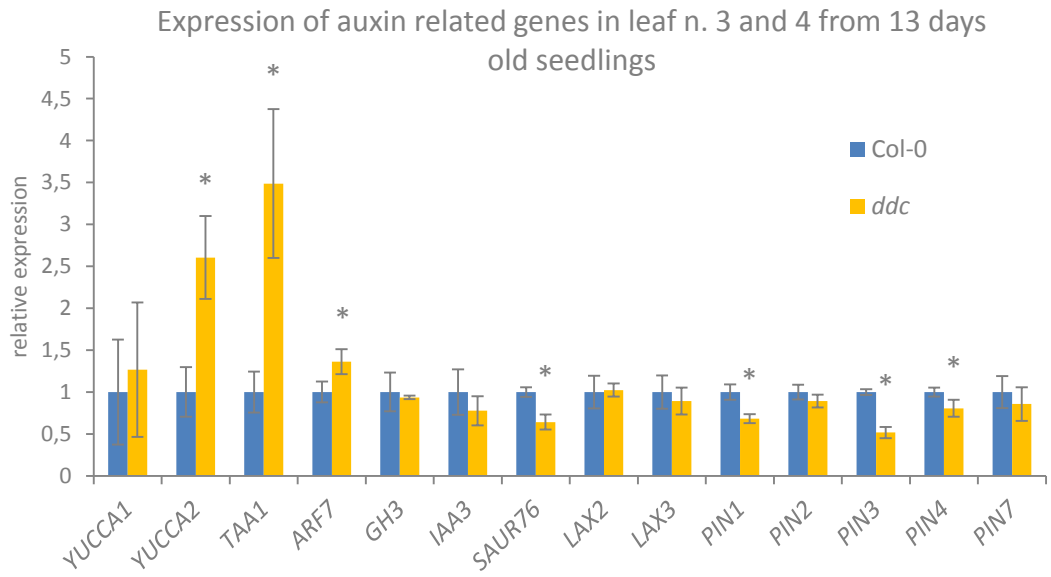

Figure 30. Expression analysis by qRT-PCR of auxin related genes in third and fourth leaf from 13 days old palnts grown on soil. The qRT-PCR data were normalized using *SAND* and *GAPDH* as housekeeping genes and analyzed by qBasePLUS software. The results represent the mean value (± standard deviation) of three independent biological replicates. Asterisks indicate significant pairwise differences using Student's t-test ($p \leq 0.05$).

On the basis of the curly phenotype and reduced epidermal cell size observed in the leaf of the *drm1 drm2 cmt3*, we decided to extend the transcriptional analysis to genes known to be involved in leaf development (Table 14).

The development of a growing leaf has been divided into three different stages: primordium initiation, primary morphogenesis and secondary morphogenesis (Donnelly *et al*., 1999). Leaf primordia initiate at the flanks of the shoot apical meristem. In the primary morphogenesis the growth is given by successive cell divisions. During secondary morphogenesis the cells cease proliferating and begin to expand. The transition from cell proliferation to cell expansion is like a gradient which proceed down the leaf, with stopping of cell division first in the tip and progressively down the longitudinal axis (Kazama *et al*., 2010). Then the cells start to expand increasing their

volume. The overall size of a growing leaf depends on the balance between cell growth and division.

Leaves 3 and 4 of 13 days old plants were selected for further investigating mechanisms of regulation involved in leaf growth. Indeed, at this particular developmental stage the majority of cells at the leaf base began to expand (Andiankaja *et al*., 2012).

Genes involved in leaf development	
AS1	***TCP2***
AS2	***TCP4***
STM	***DA1***
EXP10	***DELLA***
CLF	***RPT2a***
KNAT1	***SAUR19***
KNAT2	***SAUR36***
KNAT6	***MED25***

Table 14. Leaf development genes.

Interestingly, qRT-PCR analysis evidenced a significant down-regulation of two genes involved in the cell size regulation such as *EXP10* (*EXPANSIN 10*) and *TCP2* (*TCP FAMILY TRANSCRIPTION FACTOR 2) which* enhance cell expansion (Cho and Cosgrove, 2000; Ballester *et al*., 2014). Genes such as *SAUR19* (*Small Auxin Up-RNA19)* which promotes cell expansion (Spartz *et al*., 2012) and *SAUR36* (*Small Auxin Up-RNA36)* which negatively regulate cell growth (Hou *et al*., 2013) were not differentially expressed (Fig. 31).

Leaf final size strongly relies on the duration of the cell division phase and the proliferation rate. Therefore we also tested the expression levels of several genes involved in these processes such as *TCP4 (TCP FAMILY TRANSCRIPTION FACTOR 4), DA1(LARGE IN CHINESE), RPT2a (REGULATORY PARTICLE AAA-ATPASE 2A) and MED25 (MEDIATOR 25)* but no difference was found between triple methylation mutant and wild type (Fig. 31).

Subsequently, we decided to look more into the genes which have a role in organogenesis processes in the SAM. In leaf primordia initiation event which takes place in the shoot apical meristem, a complex network of two different families of transcription factors, class 1 KNOX and ARP [ASYMMETRIC LEAVES1 (AS1), ROUGH SHEATH2 (RS2), PHANTASTICA] (Byrne *et al*., 2002; Hay and Tsiantis, 2006, 2010), play

antagonistic roles in the regulation of the emergence of a young primordium. Class 1 *KNOX* genes are required for meristem function and the determination of leaf identity upon their down regulation.

In Arabidopsis AS1-AS2 complex functions as promoter of differentiation in leaf primordium by repressing class 1 *KNOX* homeobox genes in the shoot apical meristem (Byrne *et al*., 2002), indeed most of the class 1 *KNOX* genes are expressed in the shoot apical meristem and excluded from leaf primordia.

In *drm1 drm2 cmt3* we found levels of mRNA encoding for both components of the AS1-AS2 complex (ASYMMETRIC LEAVES 1 and 2) lower than wild type in leaf tissue (Fig. 31).

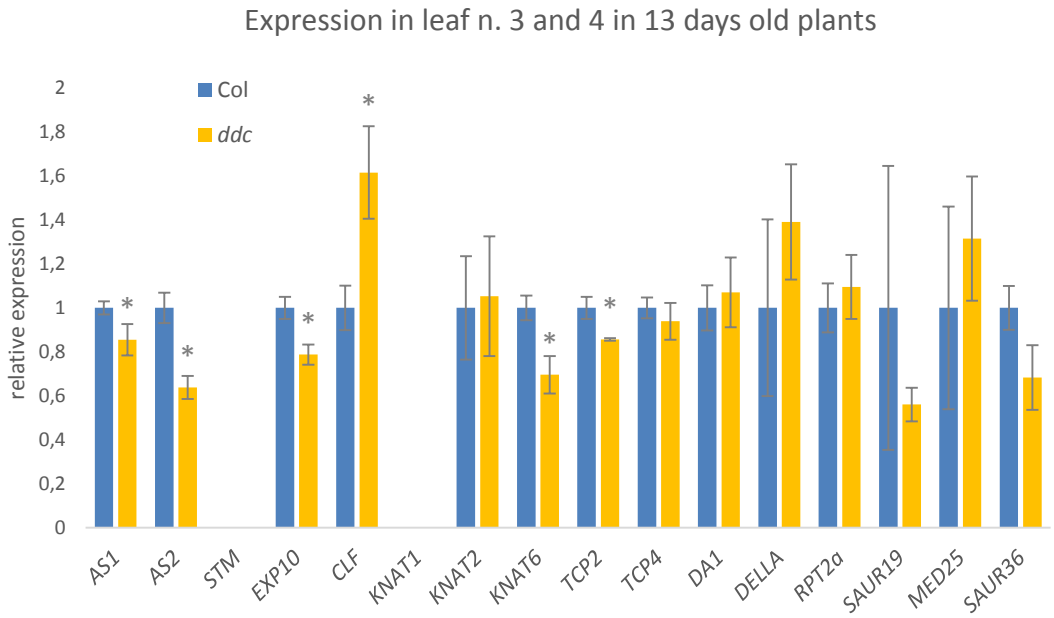

Figure 31. Expression analysis by qRT-PCR of leaf growth regulation in third and fourth leaf from 13 days old palnts grown on soil. The qRT-PCR data were normalized using *SAND* and *GAPDH* as housekeeping genes and analyzed by qBasePLUS software. The results represent the mean value (± standard deviation) of three independent biological replicates. Asterisks indicate significant pairwise differences using Student's t-test ($p \leq 0.05$).

Conversely than expected, no ectopic expression of *KNAT1* (*KNOTTED-LIKE FROM ARABIDOPSIS THALIANA 1*) and *STM* (*SHOOTMERISTEMLESS*) due to the *AS1* and *AS2* down-regulation were detected in leaves (Fig. 32).

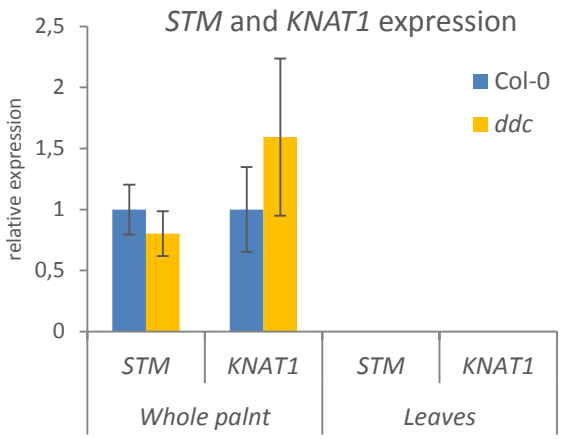

Figure 32. Expression analysis by qRT-PCR of *STM* and *BP/KNAT1* genes on whole plant and tissue from 3rd and 4th leaf of 13 days old seedlings. The qRT-PCR data were normalized using *SAND* and *GAPDH* as housekeeping genes and analyzed by qBasePLUS software. The results represent the mean value (± standard deviation) of three independent biological replicates. Asterisks indicate significant pairwise differences using Student's t-test ($p \leq 0.05$).

We also found differences in gene expression of *CLF* (*CURLY LEAF*) and *KNAT6* (*KNOTTED1-LIKE HOMEOBOX GENE 6*) which were up- and down-regulated respectively, in the third and fourth rosette leaves from 13 days old plants of *drm1 drm2 cmt3* (Fig. 31).

3.11 Methylation levels of up-regulated auxin genes in Arabidopsis *drm1 drm2 cmt3* mutant through MeDIP analysis.

As above mentioned, DNA methylation has been observed to play a role in mediating gene expression. Globally, these studies showed that more methylation at and near gene promoters is correlated with low or no transcription (Suzuki and Bird, 2008).

In this context, in the last part of the present study we aimed to investigate whether auxin genes overexpressed in the mutant were direct target of this epigenetic mechanism by testing the DNA methylation levels in their promoters. In order to get this information we decided to adopt a molecular biology approach performing Methylated DNA Immunoprecipitation experiment (MeDIP).

From published data there is a genomic region in *Arabidopsis thaliana* with intriguing requirement for components of the RdDM (RNA directed DNA Methylation) pathway. The region corresponds to the 5' UTR of the *HEI10* gene. Individual locus bisulfite sequencing of *HEI10* revealed that DNA methylation in all sequence contexts

(CG, CHG, CHH) was impaired in the *drm1 drm2 cmt3* methyltransferase mutant (Yang *et al*., 2016) (Fig. 33).

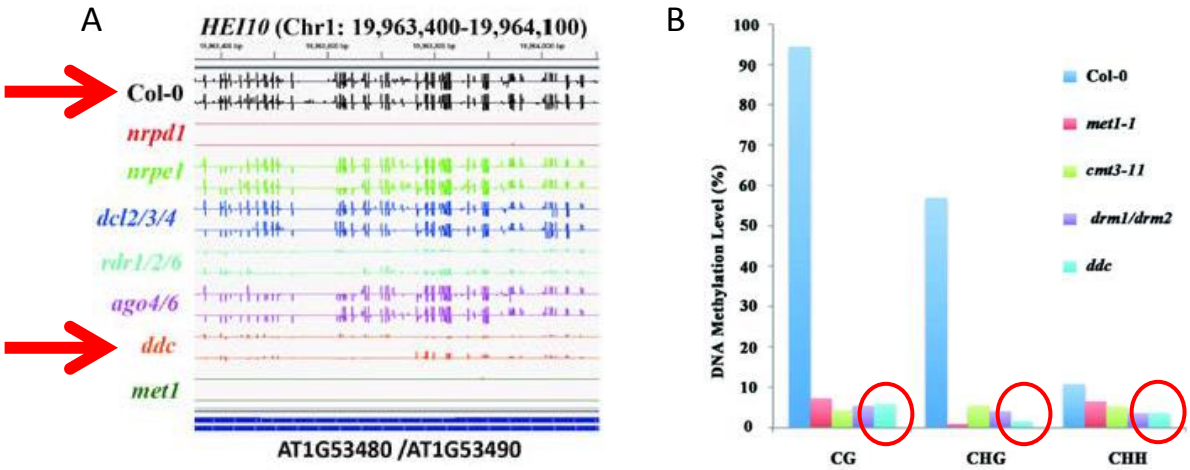

Figure 33. (**A**) IGV genome browser screenshots of DNA methylation levels at *HEI10* locus. DNA methylation levels are indicated by the height of the vertical bars in each row (Yang *et al*., 2016). Red arrows indicate Col-0 and *drm1 drm2 cmt3* mutant. (**B**) DNA methylation levels at the 5' UTR region of *HEI10* found by sodium bisulfite sequencing. Red circles indicate *drm1 drm2 cmt3* DNA methylation mutant (Yang *et al*., 2016).

We decided to use this region as control sample in MeDIP assays. First, the focus was to establish optimal experimental conditions and to minimize high background got in the pilot experiment which is often caused by too high concentration of antibody. After attempts with different concentration of antibody we found that the optimal conditions were obtained using 2 µg of antibody per reaction (Fig. 34). The good efficiency of the experiments was supported by the result obtained for the 5' UTR of the *HEI10* gene used as control that was hypomethylated in the mutant confirming data already known (Yang *et al*., 2016). Methylation levels are defined as the normalized ratio of IP enriched sample to Input sample, furthermore all the samples were normalized to *ACTIN7* gene.

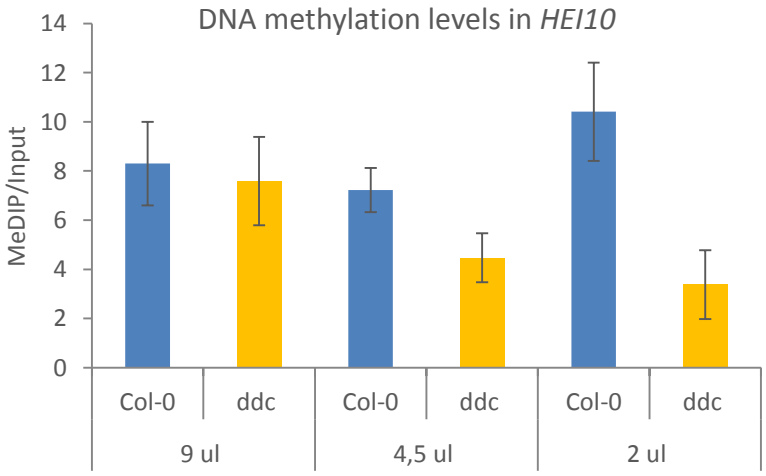

Figure 34. MeDIP experiment optimization by using different concentration of antibody anti 5-methylcytosine. The 5'UTR region was analyzed and relative amount of immunoprecipitation DNA fragments is determined by real-time PCR compared to wild-type. The immunoprecipitated fraction were normalized versus both input and the *ACTIN7* gene. The results represent the mean value (± standard deviation) of three independent biological replicates.

First we tested the DNA methylation levels in 21 days old whole seedling by MeDIP-qPCR.

Primers were designed for regions within the coding sequence and upstream the transcription start site of the *GH3* and *PIN2* genes. From the qRT-PCR analysis, indeed, these genes resulted to be overexpressed in 21 days old whole seedling. No significant differences were found in methylation levels within the regions tested of *GH3* and *PIN2* (Fig. 35).

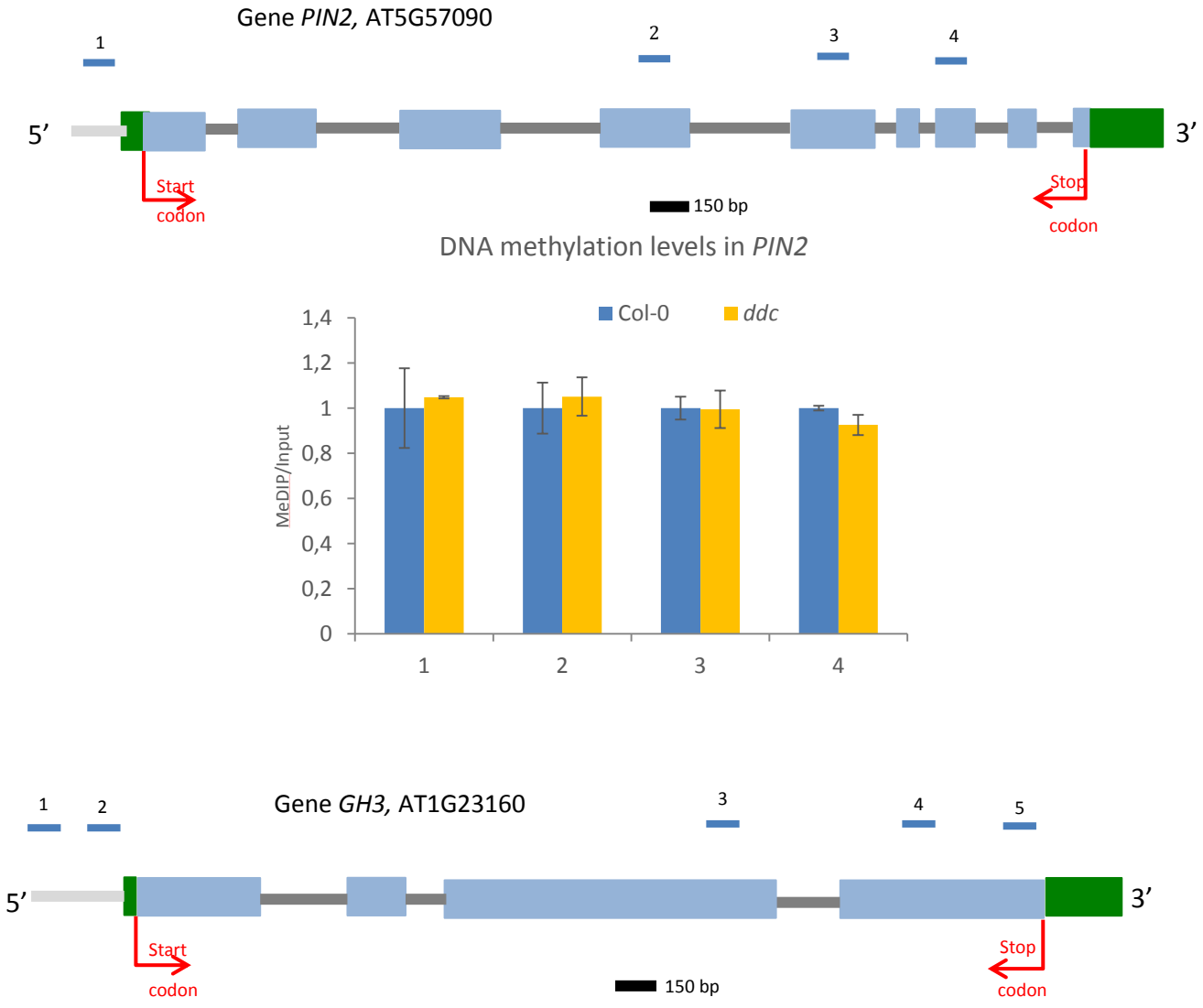

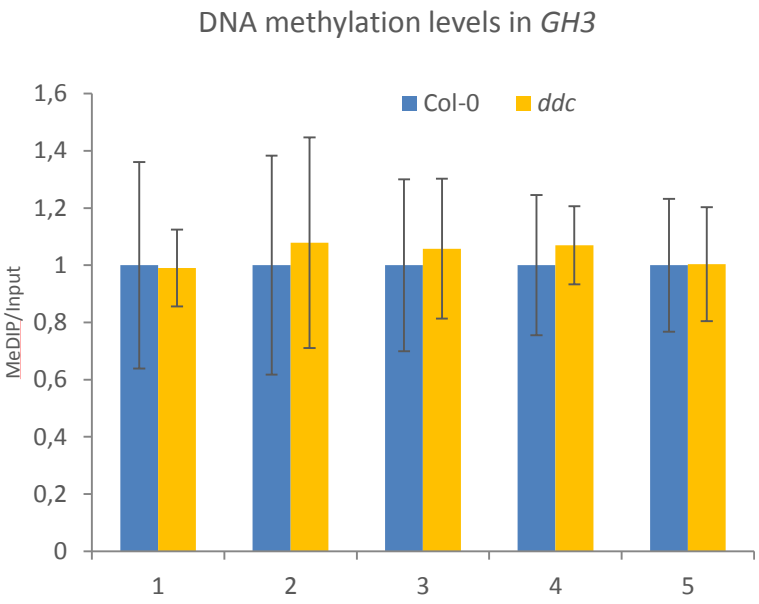

Figure 35. MeDIP Analysis at *PIN2* and *GH3* genes in 21 days old whole seedlings. On top the structures of every gene and the position of primers are indicated. Green and blue boxes represent untranslated region and exons, respectively; red arrows represent the start and the stop codon, respectively. The graphs show relative amount of immunoprecipitation DNA fragments determined by real-time PCR. The immunoprecipitated fraction were normalized versus both input and the *ACTIN7* gene. The results represent the mean value (± standard deviation) of three independent biological replicates. Asterisks indicate significant pairwise differences using Student's t-test ($p \leq 0.05$).

Based on the hypothesis that both transcription of certain genes and DNA methylation pattern might be somehow organ-specific we focused our attention on the leaves where major differences were found at both morphological and transcriptional level.

So enrichment analysis of methylated genomic DNA fragments from whole leaf genome was carried out by MeDIP-qPCR. Primers were designed for regions within *YUCCA2*, *TAA1* and *ARF7* promoters. Lower DNA methylation levels were found around 1,2 kb upstream the ATG site of *YUCCA2* gene in *drm1 drm2 cmt3* compared to Col-0 (Fig. 36).

This result is consistent with the up-regulation of this gene in leaves of the triple mutant. No significant differences were found in methylation levels within other regions tested in *TAA1* and *ARF7* (Fig. 36).

Gene *YUCCA2,* AT4G13260

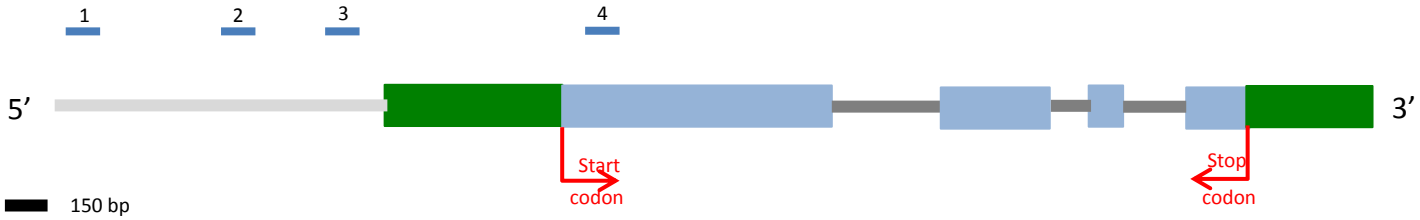

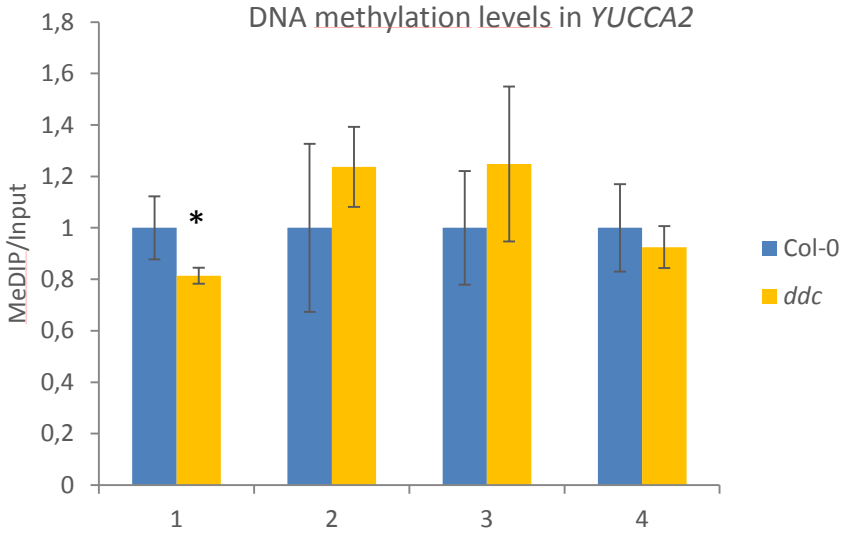

Gene *TAA1,* AT1G70560

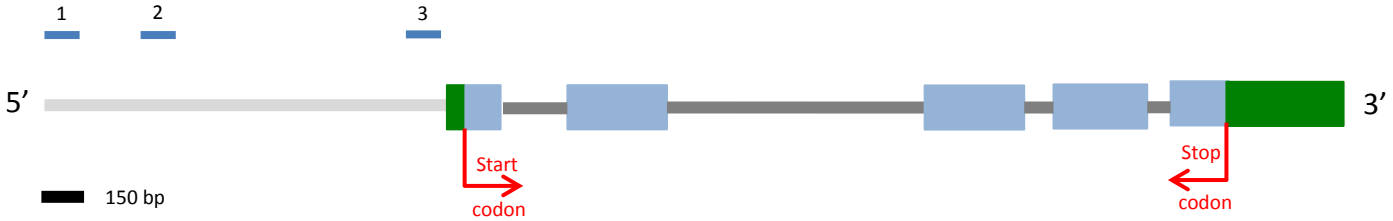

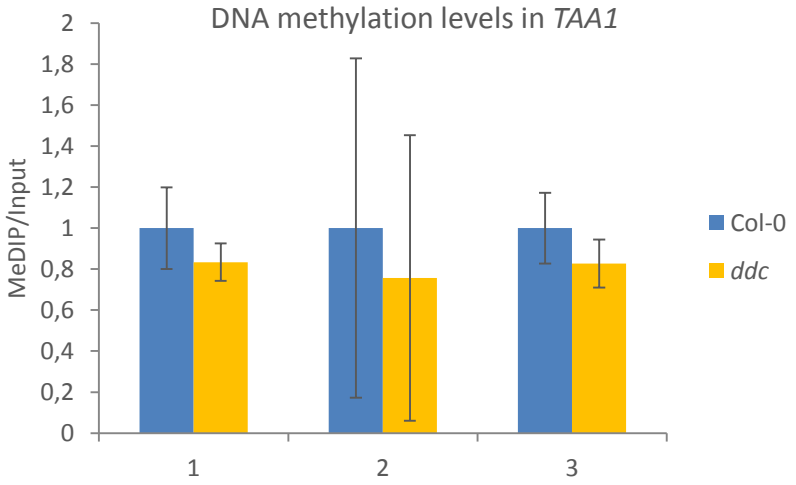

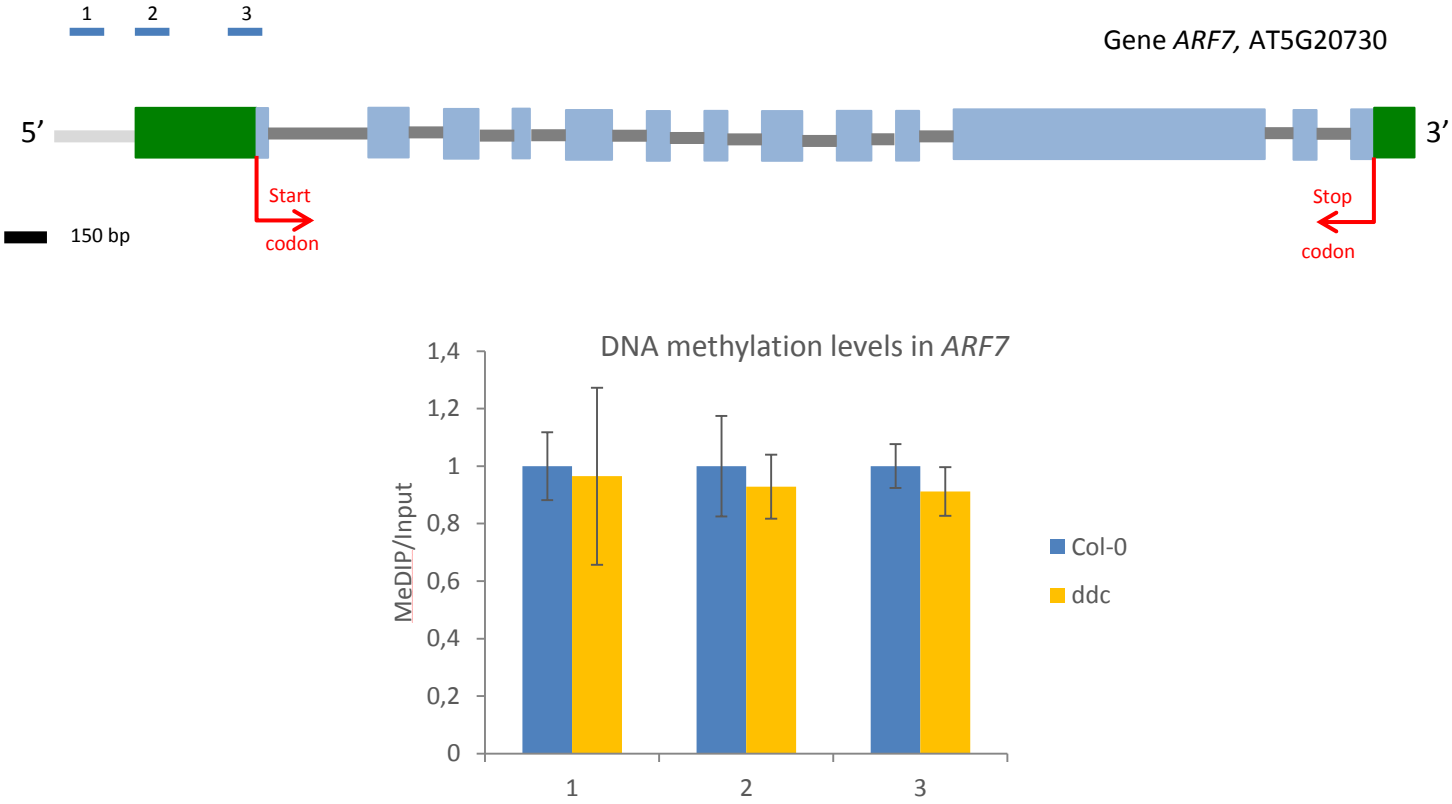

Figure 36. MeDIP Analysis at *YUCCA2, TAA1* and *ARF7* genes in leaf tissue. On top the structures of every gene and the position of primers are indicated. Green and blue boxes represent untranslated region and exons, respectively; red arrows represent the start and the stop codon, respectively. The graphs show relative amount of immunoprecipitation DNA fragments determined by real-time PCR. The immunoprecipitated fraction were normalized versus both input and the *ACTIN7* gene. The results represent the mean value (± standard deviation) of three independent biological replicates. Asterisks indicate significant pairwise differences using Student's t-test ($p \leq 0.05$).

3.12 ChIP analysis of CLF target genes.

We above discussed the documented interaction between different epigenetic mechanisms in controlling gene expression. In our study we found that among genes missregulated in the *drm1 drm2 cmt3* mutant there was *CLF* gene which encodes a component of PRC2 complex responsible for catalyzing H3K27 methylation together with MEA (MEDEA) and SWN (SWINGER) (Yu *et al.*, 2009). MEDEA works specifically in the female gametophyte and during seeds development (Grossniklaus *et al.*, 1998). SWN has a partially redundant function with CLF in regulating both vegetative and reproductive development. *CLF* gene is widely expressed in Arabidopsis during

development. It is involved in the control of leaf and flower morphology, as well as flowering time, via repressing floral homeotic gene *AG* (*AGAMOUS*) and the class *1 KNOX* gene *STM* by H3K27me3 (Goodrich *et al*. 1997; Schubert *et al*. 2006).

H3K27me3 accumulation marks silence developmental genes. The published dataset about whole genome analysis of histone H3 lysine 27 trimethylation in *Arabidopsis thaliana* shows that both *AS2*, *KNAT6* and *TCP2* genes are target of this kind of histone modification (Zhang *et al*., 2007). Thus, on the basis of the expression pattern of these genes in the leaf of triple mutant, our work hypothesis was that the down regulation of *AS1, AS2, KNAT6* and *TCP2* might be due to the overexpression *CLF* gene.

In order to verify such hypothesis we performed chromatin immunoprecipitation (ChIP) assay to verify whether in the *drm1 drm2 cmt3* mutant the level of H3K27me3 in *AS2, KNAT6* and *TCP2* genes was affected compared to wild type.

A new set of primers complementary to the promoter region and the transcription starting site (TSS) of *AS2* and the promoter region and the coding sequence of *TCP2* were designed. From published data we also picked up additional primer sequences, corresponding to genomic regions that were known to be target of histone methylation, complementary to the promoter region and the exon of *AS2* (Chen *et al*., 2013), to the promoter region and the body of the *KNAT6* gene (Lafos *et al*., 2011; Zhao *et al*., 2015), and to the body of the *TCP2* gene (Lafos *et al*., 2011) (Fig. 37). The relative enrichment of H3k27me3 levels was determined by real-time PCR. The results were normalized versus both Input sample and *ACTIN2* gene.

Increased H3K27me3 levels were detected in the proximal promoter region of *KNAT6* gene (*KNAT6-3* primers) in *drm1 drm2 cmt3*. The higher relative enrichment of H3k27me3 levels observed in this region is consistent on one hand with the down-regulation of the *KNAT6* gene expression and on the other hand with the up-regulation of the *CLF* gene expression in the mutant. By contrast, the H3K27me3 levels of the other tested regions in *KNAT6*, *AS2* and *TCP2* were not significantly altered in the mutant compared to Col-0 (Fig. 37).

Gene *AS2,* AT1G65620

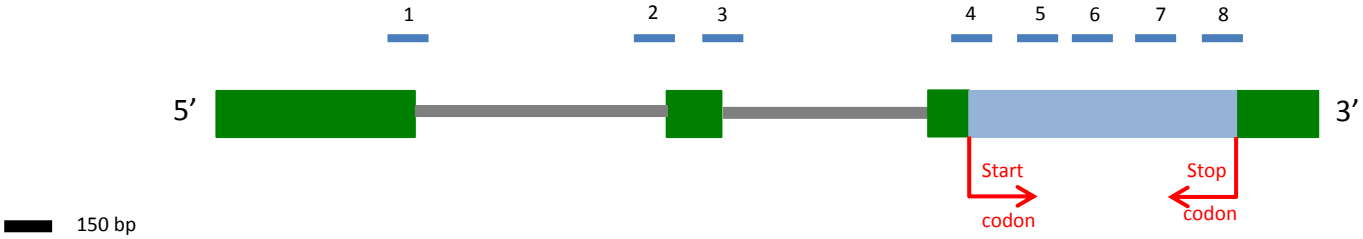

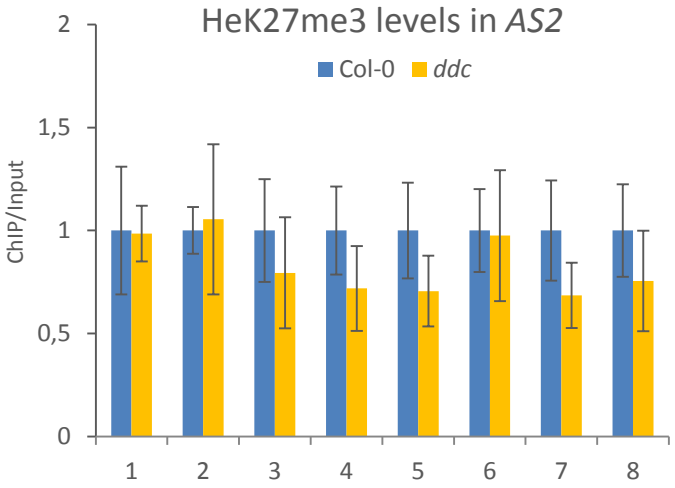

Gene *KNAT6,* AT1G23380

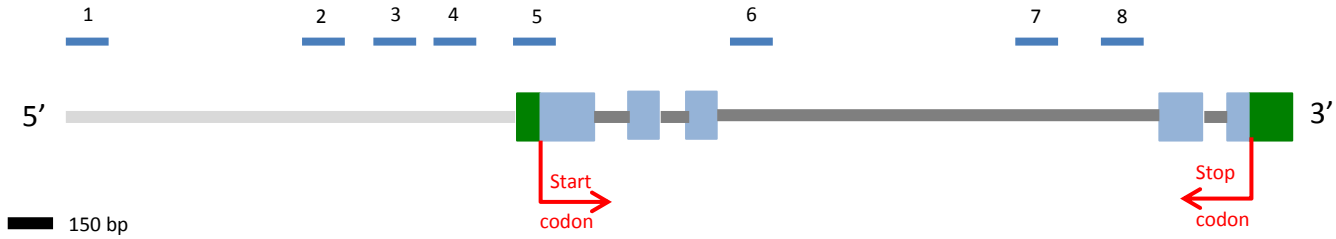

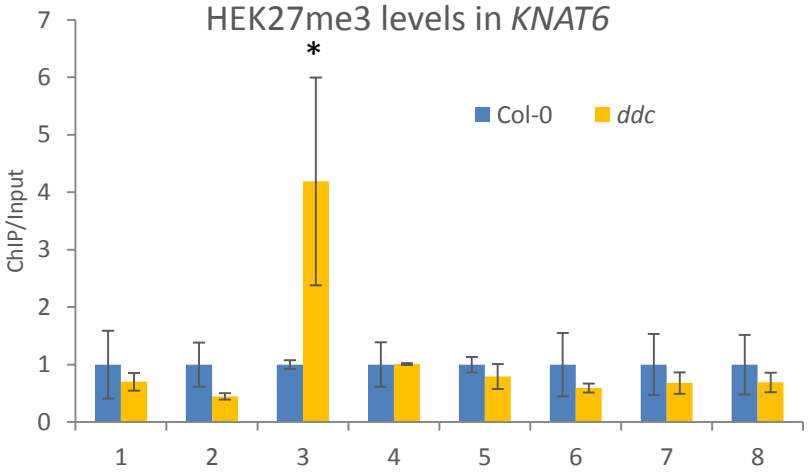

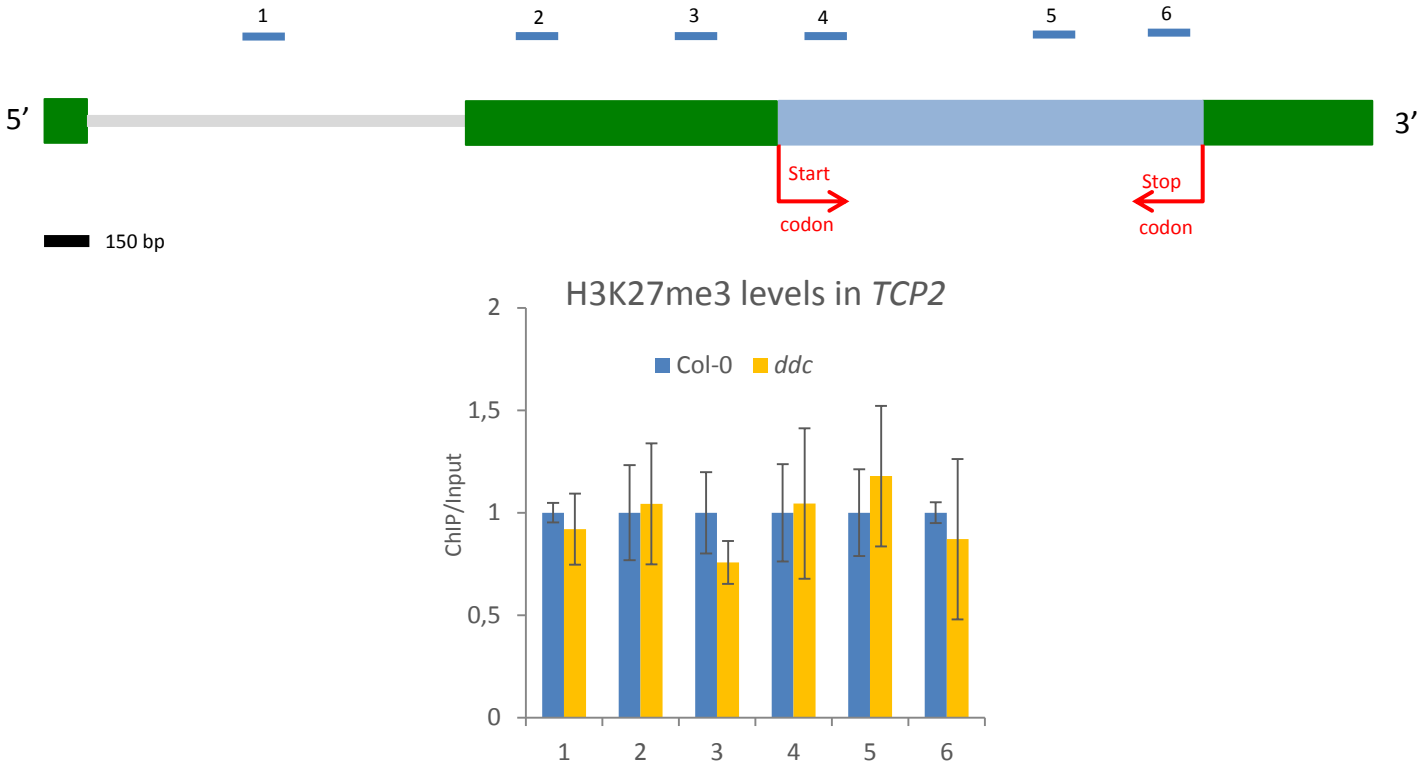

Figure 37. ChIP Analysis of H3K27me3 at *AS2, KNAT6* and *TCP2* genes in leaf tissue. On top the structures of every gene and the position of primers are indicated. Green and blue boxes represent untranslated region and exons, respectively; red arrows represent the start and the stop codon, respectively. The graphs show relative amount of immunoprecipitation DNA fragments determined by real-time PCR. The immunoprecipitated fraction were normalized versus both input and the *ACTIN2* gene. The results represent the mean value (± standard deviation) of three independent biological replicates. Asterisks indicate significant pairwise differences using Student's t-test ($p \leq 0.05$).

CHAPTER 4: DISCUSSION

Unlike other organisms where DNA methylation mutants are unviable because lethal, the model plant *Arabidopsis thaliana* can tolerate mutations that eliminate methylation, allowing for further investigations. Thus, the large collections of *Arabidopsis thaliana* T-DNA insertion mutants are among the most important resources that can be employed in the study of this epigenetic modification.

Previously characterized methylation-deficient Arabidopsis lines with defects in either the *SWI2/SNF2* chromatin remodeling factor-related gene *DDM1* (Kakutani *et al*., 1996) or the Dnmt1-related *MET1* gene displayed developmental abnormalities (Finnegan *et al*., 1996; Ronemus *et al*., 1996) such as the reduced vegetative growth and the impaired female and male gametogenesis, embryogenesis and seed viability detected in *met1* (Xiao *et al*., 2006). In contrast to *met1* single mutant, mutations in either DRMs or CMT3 do not result into visible phenotypes (Lindroth *et al*., 2001; Cao and Jacobsen, 2002b). Therefore, it has been proposed that DRMs and CMT3 act in a partially redundant and locus-specific manner to control non-CG methylations (Cao and Jacobsen, 2002a). In the Landsberg erecta (Ler) ecotype the *drm1 drm2* double mutant neither showed morphological differences from the wild type. Whereas the triple *drm1 drm2 cmt3* mutant evidenced pleiotropic phenotypic abnormalities, dealing with plant size, leaf shape and seed production (Cao and Jacobsen, 2002a; Chan *et al*., 2006) likely due to the functional redundancy of DRMs and CMT3.

In the present study, we identified similar and novel developmental defects in the *Arabidopsis thaliana* triple DNA methylation mutant *drm1 drm2 cmt3* in Columbia background. In particular these novel defects deal with a reduced and agravitropic root growth as well as with an altered differentiation pattern of the leaf as evidenced by reduced cell size and increased stomatal density and index.

Preliminarily, in order to better understand the impact of methylation status on the pattern and growth of plant organs we investigated the expression level of the genes *DRM1*, *DRM2* and *CMT3,* that are interrupted by the T-DNA insertion in the triple mutant *drm1 drm2 cmt3*, in the different organs of Arabidopsis wild-type plants with the aim to asses possible organ/tissue specific function (Fig. 8) . Globally, all the genes resulted expressed in the various organs although in some of them at very different levels. In particular, *DRM1* and *CMT3* genes exhibited the highest expression in the flower suggesting a their pivotal role in the development of this organ. Despite this

result, no visible alteration in the flower structure was detected in the triple mutant. Indeed, we did not observe defects commonly seen in the *ddm1* and *met1* methylation mutants, such as *clavata*-like flowers, *apetala2*-like flowers, *agamous*-like flowers, *sup*-like flowers, or extreme late flowering (Finnegan *et al*., 2006; Ronemus *et al*., 1996; Grossniklaus *et al*., 1998; Jacobsen *et al*., 2000). However it must be underlined that when gene expression was analyzed at different developmental stage of the flower, differences in *CMT3* and *DRM1* expression, consisting into a lower transcript level, were detected only starting from the second and third stage, respectively (Fig. 12). Since these two stages are related to gamete formation and fertilization process rather than flower organ formation, these results are consistent with the reduced seed density observed in the siliques of the triple mutant. Notwithstanding, the role of these methyltransferases in flower development processes remains still poorly understood.

Conversely than expected, the major defects were found in the root and leaves of the *drm1 drm2 cmt3* mutant. Concerning the root, the mutant exhibited a reduced length and a stronger bending of primary root compared to those of the wild type Col-0 (Fig. 18 A and 20). Similar defects in root gravitropic growth were found in auxin related mutants *aux1-7* (Swarup *et al*., 2001), *pin2 eir1-1* (Müller *et al*., 1998), suggesting that the root phenotype of the *drm1 drm2 cmt3* was somehow connected with the auxin pathway. Namely, auxin is crucial for proper development of the root, and is involved in several physiological mechanisms, such as gravity response acting as central mediator of gravitropic stimulus (Chen *et al*. 2002). According to the role of auxin in root growth, the use of the construct *proDR5:GFP* revealed a lower accumulation of this hormone in the primary root of the *drm1 drm2 cmt3* triple mutant compared to the wild-type and mainly in the root calyptra which represents the gravity sensing tissue (Fig. 25).

A higher accumulation of auxin was instead detected in the leaves of *drm1 drm2 cmt3* mutant (Fig. 27) consistently with the curly leaf phenotype and the altered leaf patterning which is tightly controlled by auxin (Zažímalová *et al*., 2014). Interestingly such extra-accumulation of auxin in the leaf of mutant was found to be associated to an enhanced expression level of auxin-related genes, including *YUCCA2,* which modulate the biosynthesis of this hormone (Fig. 30). In addition a downregulation of several members of the *PIN* family genes was also detected in the leaf of the *drm1 drm2 cmt3* mutant. It is known that shift in PINs polarization, from a polarization towards the auxin maximum of primordium to a basal localization towards the developing leaf, is quite essential for leaf growth and differentiation (Bar and Ori, 2014). Thus the obtained results strongly support the idea that hyper-production of auxin was coupled to an

impaired translocation through the membrane-localized PIN proteins that directly influence the amount and direction of auxin flow during leaf development (Bennet *et al*., 2014). Accordingly, there are evidences that mutations in members of auxin transporters are associated with spatially disorganized initiation of leaf primordia as well as with narrow and downwardly rolled rosette leaves (Bainbridge *et al*., 2008) confirming the role of auxin transport in in leaves and plant architecture.

All the above discussed results clearly demonstrated that methylation status impact on auxin pathway (metabolism, transport, perception, and signaling) in an organ specific manner.

In addition, we tested the response to exogenous auxin supply on the growth of different plant organs such as root, hypocotyl as reported in supplemental material. The preliminary results results indicate that the sensitivity of *drm1 drm2 cmt3* to the exogenous IAA is felt in an organ specific manner and looks slightly different compared to wild type.

Moreover, our findings also demonstrated that there is a direct organ-specific modulation of auxin biosynthetic pathways by DNA methylation. Namely, hypomethylation was detected by MeDIP assay in the promoter region of the *YUCCA2* gene in the *drm1 drm2 cmt3* mutant (Fig. 36) indicating that this genomic region is a direct target for methylation carried out by DRMs or CMT3 methyltransferases which in turn can result into the overexpression of the gene.

Among the genes differentially expressed in the leaf of the *drm1 drm2 cmt3* mutant compared to Col-0 we also found *KNAT6,* a class 1 *KNOX* gene, and *AS2* (Fig. 31). As above discussed, these two genes are component of the complex genetic network involved in the regulation of leaf development, from primordia initiation to abaxial/adaxial polarity and blade growth, thus contributing to determine the leaf patterning and its final size and shape (Goodrich *et al*. 1997; Schubert *et al*. 2006). In particular, it is known that a transient indeterminate growth is maintained in specific regions of the growing leaf such as at the leaf base or the leaf tip, depending on the species (Tsukaya, 2014), and above all at the leaf margin that possess organogenic potential (i.e marginal blastozones). Several studies have shown that KNOX proteins also play important roles in maintaining this transient morphogenetic window during leaf development (Hay and Tsiantis, 2010). On the other hand *AS2* is involved in the differentiation of abaxial/adaxial cell fate which is critical for leaf function determining leaf polarity (Barkoulas *et al*., 2007). Hence, the reduced growth of the triple mutant leaves which involved a reduced expansion of epidermal cells as well as the alteration of

its differentiation pattern might be linked to the altered expression pattern of these genes.

Many studies have demonstrated that the different epigenetic mechanisms interplay with each other rather than work independently. On this basis our attention was focused on the regulation of *CLF* gene, which resulted over-expressed in the leaf of *drm1 drm2 cmt3* (Fig. 31). CLF is one of the components of PCR2 complex that establishes and maintains trimethylation of histone H3 lysine 27 in both plants and animals. Trimethylation of histone H3 lysine 27 is an epigenetic mark associated with transcriptional repression of a large number of genes in Arabidopsis (about 4400) acting through chromatin remodeling (Zhang *et al*., 2007). However, despite its relevant role how PRC2 is recruited to specific regions of plant genomes is still not clear (Simon and Kingston, 2009).

High-resolution genome-wide mapping and functional analysis of DNA methylation and histone modifications in Arabidopsis revealed interesting interaction between H3K9me2 and DNA methylation (Bernatavichute *et al*., 2008). Namely, it has been demonstrated that the SRA domain of KYP/SUVH4, which is the H3K9me2 specific histone methyltransferase, binds directly to methylated CG sequence contexts, suggesting a role of DNA methylation in recruiting H3K9 methyltransferases. In turn, CMT3 contains a chromodomain that interacts with H3K9me2 in vitro, indicating maintenance of non-CpG methylation requires di-methylation of H3K9 (Johnson *et al*., 2002). So far, only an indirect correlation has been postulated between H3K27me3 and DNA methylation in Arabidopsis, where regions enriched by H3K27me3 are significantly hypomethylated (Zhang *et al*., 2007).

In this context, given *CLF* overexpression in *drm1 drm2 cmt3* mutant we moved our focus on a subset of genes, downregulated in the leaf of the triple mutant, which are target of H3K27me3 (Zhang *et al*., 2007). Among all the investigated genes we found increased H3K27me3 levels in the region upstream of the transcription start site of *KNAT6* gene (Fig. 37). We postulate that the increased H3K27me3 epigenetic modification by increased *CLF* expression, directly or indirectly related to the hypomethylation status of the triple mutant, might explain the downregulation of *KNAT6*. Further investigation are in progress to fully understand the framework of such novel correlation between these two epigenetic marks.

Conclusion

In summary, through the study of a triple DNA methylation mutant of *Arabidopsis thaliana*, we demonstrated that DNA methylation play a key role in the transcriptional control of genes which are relevant in the regulation of plant development. For some of these genes an organ-specific modulation has been assessed showing that, in the interweaved landscape of different networks that control gene expression, the pattern of DNA methylation is dynamic and related to the organ-specific growth.

We also demonstrated that most of the genes differentially expressed in the mutant were related to auxin hormone pathway, from biosynthesis to transport and signaling. A concomitance between differential expression of auxin-related genes and altered auxin accumulation in the plant organs has been verified.

In addition through MeDIP technology, which allows to identify genomic differences in DNA methylation, for some of these genes a direct relationship between methylation pattern and expression level has been demonstrated. Moreover we optimized the method and improved the efficiency of this technique making it a powerful tool for the comparative analysis of methylated regions.

Finally, we discovered a way through which DNA methylation can indirectly interacts with H3K27me3 and identified some of the genes which are ultimate target of this interplaying epigenetic regulation.

On the basis of these results, taking as model the leaf where major results have been so far obtained, below we would like to propose a partial model of the molecular framework underlying the relationship between DNA methylation status and plant development.

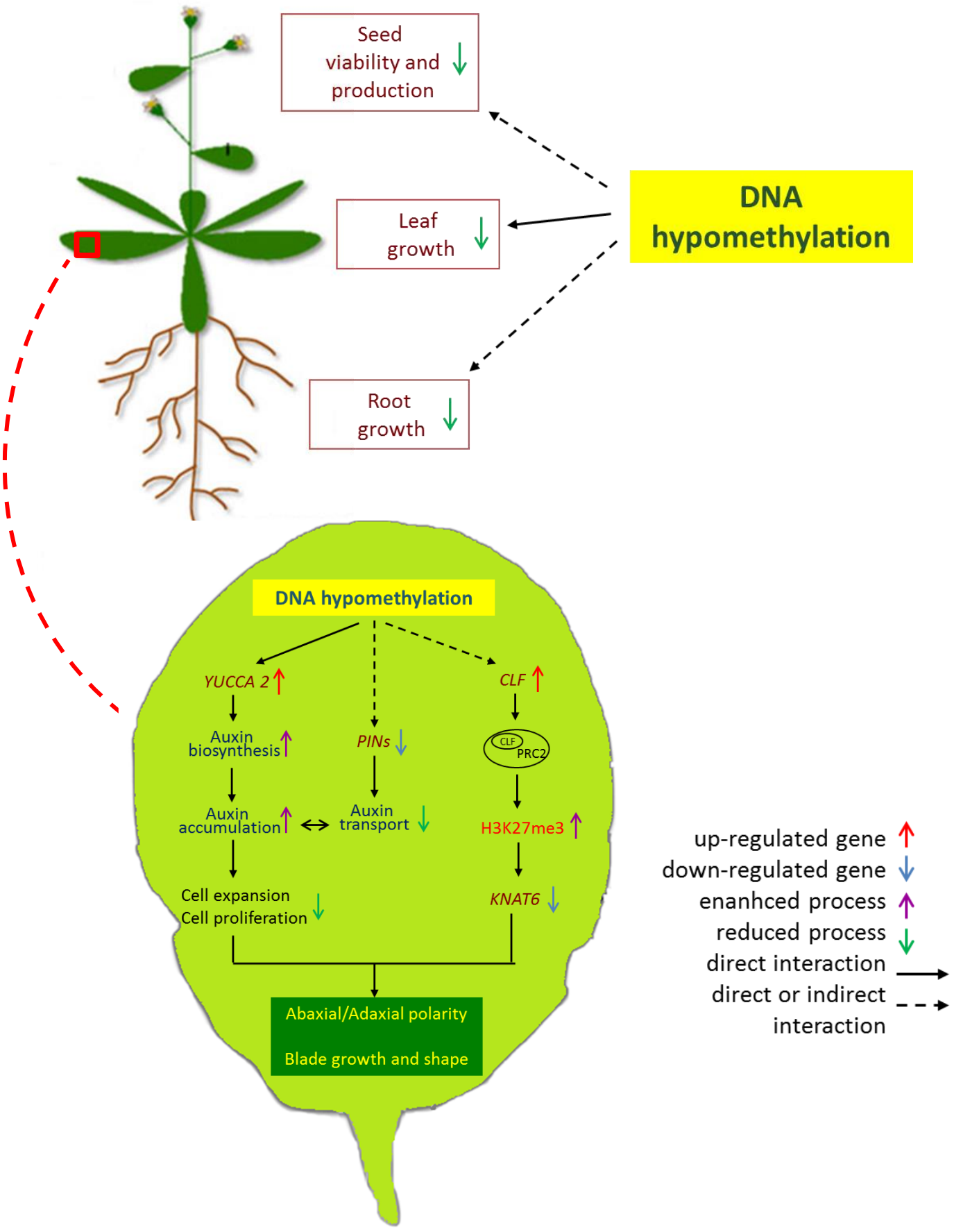
Seed viability and production
Leaf growth
Root growth
DNA hypomethylation
DNA hypomethylation
YUCCA 2
Auxin biosynthesis
Auxin accumulation
PINs
Auxin transport
CLF
CLF
PRC2
H3K27me3
KNAT6
Cell expansion
Cell proliferation
Abaxial/Adaxial polarity
Blade growth and shape
up-regulated gene
down-regulated gene
enanhced process
reduced process
direct interaction
direct or indirect interaction

Figure 38. Scheme shows: (i) the organs of Arabidopsis plant where DNA hypomethylation status caused a phenotype (ii) the genetic network underling the relationship between DNA methylation status and leaf development: DNA methylation is responsible for a reduced seed production and viability, abnormal leaf growth with smaller epidermal cells resulting in a curly shape, reduced primary root growth and agravitropic behaviour. In particular, leaf phenotype is clearly related to a missexpression of auxin-related genes which causes an extra-accumulation of the hormone due to an enhanced biosynthesis and a reduced translocation away from the leaf . Hypomethylation status directly impact on this pathway through the hypomethylation of promoter region of *YUCCA 2* gene, involved in auxin biosynthesis, which in turn results into its overexpression. An indirect interaction between DNA methylation and H3K27me3 epigenetic mark is proposed in that the overexpression of *CLF* gene, a component of PCR2 complex that performs trimethylation of histone H3 lysine 27, is accompanied by a high level of histone methylation and by a consequent down-regulation of *KNAT6* gene which play a role in defining leaf abaxial/adaxial polarity and in blade growth.

Supplemental material

As largely discussed in the thesis several developmental processes are directed to a large degree by transcription factors, which connect hormone and other signal transduction pathways with the regulation of specific genes important for directly altering plant growth and architecture (Kaufmann *et al*., 2010). Accordingly, in our work we observed that most of the genes differentially expressed in the mutant were related to auxin hormone pathway in an organ-specific manner. This prompted us to perform some preliminary experiments to verify the effect of exogenous auxin supply on the growth of different plant organs such as root, hypocotyl and cotyledon. Namely, mutant seedlings with alterations in auxin levels or auxin perception could exhibit different sensitivity to such treatment or even display the complete opposite response, elongating in the presence of exogenous hormone.

Here, we report the dose response curves for root and hypocotyl length and cotyledon area of seedlings grown in the presence of exogenous indole-3-acetic acid (IAA) (Fig. S1, S2 and S3). The following concentrations: 0 - 0.02 - 0.2 - 1 µM IAA; seedlings were grown under 16 hours light - 8 hours dark conditions.

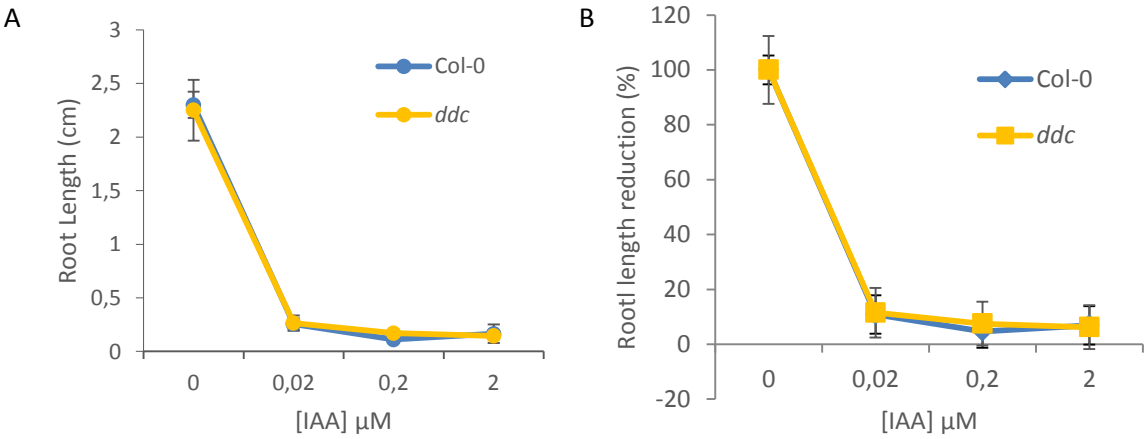

Figure S1. Dose responses of root length (cm) to IAA in Col-0 and *drm1 drm2 cmt3*. Root length was measured at 6 days. Data represent (**A**) the mean value of 30 seedlings expressed and (**B**) the percentage (%) of root length reduction. Error bars represent the standard deviation.

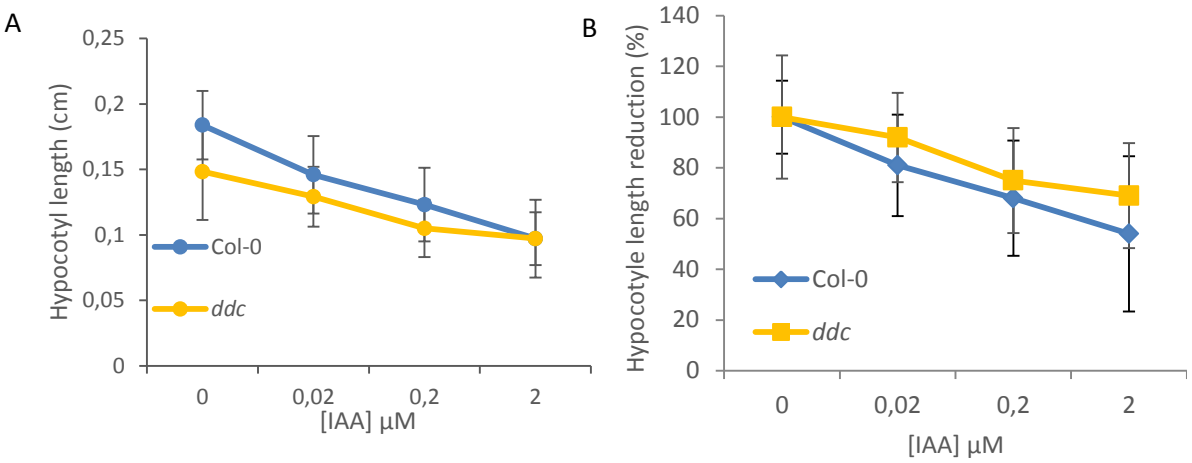

Figure S2. Dose responses of hypocotyl length (cm) to IAA in Col-0 and *drm1 drm2 cmt3*. Hypocotyl length was measured at 6 days. Data represent (**A**) the mean value of 30 seedlings expressed and (**B**) the percentage (%) of hypocotyl length reduction. Error bars represent the standard deviation.

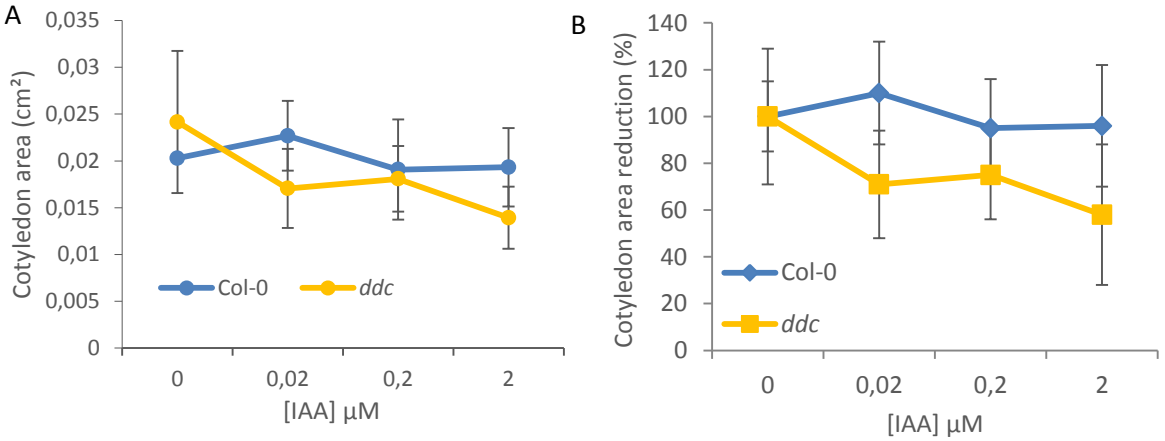

Figure S3. Dose responses of cotyledon area (cm^2) to IAA in Col-0 and *drm1 drm2 cmt3*. Cotyledon area was measured at 6 days. Data represent (**A**) the mean value of 30 seedlings expressed and (**B**) the percentage (%) of cotyledon area reduction. Error bars represent the standard deviation.

As evident in figure S1, S2, and S3, in our conditions, IAA does not promote the growth of *drm1 drm2 cmt3* and Col-0 seedlings at any concentration tested. Conversely, the tested concentration resulted to be inhibitory for root growth of both Col-0 and mutant (Fig. S1) suggesting that lower concentrations and/or different light conditions needs to be analysed, to verify whether *drm1 drm2 cmt3* response can be reversed.

A trend for a reduction of hypocotyl length was also observed in both *drm1 drm2 cmt3* and wild type (Fig. S2 B). However, even if differences were not statistically significant (Fig. S2 A and B) at 2 µM of IAA the mutant showed a minor reduction of the

hypocotyl in terms of percentage compared to Col-0. Therefore a different sensitivity of the mutant to IAA seems to emerge which deserves further investigations by testing different IAA concentrations and/or different light conditions.

Conversely, in cotyledons a trend for a reduction of the area was visible only in the triple mutant, although not statistically significant, whereas Col-0 was not affected by the different concentration of exogenous auxin (Fig. S3 A and B). This results thus confirms the hypothesis of a different sensitivity to IAA of the mutant compared to the wild type, even if in an opposite way with respect to hypocotyl (i.e. major vs minor sensitivity in cotyledons and hypocotyl, respectively). That is not surprising, since it is well documented that in plants different organs respond to the same hormone in different way (Davies, 2010).

In summary, these preliminary results indicate that the sensitivity of *drm1 drm2 cmt3* to the exogenous IAA is felt in an organ specific manner and looks slightly different compared to wild type.

These findings prompt us to investigate in the future about the optimal concentrations of IAA in order to get visible difference in the response to the treatment with exogenous auxin. The different approach may open new perspectives and clarify the relationship between hypomethylation status of the plant and auxin hormone.

Acknowledgements

It would not have been possible to write this doctoral thesis without the help and support of the kind people around me. There are so many people to thank for helping me during the last three years.

First, I express my deep gratitude to Prof. Maria Beatrice Bitonti and my supervisor Dott. Leonardo Bruno for providing me a PhD position and the exceptional opportunity to work in their research group as well as considerable support in this thesis. I thank you once again for their constructive criticism and for giving me the opportunity to have a scientific experience abroad. I would also like to extend a thank you to Prof. Adriana Chiappetta for all her contributions of time and suggestions.

Special thanks go to all the lab mates: Antonella, Olimpia, Marianna, Lia, Michele, Davide, Bernardo, Liam and Felicity. I want to thank you for the friendly work environment that you contributed to create. In the lab I found colleagues but mainly friends with which share positive and negative moments, a lot of laughs and good times.

I am grateful to Prof. Mieke Van Lijsebettens that gave me the possibility to work in her lab at Plant System Biology in Ghent. It was a honor to be part of her research group for fourteen months. Thank you so much for the scientific discussions, good ideas, motivations and the moral support in addition to her amazing optimism. Much of my experimental work would have not been performed without the teachings of Magdalena Woloszynska that guided me to optimize the experimental conditions, data analysis and gave me many scientific advices.

Special words go also to all the members of the Chromatin and Growth Control Group: Pia, Liz, Sabine, Griet, Carina, Martin, Stijn and Mike. I would like to thank you all for the nice chats during the lunch and the coffee break.

Thank you to all the people I met in Ghent with which I spent my free time. Together with the lab colleagues they contributed for making me feel at home.

A huge thanks goes out to all my flat mates Alessandro, Tonino, Benny, Salvatore and to all the friends in Palmi. They really tolerated me over all these years. So many stories to tell and funny times.

I am thankful to my parents, my brothers, my aunts, my uncles and my cousins for supporting me spiritually throughout all these three years and my life in general. Thanks to my mother for her love and all the luggage full of clothes and food. Thanks to

my father for his “good luck” said before jumping on the train every week. Thank you for always believing in me. I always feel you by my side.

Last but not the least, loving thanks to my half of the apple, Mariagrazia. Without her encouragement, understanding, love and patience it would have been impossible for me to finish this work.

References:

Aida M, Beis D, Heidstra R, Willemsen V, Blilou I, Galinha C, Nussaume L, Noh YS, Amasino R, Scheres B (2004) The PLETHORA genes mediate patterning of the Arabidopsis root stem cell niche. *Cell* 119(1):109-20.

Andriankaja M, Dhondt S, De Bodt S, Vanhaeren H, Coppens F,DeMilde L, Mühlenbock P, Skirycz A, Gonzalez N, Beemster GT, and Inzé D (2012) Exit from proliferation during leaf development in Arabidopsis thaliana: a not-so-gradual process. *Dev Cell* 22(1): 64–78.

Ausiò J (2006) Histone variants—the structure behind the function. *Brief Funct Genomic Proteomic* 5(3):228-43.

Bainbridge K, Guyomarc'h S, Bayer E, Swarup R, Bennett M, Mandel T, Kuhlemeier C (2008) Auxin influx carriers stabilize phyllotactic patterning. *Genes Dev* 22(6):810-23.

Ballester P, Navarrete-Gómez M, Carbonero P, Oñate-Sánchez L, Ferrándiz C (2015) Leaf expansion in Arabidopsis is controlled by a TCP-NGA regulatory module likely conserved in distantly related species. *Physiol Plant* 155(1):21-32.

Bar M and Ori N (2014) Leaf development and morphogenesis. *Development* 141(22):4219-30.

Barkoulas M, Galinha C, Grigg SP, Tsiantis M (2007) From genes to shape: regulatory interactions in leaf development. *Curr Opin Plant Biol* 10(6):660-6.

Benková E, Michniewicz M, Sauer M, Teichmann T, Seifertová D, Jürgens G, Friml J (2003) Local, efflux-dependent auxin gradients as a common module for plant organ formation. *Cell* 115(5):591-602.

Bennett T, Hines G, Leyser O (2014) Canalization: what the flux? *Trends Genet* 30(2):41-8.

Berger SL, Kouzarides T, Shiekhattar R, Shilatifard A (2009) An operational definition of epigenetics. *Genes Dev* 23(7):781-3.

Bernatavichute YV, Zhang X, Cokus S, Pellegrini M, Jacobsen SE (2008) Genome-wide association of histone H3 lysine nine methylation with CHG DNA methylation in *Arabidopsis thaliana*. *PLoS One* 3(9):e3156.

Bickle TA, Krüger DH (1993) Biology of DNA restriction. *Microbiol Rev* 57(2):434-50.

Bitonti MB, Chiappetta A (2010) "Root apical meristem pattern: hormone circuitry and transcriptional networks". In *Progress in Botany*, Luttge U, Beyschlag W, Büdel B, Francis D (a cura di), : Springer-Verlag, , Vol. 72, pp. 37-71.

Bitonti MB, Cozza R, Chiappetta A, Giannino D, Ruffini Castiglione M, Dewitte W, Mariotti D, Van Onckelen H, Innocenti AM (2002) Distinct nuclear organization, DNA methylation pattern and cytokinin distribution mark juvenile, juvenile-like and adult vegetative apical meristems in peach (Prunus persica (L.) Batsch). *J Exp Bot* 53(371):1047-54.

Blilou I, Xu J, Wildwater M, Willemsen V, Paponov I, Friml J, Heidstra R, Aida M, Palme K, Scheres B (2005) The PIN auxin efflux facilitator network controls growth and patterning in *Arabidopsis* roots. *Nature* 433(7021):39-44.

Boyes J, Bird A (1991) DNA methylation inhibits transcription indirectly via a methyl-CpG binding protein. *Cell* 64(6):1123-1134.

Braybrook SA, Kuhlemeier C (2010) How a plant builds leaves. *Plant Cell* 22(4):1006-18.

Byrne ME, Barley R, Curtis M, Arroyo JM, Dunham M, Hudson A, Martienssen RA (2000) Asymmetric leaves1 mediates leaf patterning and stem cell function in Arabidopsis. *Nature* 408(6815):967-71.

Byrne ME, Simorowski J, Martienssen RA (2002) ASYMMETRIC LEAVES1 reveals knox gene redundancy in *Arabidopsis*. *Development* 129(8): 1957–1965.

Cao J and Yan Q (2012) Histone ubiquitination and deubiquitination in transcription, DNA damage response, and cancer. *Front Oncol* 12;2:26.

Cao X, Aufsatz W, Zilberman D, Mette MF, Huang MS, Matzke M, Jacobsen SE (2003) Role of the *DRM* and *CMT3* methyltransferases in RNA-directed DNA methylation. *Current Biology* 13(24):212–2217.

Cao X, Jacobsen SE (2002a) Locus-specific control of asymmetric and CpNpG methylation by the DRM and CMT3 methyltransferase genes. *Proc Natl Acad Sci* USA 99:16491–16498.

Cao X, Jacobsen SE (2002b) Role of the arabidopsis DRM methyltransferases in de novo DNA methylation and gene silencing. *Curr Biol* 12(13):1138-44.

Casamitjana-Martínez E, Hofhuis HF, Xu J, Liu CM, Heidstra R, Scheres B (2003) Root-specific CLE19 overexpression and the sol1/2 suppressors implicate a CLV-like pathway in the control of Arabidopsis root meristem maintenance. *Curr Biol* 13(16):1435-41.

Chan SW and Blackburn EH (2002) New ways not to make ends meet: telomerase, DNA damage proteins and heterochromatin. *Oncogene* 21(4):553-63.

Chan SW, Henderson IR, Jacobsen SE (2005) Gardening the genome: DNA methylation in Arabidopsis thaliana. *Nat Rev Genet* 6(5):351-360.

Chen R, Guan C, Boonsirichai K, Masson PH (2002) Complex physiological and molecular processes underlying root gravitropism. *Plant Mol Biol* 49(3-4):305-17.

Chen X, Wang H, Li J, Huang H, Xu L(2013) Quantitative control of ASYMMETRIC LEAVES2 expression is critical for leaf axial patterning in Arabidopsis. *J Exp Bot* 64(16):4895-905.

Cheng X, and Blumenthal RM, (2008) Mammalian DNA methyltransferases: a structural perspective. *Structure* 16(3):341-50.

Cheng Y, Dai X, Zhao Y (2007) Auxin Synthesized by the YUCCA Flavin Monooxygenases Is Essential for Embryogenesis and Leaf Formation in Arabidopsis. *Plant Cell* 19(8) 2430-2439.

Cho T, Cosgrove DJ (2000) Altered expression of expansin modulates leaf growth and pedicel abscission in *Arabidopsis thaliana*. *Proc Natl Acad Sci* 97(17): 9783-9788.

Chow J, Yen Z, Ziesche S, Brown C (2005) Silencing of the mammalian X chromosome. *Annu Rev Genomics Hum Genet* 6:69-92.

Clark SE, Jacobsen SE, Levin JZ, Meyerowitz EM (1996) The CLAVATA and SHOOT MERISTEMLESS loci competitively regulate meristem activity in *Arabidopsis*. *Development* 122(5):1567-75.

Czechowski T, Stitt M, Altmann T, Udvardi MK, Scheible WR (2005) Genome-wide identification and testing of superior reference genes for transcript normalization in *Arabidopsis. Plant Physiol* 139(1):5-17.

Das PP, Bagijn MP, Goldstein LD, Woolford JR, Lehrbach NJ, Sapetschnig A, Buhecha HR, Gilchrist MJ, Howe KL, Stark R, Matthews N, Berezikov E, Ketting RF, Tavaré S, Miska EA (2008) Piwi and piRNAs act upstream of an endogenous siRNA pathway to suppress Tc3 transposon mobility in the *Caenorhabditis elegans* germline. *Mol Cell* 31(1):79-90.

Davies PJ (2010) The Plant Hormones: Their Nature, Occurrence, and Functions. Plant Hormones. Dordrecht: Springer.

Dennis ES, Bilodeau P, Burn J, Finnegan EJ, Genger R, Helliwell C, Kang BJ, Sheldon CC, Peacock WJ (1998) Methylation controls the low temperature induction of flowering in Arabidopsis. Symposia of the Society for Experimental Biology 51:97–103.

Donnelly PM, Bonetta D, Tsukaya H, Dengler RE, Dengler NG (1999) Cell cycling and cell enlargement in developing leaves of Arabidopsis. *Dev Biol* 215(2):407-19.

Du J, Zhong X, Bernatavichute YV, Stroud H, Feng S, Caro E, Vashisht AA, Terragni J, Chin HG, Tu A, Hetzel J, Wohlschlegel JA, Pradhan S, Patel DJ, Jacobsen SE (2012) Dual binding of chromomethylase domains to H3K9me2-containing nucleosomes directs DNA methylation in plants. *Cell* 151(1):167-80.

Eckhardt F, Lewin J, Cortese R, Rakyan VK, Attwood J, Burger M, Burton J, Cox TV, Davies R, Down TA, Haefliger C, Horton R, Howe K, Jackson DK, Kunde J, Koenig C, Liddle J, Niblett D, Otto T, Pettett R, Seemann S, Thompson C, West T, Rogers J, Olek A, Berlin K, Beck S (2006). DNA methylation profiling of human chromosomes 6, 20 and 22. *Nat Genet* 38(12):1378-85.

Feinberg AP and Vogelstein B (1983) Hypomethylation of ras oncogenes in primary human cancers. *Biochem Biophys Res Commun* 111(1):47-54.

Feraru E, Friml J (2008) PIN polar targeting. *Plant Physiol* 147(4):1553-9.

Finnegan EJ, Brettell RI, Dennis ES (1993) The role of DNA methylation in the regulation of plant gene expression. *EXS* 64:218–261.

Finnegan EJ, Peacock WJ, Dennis ES (1996) Reduced DNA methylation in *Arabidopsis thaliana* results in abnormal plant development. *Proc Natl Acad Sci* 93(16):8449-54.

Flores I, Cayuela ML, Blasco MA (2005) Effects of telomerase and telomere length on epidermal stem cell behavior. *Science* 309(5738):1253-6.

Fojtova M, Van Houdt H, Depicker A, Kovarik A (2003) Epigenetic switch from posttranscriptional to transcriptional silencing is correlated with promoter hypermethylation. *Plant Physiol* 133(3):1240-50.

Friml J, Benková E, Blilou I, Wisniewska J, Hamann T, Ljung K, Woody S, Sandberg G, Scheres B, Jürgens G, Palme K (2002) AtPIN4 mediates sink-driven auxin gradients and root patterning in Arabidopsis. *Cell* 108(5):661-73.

Friml J, Wiśniewska J, Benková E, Mendgen K, Palme K (2002) Lateral relocation of auxin efflux regulator PIN3 mediates tropism in Arabidopsis. *Nature* 415(6873):806-9.

Fujimoto D, Srinivasan PR, Borek E (1965) On the nature of the deoxyribonucleic acid methylases. Biological evidence for the multiple nature of the enzymes. *Biochemistry* 4(12):2849-55.

Gao Z, Liu HL, Daxinger L, Pontes O, He X, Qian W, Lin H, Xie M, Lorkovic ZJ, Zhang S, Miki D, Zhan X, Pontier D, Lagrange T, Jin H, Matzke AJ, Matzke M, Pikaard CS, Zhu JK (2010) An RNA polymerase II- and AGO4-associated protein acts in RNA-directed DNA methylation. *Nature* 465(7294):106-109.

Gonzalo S, Jaco I, Fraga MF, Chen T, Li E, Esteller M, Blasco MA (2006) DNA methyltransferases control telomere length and telomere recombination in mammalian cells. *Nature Cell Biol* 8(4):416-24.

Goodrich J, Puangsomlee P, Martin M, Long D, Meyerowitz EM, Coupland G (1997) A Polycomb-group gene regulates homeotic gene expression in Arabidopsis. *Nature* 386(6620):44-51.

Gray WM (2004) Hormonal regulation of plant growth and development. *PLoS Biol* 2(9):E311.

Greco M, Chiappetta A, Bruno L, Bitonti M (2012) In Posidonia oceanica cadmium induces changes in DNA methylation and chromatin patterning. *J Exp Bot* 63(2):695-709.

Griffith JS, Mahler HR (1969) DNA ticketing theory of memory. *Nature* 223(5206):580-2.

Grossniklaus U, Vielle-Calzada JP, Hoeppner MA, Gagliano WB (1998) Maternal control of embryogenesis by MEDEA, a polycomb group gene in *Arabidopsis*. *Science* 280(5362):446-50.

Haag JR, Pikaard CS (2011) Multisubunit RNA polymerases IV and V: purveyors of non-coding RNA for plant gene silencing. *Nature Rev Mol Cell Biol* 12(8):483-492.

Hay A, Tsiantis M (2006) The genetic basis for differences in leaf form between Arabidopsis thaliana and its wild relative Cardamine hirsuta. *Nat Genet* 38(8):942-7.

Hay A, Tsiantis M (2010) KNOX genes: versatile regulators of plant development and diversity. *Development* 137(19):3153-65.

Hayatsu H (2008) Discovery of bisulfite-mediated cytosine conversion to uracil, the key reaction for DNA methylation analysis - a personal account. *Proc Jpn Acad Ser B Phys Biol Sci* 84(8):321-330.

Henderson IR and Jacobsen SE (2007) Epigenetic inheritance in plants. *Nature* 447(7143):418-24.

Henderson IR and Jacobsen SE (2008) Tandem repeats upstream of the Arabidopsis endogene SDC recruit non-CG DNA methylation and initiate siRNA spreading. *Genes Dev* 22(12):1597-606.

Henikoff S, Comai, L (1998) A DNA methyltransferase homolog with a chromodomain exists in multiple polymorphic forms in Arabidopsis. *Genetics* 149(1):307-318.

Hohn T, Corsten S, Rieke S, Müller M, Rothnie H. (1996) Methylation of coding region alone inhibits gene expression in plant protoplasts. *Proc Natl Acad Sci USA* 93(16):8334-8339.

Holliday R and Pugh JE (1975) DNA modification mechanisms and gene activity during development. *Science* 187(4173):226-32.

Hotchkiss RD (1948) The quantitative separation of purines, pyrimidines, and nucleosides by paper chromatography. *J Biol Chem* 175(1):315-32.

Hou K, Wu W, Gan SS (2013) *SAUR36*, a SMALL AUXIN UP RNA gene, is involved in the promotion of leaf senescence in Arabidopsis. *Plant Physiol* 161(2): 1002-1009.

Hruz T, Laule O, Szabo G, Wessendorp F, Bleuler S, Oertle L, Widmayer P, Gruissem W and P Zimmermann (2008) Genevestigator V3: a reference expression database for the meta-analysis of transcriptomes. *Advances in Bioinformatics* 420747.

Irizarry RA, Ladd-Acosta C, Carvalho B, Wu H, Brandenburg SA, Jeddeloh JA, Wen B, Feinberg AP (2008) Comprehensive high-throughput arrays for relative methylation (CHARM). *Genome Res* 18(5):780-790.

Issa JP (2000) CpG-island methylation in aging and cancer. *Curr Top Microbiol Immunol* 249:101-18.

Jackson JP, Lindroth AM, Cao X, Jacobsen SE (2002) Control of CpNpG DNA methylation by the KRYPTONITE histone H3 methyltransferase. *Nature* 416(6880):556-560.

Jacobsen SE, Sakai H, Finnegan EJ, Cao X, Meyerowitz EM (2000) Ectopic hypermethylation of flower-specific genes in *Arabidopsis*. *Curr Biol* 10(4):179-86.

Jenik PD, Barton MK (2005) Surge and destroy: the role of auxin in plant embryogenesis. *Development* 132(16):3577-85.

Johnson L, Cao X, Jacobsen S (2002) Interplay between two epigenetic marks. DNA methylation and histone H3 lysine 9 methylation. *Curr Biol* 12(16):1360-7.

Jullien PE, Susaki D, Yelagandula R, Higashiyama T, Berger F (2012) DNA methylation dynamics during sexual reproduction in Arabidopsis thaliana. *Curr Biol* 22(19):1825-30.

Kakutani T, Jeddeloh JA, Flowers SK, Munakata K, Richards EJ (1996) Developmental abnormalities and epimutations associated with DNA hypomethylation mutations. *Proc Natl Acad Sci* 93(22):12406-11.

Kaufmann K, Pajoro A, Angenent GC (2010) Regulation of transcription in plants: mechanisms controlling developmental switches. *Nat Rev Genet* 11(12):830-42.

Kazama T, Ichihashi Y, Murata S, Tsukaya H (2010) The mechanism of cell cycle arrest front progression explained by a KLUH/CYP78A5-dependent mobile growth factor in developing leaves of Arabidopsis thaliana. *Plant Cell Physiol* 51(6): 1046–1054.

Kerk NM, Ceserani T, Tausta SL, Sussex IM, Nelson TM (2003) Laser capture microdissection of cells from plant tissues. *Plant Physiol* 132(1):27-35.

Kornberg RD and Lorch Y (1999) Twenty-five years of the nucleosome, fundamental particle of the eukaryote chromosome. *Cell* 98(3):285-94.

Kouzarides T (2002) Histone methylation in transcriptional control. *Curr Opin Genet Dev* 12(2):198-209.

Krysan PJ, Young JC, Sussman MR (1999) T-DNA as an insertional mutagen in Arabidopsis. *Plant Cell* 11(12):2283-90.

Lafos M, Kroll P, Hohenstatt ML, Thorpe FL, Clarenz O, Schubert D (2011) Dynamic regulation of H3K27 trimethylation during Arabidopsis differentiation. *PLoS Genet* 7(4):e1002040.

Laird PW (2010) Principles and challenges of genomewide DNA methylation analysis. *Nat Rev Genet* 11(3):191-203.

Law JA, Ausin I, Johnson LM, Vashisht AA, Zhu JK, Wohlschlegel JA, Jacobsen SE (2010) A protein complex required for polymerase V transcripts and RNA- directed DNA methylation in Arabidopsis. *Curr Biol* 20(10):951-6.

Law JA, Jacobsen SE (2010) Establishing, maintaining and modifying DNA methylation patterns in plants and animals. *Nat Rev Genet* 11(3):204-220.

Li E, Bestor TH, Jaenisch R (1992) Targeted mutation of the DNA methyltransferase gene results in embryonic lethality. *Cell* 69(6):915-26.

Lindroth AM, Cao X, Jackson JP, Zilberman D, McCallum CM, Henikoff S, Jacobsen SE (2001) Requirement of CHROMOMETHYLASE3 for maintenance of CpXpG methylation. *Science* 292(5524):2077-80.

Lisch D (2009) Epigenetic Regulation of Transposable Elements in Plants. *Annu Rev Plant Biol 60:43-66.*

Lister R, Mukamel EA, Nery JR, Urich M, Puddifoot CA, Johnson ND, Lucero J, Huang Y, Dwork AJ, Schultz MD, Yu M, Tonti-Filippini J, Heyn H, Hu S, Wu JC, Rao A, Esteller M, He C, Haghighi FG, Sejnowski TJ, Behrens MM, Ecker JR (2013) Global epigenomic reconfiguration during mammalian brain development. *Science* 341(6146):1237905.

Lister R, O'Malley RC, Tonti-Filippini J, Gregory BD, Berry CC, Millar AH, Ecker JR (2008) Highly integrated single-base resolution maps of the epigenome in *Arabidopsis*. *Cell* 133(3):523-36.

Lodha M, Marco CF, Timmermans MC (2013) The ASYMMETRIC LEAVES complex maintains repression of KNOX homeobox genes via direct recruitment of Polycomb-repressive complex2. *Genes Dev* 27(6):596-601.

Luo M, Yu CW, Chen FF, Zhao L, Tian G, Liu X, Cui Y, Yang JY, Wu K (2012) Histone deacetylase HDA6 is functionally associated with AS1 in repression of KNOX genes in arabidopsis. *PLoS Genet* 8(12):e1003114.

Mallory A and Vaucheret H (2010) Form, function, and regulation of ARGONAUTE proteins. *Plant Cell* 22(12):3879-89.

Matzke M, Matzke AJ, Kooter JM (2001) RNA: guiding gene silencing. *Science* 293(5532):1080-3.

Matzke MA, Mosher RA (2014) RNA-directed DNA methylation: an epigenetic pathway of increasing complexity. *Nat Rev Genet* 15(6):394-408.

Medford JI, Behringer FJ, Callos JD, Feldmann KA (1992) Normal and abnormal development in the *Arabidopsis* vegetative shoot apex. *Plant Cell* 4(6):631-643.

Mitchell Olds T (2001) *Arabidopsis thaliana* and its wild relatives: a model system for ecology and evolution. *TRENDS in Ecology & Evolution* Vol. 16 No. 12 December.

Moazed D (2009) Small RNAs in transcriptional gene silencing and genome defence. *Nature* 457(7228):413-20.

Mohn F, Weber M, Schübeler D, Roloff TC (2009) Methylated DNA immunoprecipitation (MeDIP). *Methods Mol Biol* 507:55-64.

Mukhopadhyay R, Yu W, Whitehead J, Xu J, Lezcano M, Pack S, Kanduri C, Kanduri M, Ginjala V, Vostrov A, Quitschke W, Chernukhin I, Klenova E, Lobanenkov V, Ohlsson R (2004) The binding sites for the chromatin insulator protein CTCF map to DNA methylation-free domains genome-wide. *Genome Res*. 14(8):1594-1602.

Müller A, Guan CH, Galweiler L, Tanzler P, Huijser P, Marchant A, Parry G, Bennett M, Wisman E, Palme K (1998) AtPIN2 defines a locus of *Arabidopsis* for root gravitropism control. *EMBO J* 17(23):6903-11.

Musco G and Peterson P (2008) PHD finger of autoimmune regulator: an epigenetic link between the histone modifications and tissue-specific antigen expression in thymus. *Epigenetics* 3(6):310-4.

Nakajima K, Sena G, Nawy T, Benfey PN (2001) Benfey Intercellular movement of the putative transcription factor SHR in root patterning. *Nature* 413(6853):307-11.

Nakazono M, Qiu F, Borsuk LA, Schnable PS (2003) Laser-capture microdissection, a tool for the global analysis of gene expression in specific plant cell types: identification of genes expressed differentially in epidermal cells or vascular tissues of maize. *Plant Cell* 15(3):583-96.

Nathan D, Ingvarsdottir K, Sterner DE, Bylebyl GR, Dokmanovic M, Dorsey JA, Whelan KA, Krsmanovic M, Lane WS, Meluh PB, Johnson ES, Berger SL (2006) Histone sumoylation is a negative regulator in *Saccharomyces cerevisiae* and shows dynamic interplay with positive-acting histone modifications. *Genes Dev* 20(8):966–76.

Nelissen H, Boccardi TM, Himanen K, Van Lijsebettens M (2007) Impact of core histone modifications on transcriptional regulation and plant growth. *Crit Rev Plant Sci* 26:243–63.

Nelissen H, De Groeve S, Fleury D, Neyt P, Bruno L, Bitonti MB, Vandenbussche F, Van der Straeten D, Yamaguchi T, Tsukaya H, Witters E, De Jaeger G, Houben A, Van Lijsebettens M (2010) Plant Elongator regulates auxin-related genes during RNA polymerase II transcription elongation. *Proc Natl Acad Sci* 107(4):1678-83.

Niederhuth CE, Bewick AJ, Ji L, Alabady MS, Kim KD, Li Q, Rohr NA, Rambani A, Burke JM, Udall JA, Egesi C, Schmutz J, Grimwood J, Jackson SA, Springer NM, Schmitz RJ (2016) Widespread natural variation of DNA methylation within angiosperms. *Genome Biol* 17(1):194.

Okano M, Bell DW, Haber DA, Li E (1999) DNAmethyltransferases Dnmt3a and Dnmt3b are essential for de novomethylation and mammalian development. *Cell* 99(3):247-57.

Ooi SK, Qiu C, Bernstein E, Li K, Jia D, Yang Z, Erdjument-Bromage H, Tempst P, Lin SP, Allis CD, Cheng X, Bestor TH (2007) DNMT3L connects unmethylated lysine 4 of histone H3 to de novo methylation of DNA. *Nature* 448(7154):714-7.

Palme K, Galweiler L (1999) PIN-pointing the molecular basis of auxin transport. *Curr Opin Plant Biol* 2(5): 375-81.

Petrásek J, Mravec J, Bouchard R, Blakeslee JJ, Abas M, Seifertová D, Wisniewska J, Tadele Z, Kubes M, Covanová M, Dhonukshe P, Skupa P, Benková E, Perry L, Krecek P, Lee OR, Fink GR, Geisler M, Murphy AS, Luschnig C, Zažímalová E, Friml J (2006) PIN proteins perform a rate-limiting function in cellular auxin efflux. *Science* 312(5775):914-8.

Petricka JJ, Winter CM, Benfey PN (2012) Control of Arabidopsis root development. *Annu Rev Plant Biol* 63:563-90.

Pfeiffer A, Wenzl C, Lohmann JU (2016) Beyond flexibility: controlling stem cells in an ever changing environment. *Curr Opin Plant Biol* 35:117-123.

Pray L (2008) Transposons: The jumping genes. *Nature Education* 1(1):204.

Ramsahoye BH, Biniszkiewicz D, Lyko F, Clark V, Bird AP, Jaenisch R (2000) Non-CpG methylation is prevalent in embryonic stem cells and may be mediated by DNA methyltransferase 3a. *Proc Natl Acad Sci USA* 97(10):5237-42.

Razin A and Cedar H (1993) DNA methylation and embryogenesis. *EXS* 64, 343-57.

Reinhardt D, Mandel T, Kuhlemeier C (2000) Auxin regulates the initiation and radial position of plant lateral organs. *Plant Cell* 12(4):507-18.

Relton CL, Davey Smith G (2010) Epigenetic epidemiology of common complex disease: prospects for prediction, prevention, and treatment. *PLoS Med* 7(10):e1000356.

Rinn JL, Chang HY (2012) Genome regulation by long noncoding RNAs. *Annu Rev Biochem* 81:145-66.

Ronemus MJ, Galbiati M, Ticknor C, Chen J, Dellaporta SL (1996) Demethylation-induced developmental pleiotropy in *Arabidopsis*. *Science* 273(5275):654-7.

Roudier F, Ahmed I, Bérard C, Sarazin A, Mary-Huard T, Cortijo S, Bouyer D, Caillieux E, Duvernois-Berthet E, Al-Shikhley L, Giraut L, Després B, Drevensek S, Barneche F, Dèrozier S, Brunaud V, Aubourg S, Schnittger A, Bowler C, Martin-Magniette ML, Robin S, Caboche M, Colot V (2011) Integrative epigenomic mapping defines four main chromatin states in *Arabidopsis*. *EMBO J* 30(10):1928-38.

Sabatini S, Heidstra R, Wildwater M, Scheres B (2003) SCARECROW is involved in positioning the stem cell niche in the Arabidopsis root meristem. *Genes Dev* 17(3)354-8.

Satina S, Blakeslee AF, Avery AG (1940) Demonstration of the three germ layers in the shoot apex of Datura by means of induced polyploidy in periclinal chimeras. *Am J Bot* 27:895-905.

Scarpella E, Marcos D, Friml J, Berleth T (2006) Control of leaf vascular patterning by polar auxin transport. *Genes Dev* 20(8):1015-27.

Schubert D, Primavesi L, Bishopp A, Roberts G, Doonan J, Jenuwein T, Goodrich J (2006) Silencing by plant Polycomb-group genes requires dispersed trimethylation of histone H3 at lysine 27. *EMBO J* 25(19):4638-49.

Shukla A, Stanojevic N, Duan Z, Shadle T, Bhaumik SR (2006) Functional analysis of H2B-Lys-123 ubiquitination in regulation of H3-Lys-4 methylation and recruitment of RNA polymerase II at the coding sequences of several active genes in vivo. *J Biol Chem* 281(28):19045-54.

Simon JA and Kingston RE (2009) Mechanisms of polycomb gene silencing: knowns and unknowns. *Nat Rev Mol Cell Biol* 10(10):697-708.

Soppe WJ, Jacobsen SE, Alonso-Blanco C, Jackson JP, Kakutani T, Koornneef M, Peeters AJ (2000) The late flowering phenotype of fwa mutants is caused by gain-of-function epigenetic alleles of a homeodomain gene. *Mol Cell* 6(4):791-802.

Soppe WJ, Jasencakova Z, Houben A, Kakutani T, Meister A, Huang MS, Jacobsen SE, Schubert I, Fransz PF (2002) DNA methylation controls histone H3 lysine 9 methylation and heterochromatin assembly in *Arabidopsis*. *EMBO J* 21(23):6549-59.

Soyars CL, James SR, Nimchuk ZL (2016) Ready, aim, shoot: stem cell regulation of the shoot apical meristem. *Curr Opin Plant Biol* 29:163-8.

Spartz AK, Lee SH, Wenger JP, Gonzalez N, Itoh H, Inzé D, Peer WA, Murphy AS, Overvoorde PJ, Gray WM (2012) The *SAUR19* subfamily of *SMALL AUXIN UP RNA* genes promote cell expansion. *Plant J* 70(6): 978-990.

Stroud H, Do T, Du J, Zhong X, Feng S, Johnson L, Patel DJ, Jacobsen SE (2014) Non-CG methylation patterns shape the epigenetic landscape in Arabidopsis. *Nat Struct Mol Biol* 21(1):64-72.

Surani MA Barton SC Norris ML (1984) Development of reconstituted mouse eggs suggests imprinting of the genome during gametogenesis. *Nature* 308(5959):548-50.

Suzuki M, Bird, A (2008) DNA methylation landscapes: Provocative insights from epigenomics. *Nature Reviews Genetics* 9(6):465-76.

Swarup R, Friml J, Marchant A, Ljung K, Sandberg G, Palme K, Bennett M (2001) Localization of the auxin permease AUX1 suggests two functionally distinct hormone transport pathways operate in the Arabidopsis root apex. *Genes Dev* 15(20):2648-53.

Tazi J and Bird A (1990) Alternative chromatin structure at CpG islands. *Cell* 60(6):909-20.

Tompa R, McCallum CM, Delrow J, Henikoff JG, van Steensel B, Henikoff S (2002) Genome-wide profiling of DNA methylation reveals transposon targets of CHROMOMETHYLASE3. *Curr Biol* 12(1):65-68.

Trewavas A (1981) How do plant growth substances work? *Plant Cell Environ* 4:203–228.

Tsukaya H (2014) Comparative leaf development in angiosperms. *Curr Opin Plant Biol* 17: 103–109.

Turner BM (2000) Histone acetylation and an epigenetic code. *Bioessays* 22(9):836-45.

Verdel A, Jia S, Gerber S, Sugiyama T, Gygi S, Grewal SI, Moazed D. (2004) RNAi-mediated targeting of heterochromatin by the RITS complex. *Science* 303(5658):672-6.

Vielle-Calzada JP, Thomas J, Spillane C, Coluccio A, Hoeppner MA, Grossniklaus U(1999) Maintenance of genomic imprinting at the Arabidopsis medea locus requires zygotic DDM1 activity. *Genes Dev* 13(22):2971-82.

Viré E, Brenner C, Deplus R, Blanchon L, Fraga M, Didelot C, Morey L, Van Eynde A, Bernard D, Vanderwinden JM, Bollen M, Esteller M, Di Croce L, de Launoit Y, Fuks F (2006) The Polycomb group protein EZH2 directly controls DNA methylation. *Nature* 439(7078):871-4.

Waddington CH (2012) The epigenotype. 1942. *Int J Epidemiol* 41(1):10-3.

Wang X, Elling AA, Li X, Li N, Peng Z, He G, Sun H, Qi Y, Liu XS, Deng XW (2009) Genome-wide and organ-specific landscapes of epigenetic modifications and their relationships to mRNA and small RNA transcriptomes in maize. *Plant Cell* 21(4):1053-69.

Weber and Schübeler. Methylated DNA Immunoprecipitation (MeDIP) (PROT33). The epigenome network of excellence.

Weber M, Davies JJ, Wittig D, Oakeley EJ, Haase M, Lam WL, Schübeler D (2005) Chromosome-wide and promoter-specific analyses identify sites of differential DNA methylation in normal and transformed human cells. *Nat Genet* 37(8):853-62.

Widman N, Feng S, Jacobsen SE, Pellegrini M (2014) Epigenetic differences between shoots and roots in Arabidopsis reveals tissue-specific regulation. *Epigenetics* 9(2):236-42.

Wyatt GR (1950) Occurrence of 5-methylcytosine in nucleic acids. *Nature* 166(4214):237-8.

Yen RW, Vertino PM, Nelkin BD, Yu JJ, el-Deiry W, Cumaraswamy A, Lennon GG, Trask BJ, Celano P, Baylin SB (1992) Isolation and characterization of the cDNA encoding human DNA methyltransferase. *Nucleic Acids Res* 20(9):2287-91.

Yoder JA, Walsh CP, Bestor TH (1997) Cytosine methylation and the ecology of intragenomic parasites. *Trends Genet*. 13(8):335-40.

Yu Y, Bu Z, Shen WH, Dong A (2009) An update on histone lysine methylation in plants. *Prog Nat Sci* 19: 407–413.

Zažímalová E, Petrasek J, Benková E (2014) Auxin and Its Role in Plant Development. Dordrecht: Springer.

Zemach A, Kim MY, Hsieh PH, Coleman-Derr D, Eshed-Williams L, Thao K, Harmer SL, Zilberman D (2013) The Arabidopsis nucleosome remodeler DDM1 allows DNA methyltransferases to access H1-containing heterochromatin. *Cell* 153(1):193-205.

Zhang X, Clarenz O, Cokus S, Bernatavichute YV, Pellegrini M, Goodrich J, Jacobsen SE (2007) Whole-Genome Analysis of Histone H3 Lysine 27 Trimethylation in *Arabidopsis*. *PLoS Biol* 5(5):e129.

Zhang X, Yazaki J, Sundaresan A, Cokus S, Chan SW, Chen H, Henderson IR, Shinn P, Pellegrini M, Jacobsen SE, Ecker JR (2006) Genome-wide High-Resolution Mapping and Functional Analysis of DNA Methylation in Arabidopsis. *Cell* 126(6):1189-201.

Zhao M, Yang S, Chen CY, Li C, Shan W, Lu W, Cui Y, Liu X, Wu K (2015) Arabidopsis BREVIPEDICELLUS interacts with
the SWI2/SNF2 chromatin remodeling ATPase BRAHMA toregulate KNAT2 and K NAT6 expression in control of inflorescence architecture. *PLoS Genet* 11(3):e1005125.

Zilberman D, Gehring M, Tran RK, Ballinger T, Henikoff S (2007) Genome-wide analysis of Arabidopsis thaliana DNA methylation uncovers an interdependence between methylation and transcription. *Nat Genet* 39(1):61-9.